A PLATELET-MEDIATED PARADIGM FOR TARGETED DELIVERY OF MICROENCAPSULATED, CLOT-AUGMENTING BIOTHERAPEUTICS

A Dissertation
Presented to
The Academic Faculty

by

Caroline E. Hansen

In Partial Fulfillment
of the Requirements for the Degree
Doctor of Philosophy in the
School of Chemistry and Biochemistry

Georgia Institute of Technology
August 2017

A PLATELET-MEDIATED PARADIGM FOR TARGETED DELIVERY OF MICROENCAPSULATED, CLOT-AUGMENTING BIOTHERAPEUTICS

Approved by:

Dr. Wilbur A. Lam, Co-Advisor
School of Biomedical Engineering
Georgia Institute of Technology

Dr. M. G. Finn
School of Chemistry and Biochemistry
Georgia Institute of Technology

Dr. L. Andrew Lyon, Co-Advisor
College of Science
Chapman University

Dr. Stefan France
School of Chemistry and Biochemistry
Georgia Institute of Technology

Dr. Adegboyega Oyelere
School of Chemistry and Biochemistry
Georgia Institute of Technology

Date Approved: July 5, 2017

ACKNOWLEDGEMENTS

First and foremost, I would like to thank all of my family members for their incredible support through this academic pursuit. I would especially like to thank my Mother, Lula Hansen, for her unwavering support and belief in my capabilities and my Father, for keeping me focused and grounded. I would also like to thank my Brother, Steven Hansen, for supporting and believing in me as well as my dog, Pippa. In addition, I would like to thank Dr. Haylee Bachman, for her emotional support during the entire graduate school process.

I would like to thank Dr. Wilbur Lam for not only taking me into his lab, put providing an immeasurable amount of guidance, support, and freedom throughout my project. Thank you to Dr. L. Andrew Lyon for giving me freedom to explore ideas but offering guidance and feedback when needed. I would also like to like my additional committee members – Drs. M. G. Finn, Yomi Oyelere, and Stefan France – for not only their valuable time, but guidance and insightful comments throughout the course of this project.

I also owe an enormous amount of gratitude to past and present lab members – Dr. Ashley Brown, Dr. Grant Hendrickson, Dr. Shalini Saxena, Dr. Margo Rollins, Dr. Elaissa Trybus Hardy, Dr. Yongzhi Qiu, Dr. Sarah Mitchell, Dr. Marcus Carden, Erika Tyburski, Meredith Fey, Jordan Ciciliano, Rob Maninno, and Jessica Lin – for their support and valuable conversations. I would especially like to thank Yumiko Sakurai for her patience in teaching me numerous experimental designs and platelet biology, Dr.

David Myers for the innumerable trouble shooting conversations regarding my project, and Dr. Reginald Tran for his immeasurable support during my graduate school career.

Thank you to everyone, this work would not be possible without you.

TABLE OF CONTENTS

LIST OF FIGURES

LIST OF SYMBOLS AND ABBREVIATIONS

ADP	Adensoine diphosphate
BSA	Bovine serum albumin
EDTA	Ethylenediaminetetraacetic acid
Fbn	fibrinogen
FITC	Fluorescein isothiocyanate
fVIII	factor VIII
GP	Glycoprotein
HyPEM	Hybridized polyelectrolyte multilayer capsule
ITI	Immune tolerance induction
LbL	Layer-by-layer
o/w	Oil-in-water
PDMS	Polydimethyl siloxane
PEM	Polyelectrolyte multilayer
PLG	Poly-L-glutamic acid
PLL	Poly-L-lysine
Plt	platelet
PPP	Platelet poor plasma
PRP	Platelet rich plasma
RBITC	Rhodamine B isothiocyanate
tPA	Tissue plasminogen activator
vWF	Von Willebrand Factor

SUMMARY

Reported herein is a paradigm-shifting, targeted drug delivery system that leverages the patient's own platelets to sense and actuate targeted delivery of a clot-augmenting therapeutic to a site of vascular injury. In this system, platelets target microencapsulated drugs through their natural aggregation behavior in the clot formation process and then deliver the drug by physically rupturing the microcapsule through contractile forces exerted during clot contraction. This cell-mediated, targeted drug delivery system utilizes polyelectrolyte multilayer capsules that hybridize with the patient's own platelets upon intravenous administration and rupture upon platelet contraction, enabling the targeted and controlled "burst" release of an encapsulated biotherapeutics (Figure 1). As platelets are the "first responders" in the blood clot formation process, this platelet-hybridized system is ideal for the targeted delivery of clot augmenting biotherapeutics wherein immediate therapeutic efficacy is required.

As proof-of-concept, we tailored this system to deliver the pro-clotting biotherapeutic, factor VIII (fVIII) for hemophilia A patients who have developed inhibitory anti-fVIII antibodies. The polyelectrolyte multilayer capsules physically shield the encapsulated fVIII from the patient's inhibitors during circulation, preserving its bioactivity until it is delivered at the target site *via* platelet contractile force. Using an *in vitro* microfluidic vascular injury model with fVIII-inhibited blood, we demonstrate a 3.8x increase in induced fibrin formation using capsules loaded with fVIII at a concentration an order of magnitude lower than that used in systemic delivery. We further demonstrate that clot formation occurs 18 minutes faster when fVIII loaded capsules are used compared to

systemic delivery at the same concentration. Because platelets are integral in the pathophysiology of thrombotic disorders, cancer, and innate immunity, this paradigm-shifting smart drug delivery system can be similarly applied to these diseases.

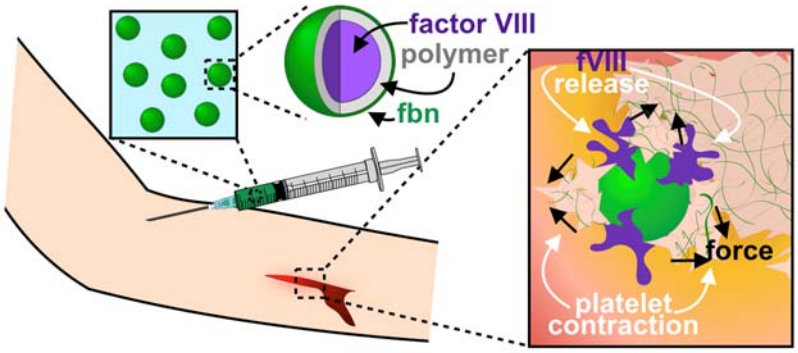

Figure 1. Illustration of platelet-mediated "burst" delivery at a site undergoing bleeding. Polyelectrolyte multilayer microcapsules loaded with a clot-promoting drug (i.e. factor VIII (fVIII)) are intravenously administered to the patient. The patient's own platelets hybridize with the microcapsule and target it to the injury site through their natural clotting behavior. Once platelets begin to contact within the clot structure, the physical force ruptures the microcapsule and delivers the full encapsulated dose to the injury site to stem bleeding. [1]

CHAPTER 1. INTRODUCTION

Intravenous administration of a "free" drug results immediate exposure of the drug to the vascular system (systemic exposure). While this may be desirable in treating certain conditions (*i.e.* acetaminophen for general muscle soreness), this can lead to off-target interactions between the administered drug and healthy environments, which can lead to life threatening complications for certain drugs. The rise of nanotechnology in recent decades has had substantial impact on the fields of chemistry, biomedical engineering, and medicine as a vast array of nanoparticles have been developed that enable targeted delivery of therapeutics that have traditionally been administered systemically. Nanoparticle-based targeted delivery has been shown to increase efficacy by altering biodistribution, increasing drug half-life and solubility, and lowering potential risk of side effects. [2-8] Commonly developed drug carrying nanoparticles, in particular ones that have achieved FDA approval, have relied upon delivery mechanisms that operate over extended time scales (*i.e.* diffusion or site-specific biodegradation).[9] While this has been shown to increase efficacy and decrease the side effect profile for several drugs (*i.e.* Doxil® - liposomal doxorubicin in treating malignant tumors),[10] several life-threatening disorders require immediate exposure of the full dose of the treatment at the diseased site, rendering these nanoparticle-based targeted delivery technologies insufficient.

1.1 Motivation

Hemostasis is an extremely sensitive system that exists on a continuum. Pathologic coagulation that requires therapeutic intervention occurs on both ends of the continuum (*i.e.* deep vein thrombosis or hemorrhage). The current clinically-used treatment standard

requires systemic administration of the appropriate treatment (small molecule, recombinant biologic, or plasma products) to break-up occlusive clotting or promote clotting for non-compressible hemorrhage.[11-14] These treatments can drive the hemostatic response to the other end of the continuum due to their off-target effects (i.e. causing hemorrhagic stroke when treating thrombosis or causing thrombosis when treating bleeds).[15,16] Additional drawbacks to these treatment options include restricted administration timeframes for thrombolytics (due to their off-target side effects), immediate access to large donor pools, storage of both frozen and freshly thawed plasma products, and adverse immunomodulatory responses for antihemorrhagics.[15,17,18]

As both platelets and red blood cells are involved in the clot formation process and are major constituents of blood clots, significant research has been conducted into cell-mediated strategies for targeted delivery of clot augmenting therapies.[19-21] However, the previously developed strategies have focused on delivery of fibrinolytics and, more importantly, do not enable an immediate "burst" release of the incorporated therapeutic. An advantageous feature of innate platelet behavior is their ability to physically contract on an underlying substrate after site-specific activation, as in the context of a clotting environment, which has yet to be used to perform targeted drug delivery. This work capitalizes upon this behavior to effect drug targeting (*via* platelet adhesion to sites of clotting) and drug delivery (*via* platelet contraction after activation).

Specifically, fibrinogen coated polyelectrolyte multilayer microcapsules (PEM capsules) that are loaded with a hemostatic drug (*i.e.* fVIII to treat bleeds in hemophilia A patients) are intravenously administered, after which the patient's own platelets adhere to the surface fibrinogen, forming a platelet hybridized PEM capsule (platelet-HyPEM)

(Figure 2A).[1] These structures circulate quiescently through healthy vascular environments (Figure 2B), but once exposed to a site undergoing active bleeding, the hybridized platelets activate and adhere the PEM capsule to the injury site (Figure 2C). Once the platelets begin to contract, the contractile force generated in the forming clot physically ruptures the PEM capsule wall, providing a "burst" release of the targeted drug for immediate exposure (Figure 2D). Utilizing the biomechanical behavior of the patient's own platelets is a previously unreported drug delivery paradigm, which could drastically advance future "smart" targeted drug delivery strategies in the context of hematological disorders.

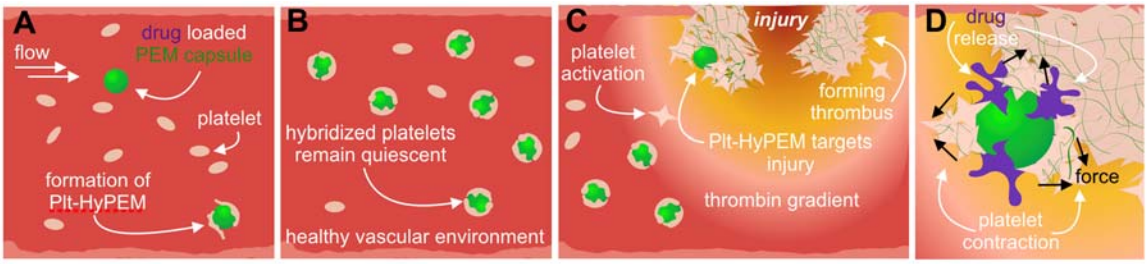

Figure 2. Illustration of "smart" drug delivery paradigm leveraging the patient's own platelets for targeted delivery and controlled release. (A) Polyelectrolyte multilayer (PEM) capsules loaded with a biotherapeutic payload are intravenously administered to the patient whereupon the patient's own platelets adhere to the PEM capsule *via* surface fibrinogen (green) during circulation to form a platelet-hybridized microcapsule (plt-HyPEM). (B) The patient's platelets that comprise the hybrid microcapsule remain quiescent during circulation. Only when the hybrid microcapsules enter an area undergoing active clotting (C), do the hybridized platelets activate upon exposure to thrombin and target the platelet-HyPEM to the site of injury by adhering to exposed collagen at the site of vascular injury and/or integrating into the forming fibrin network of the nascent clot. (D) Finally, the physical force exerted by platelet-mediated contraction within the platelet-HyPEM and nearby platelets physically ruptures the platelet-HyPEM capsule, enabling delivery of a high dose of the encapsulated biotherapeutic (purple) to the target site.

1.2 Research Objectives and Specific Aims

The *long-term goal* of this project is to develop a technology for the targeted delivery of factor VIII (fVIII) to abate bleeds in hemophilia A patients with inhibitory antibodies. The **overall objective** of this thesis was to develop a targeted drug delivery paradigm that leverages platelet biomechanical behavior (specifically site-specific aggregation and contraction) for both targeting and delivery. The **central hypothesis** of this work is that platelets will adhere onto a fibrinogen coated spherical surface (the drug loaded vehicle), and that their contraction (once activated) in a clotting environment is sufficient enough to mechanically disrupt a drug-carrying microparticle such that rupture of the particle and release of the drug is achieved. This hypothesis is substantiated upon the significant research conducted regarding platelet adhesion onto fibrinogen coated surfaces and their contractile behavior on underlying substrates that has been measured on the bulk and single-cell length scales.

1.2.1 Specific Aim 1: Feasibility of a Platelet-Mediated Targeted Drug Delivery Mechanism

The viability of a platelet-mediated drug delivery system depends on the realization of several factors, including: platelet adhesion onto microparticles to form platelet-hybridized microparticles, adhesion of the hybrid microparticles to sites of vascular injury, and the ability of the microparticle to rupture due to platelet contractile forces. Emulsion microparticles were originally investigated as the drug delivery microparticle due to their ease of fabrication and current use in several pharmaceutical formulations.[22]

In this aim, I investigated two emulsification methods for fibrinogen stabilized emulsions, and their effects on emulsion size and stability. I then developed a microfluidic

experimental assay to demonstrate two factors that are crucial to the proposed platelet-mediated targeted drug delivery paradigm. I show that not only can emulsion droplets adhere to "micro-thrombi", but also that circulating single platelets can adhere to the fibrinogen coated emulsion surface. Furthermore, I show in the developed microfluidic assay that their contractile force under ADP or thrombin activation is sufficient enough to morphologically disrupt the emulsion droplets and rupture the fibrinogen coating on the droplet surface, thereby proving the feasibility of this platelet-mediated paradigm.

1.2.2 Specific Aim 2: Modification of Polyelectrolyte Multilayer Microcapsules to Enable Platelet Contractile Force Mediated Rupture

Polyelectrolyte multilayer (PEM) capsules are well-established self-assemblies that have been heavily investigated as possible drug delivery microcapsules.[23,24] They are easily fabricated via layer-by-layer deposition of polyelectrolyte polymers onto a sacrificial templating core particle followed by core removal, enabling facile control over the mechanical properties by adjusting polyelectrolyte shell thickness.[25,26] Of particular consequence to a drug delivery paradigm based upon contractile forces is that their structural integrity has been shown to be susceptible to mechanical force generating events on the cellular level, such as cellular uptake.[27] As such, their suitability to function as drug-encapsulating microcapsules that are susceptible to platelet contraction-mediated drug release was explored. In this aim, I detail modifications to PEM capsules that were made in order to facilitate the desired interactions with platelets, specifically their ability to form hybrid complexes (platelet-HyPEMs) with quiescent platelets and rupture via contraction of activated platelets.

1.2.3 Specific Aim 3: Platelet-Mediated Targeted Delivery of Factor VIII In Vitro

Hemophilia A is a genetic bleeding disorder wherein patients cannot produce functional factor VIII, a pro-coagulant plasma protein. They therefore must receive prophylactic or on-demand injections of fVIII to prevent and abate bleeding events.[28,29] Approximately 30% of severe hemophilia patients produce an inhibitory antibody to fVIII, which renders replacement therapy ineffective due to its systemic administration.[30] These patients must then use alternative pro-clotting factors that are associated with higher risks of thrombotic side effects or have shorter half-lives.[31-34] Platelet-HyPEMs were investigated as fVIII delivery microcapsules that circumvent interaction between the patient's inhibitors and administered fVIII as an alternative therapy with the potential of lower side effects.

This chapter focuses on evaluation of the *in vitro* hemostatic efficacy of fVIII loaded platelet-HyPEMs using healthy and fVIII inhibited blood samples. A microfluidic vascular injury model was used to determine effects on fibrin formation in a clotting environment. Results show that fVIII-loaded HyPEMs enable more fibrin formation compared to "free" fVIII in fVIII-inhibited blood. In addition, a clot duration assay was used to investigate clot formation on the bulk scale, which shows that fVIII-loaded HyPEMs decrease clot formation time to that of a healthy patient compared to a fVIII-inhibited control and "free" fVIII.

1.3 Significance

This work has significance in two areas – the development of a paradigm-shifting mechanism within the targeted drug delivery field and its application to potentially

circumvent inhibitor interference in hemophilia A patients. Leveraging the naturally occurring and site-specific biomechanical behavior of the patient's own platelets, specifically their contraction after activation, to effect targeted drug delivery is a paradigm-shifting approach, with potential to not only deliver hemostatic-regulating drugs, but also chemotherapeutics and immunomodulatory therapies as platelets are involved in these biological systems as well. However, within the context of clot-augmenting drugs, this technology has immense impact as these pathologies are often immediately life threatening if left untreated. This targeted drug delivery method enables delivery of larger therapeutic dose to the target site compared to what is allowed when administering a formulation that results in systemic exposure. As such, this can be a very powerful technology in delivery biotherapeutics to quickly abate active bleeds due to non-compressible injuries or for patients who are at a high risk of hemorrhage.

For severe hemophilia A patients, prophylactic treatment with replacement factor is recommended in order to prevent spontaneous bleeding episodes; however, this treatment regimen is extremely costly, as it requires multiple infusions per week. In 2015, the 20,000 hemophilia A patients in the United States spent approximately $9.3 Billion dollars on drugs to prevent or abate bleeding episodes.[35] The subset of patients that develop inhibitors to fVIII replacement therapy are left with few treatment options to prevent or abate bleeding and spend an average of $978,955 per year on treatment costs.[35,36]

Clearly, an unmet medical need exists for an effective, yet safe, treatment for hemophilia A patients with inhibitors. Encapsulating fVIII in a polymer microcapsule affords "shielding" from the patient's inhibitors during circulation, preserving its bioactivity for when it is released on the injured site. Furthermore, imparting targeting and

"burst" delivery capabilities into the microcapsule can enhance fVIII efficacy while decreasing the risk of thrombotic side effects. Such a treatment system will drastically improve the lives of hemophilia patients with inhibitors, as they will be able to quickly and effectively treat bleeding episodes.

CHAPTER 2. BACKGROUND AND LITERATURE REVIEW

2.1 Targeted Drug Delivery

Nanoparticle-based targeted drug delivery systems offer many advantages for intravenous therapies in comparison to administration of the "free" drug (*i.e.* increased solubility, alteration of biodistribution and pharmacokinetics, and longer drug half-life).[8] Most notable is the advantage of targeting the therapy strictly to the diseased site. Theoretically, the increased drug accumulation at the diseased area can increase the efficacy of a drug while using a lower dose compared to the "free" drug that is targeted systemically. Targeting also decreases the drug's off-target interactions with healthy tissues, thereby lowering the potential risk of side effects.

A substantial amount of research has been conducted into targeted drug delivery systems for a wide range of diseases, and as such, a vast array of targeted delivery mechanisms have been developed. Generally, these can be classified into passive or active targeting.[37,38] Passive targeting mechanisms do not include a feature in the nanoparticle that can specifically target the diseased site and instead rely on a feature of the diseased site or physical characteristic of the nanoparticle for accumulation.[37] Utilization of the enhanced permeability and retention (EPR) effect for tumor-targeting formulations is a classic example of a passive targeting mechanism.[37,39,40] Targeted drug delivery systems that employ active targeting display a targeting moiety on the nanoparticle. Targeting features include biochemical moieties like peptides or antibodies specific to a receptor that is upregulated or present in a diseased state,[41-43] magnetic nanoparticles that guide the drug delivery construct to the desired site by application of an external magnet,[44,45] or cell-

mediated strategies wherein nanoparticle constructs are hybridized (covalently or non-covalently) with disease regulating cells to "hitch-hike" to the target site.[46]

In addition to active or passive targeting, incorporating a stimuli responsive delivery mechanism offers additional control by enabling site-specific release of the therapeutic.[47,48] This can be accomplished by incorporating features subject to intrinsically present or externally applied stimuli. Popular intrinsic stimuli include increased redox environments,[49] lower localized pH environments,[41] or sensitivity to specific enzymes.[50] Utilization of heat,[44] lasers,[51,52] or ultrasound[53-55] are external methods that have been extensively developed in the literature as well.

Ruan *et al.* leveraged the EPR effect and several intrinsic aspects of the tumor environment for targeted delivery of doxorubicin from a multi-particle construct.[56] Investigators synthesized gelatin nanoparticles to which they covalently coupled (*via* EDC/NHS chemistry) gold nanoparticles that were decorated with PEG and doxorubicin with a hydrazone crosslinker. The particle composites were targeted to tumors through the EPR effect, and once there, underwent gelatin degradation *via* matrix metalloprotease-2, which is over expressed in tumor sites. Gelatin degradation frees the smaller gold nanoparticle constructs, enabling further interrogation of the tumor mass. Doxorubicin is then released in the acidic environment within the tumor or after cellular uptake in the lysosome *via* the pH sensitive hydrazone bond. Utilizing an *in vivo* model of B16F10 tumor bearing mice, they were able to show minimal changes in tumor growth determine *via* volume volume over 22 days, which was statistically significant compared to free doxorubicin and the controls.

Utilization of the EPR effect for nanoparticle tumor targeting suffers from two major drawbacks: (1) nanoparticles typically undergo rapid clearance, which can only be extended by a certain extent using surface functionalization strategies (*i.e.* PEGylation), and (2) access to the full tumor tissue is severely limited due to interstitial pressure and heterogeneous vascularization.[37,40,57] To address these shortcomings, a cell-mediated strategy was developed that targets circulating monocytes after intravenous administration.[58] When these monocytes differentiate into macrophages in tumor environments, they can exhibit substantial extravasation, entering areas that are inaccessible when relying on the EPR effect alone.[59] This paradigm utilizes flat-disk shaped "backpack" particles (to circumvent cellular uptake) comprised of several layers fabricated from layer-by-layer assembly with a structural layer consisting of poly(allylamine hydrochloride) and iron oxide magnetic nanoparticles and a ligand displaying layer consisting of poly(acrylic acid) and poly(allylamine hydrochloride) functionalized with biotin. Streptavidin is then deposited on the biotin layer, followed by a biotinylated antibody of choice, enabling "hitchhiking" of monocytes. Investigators showed significant accumulation of hitchhiked backpack particles compared to free particles in inflamed tissue compared to other organs (except the heart). They then showed in a lung inflammation model, backpacks hitchhiked to monocytes significantly accumulated more in the lungs compared to other organs, which was not seen in healthy mice.

Hyaluranic acid (HA) polymeric micelles are commonly used nanoparticle constructs in chemotherapeutic delivery as HA naturally targets CD44, which has been shown to be overexpressed in several tumor cell lines.[60] Polymeric micellular constructs

have been shown to be unstable after intravenous administration, however, which results in premature and off-target drug release.[61] To combat this undesirable behavior, Han *et al.* fabricated HA polymeric micelles with redox-sensitive crosslinked cores to enhance stability in complex suspensions like whole blood.[62] This was achieved by covalently attaching a disulfide displaying polymer to the HA polymer, which after micelle formation and doxorubicin loading, was crosslinked *via* a redox reaction with dithiothreitol. Disulfide crosslinking of the particles imparts redox sensitive release to leverage the substantial higher glutathione concentration in the intracellular environment of tumor cells. *In vivo* determination using SCC7 tumor-bearing mice demonstrated significantly increased nanoparticle accumulation in tumor tissue for core crosslinked particles compared to uncrosslinked particles, which was further supported by decreased doxorubicin concentration in plasma but increased concentration in the tumor tissue. Investigators further showed a significant decrease in tumor volume and weight when core crosslinked particles were used compared to uncrosslinked core particles or free doxorubicin.

A disease target that has proven to be extremely difficult to target are circulating tumor cells (CTCs). Gao *et al.* reported a doxorubicin-loaded nanomissle constructed from a mesoporous silica nanoparticle displaying two nuclei acid aptamers to target the epithelial cell adhesion molecule (EpCAM) and CD44 on colorectal CTCs.[63] Mesoporous silica nanoparticles were chosen because of their easily adjusted porosity to tune drug loading and release, as well as facile surface modification to incorporate the aptamers for active targeting. The investigators demonstrated an 8-hour stability in blood and ability of the nanomissles to bind to CTCs in whole blood. *In vitro*, the developed nanomissle significantly downregulated SW620 (murine colorectal carcinoma cell line) adhesion to

human umbilical vein endothelial cells as well as their proliferation, suggesting a decreased ability to metastasize. Most impressively, it was then demonstrated in an *in vivo* model of colon carcinoma metastasis to the lungs that tumor metastasis was decreased from approximately 70 pulmonary sites when free doxorubicin was used compared to almost zero when the nanomissles were used.

A recent example of a multi-functional targeted drug delivery particle for photochemotherapy has been reported that utilizes both antibody targeting and near IR delivery enhancement.[51] Here, Lee and co-workers fabricated polyethyleneimine-coated double nano-emulsions that were loaded with doxorubicin and indocyanine green as a photosensitizer. The nano-emulsions displayed anti-HER2 antibodies on the surface to target HER2 positive breast cancer cells. The researchers demonstrated *in vitro* a significant decrease in viability of MDA-MB-453 cells from approximately 80% to less than 20% when samples were preoxygenated and exposed to near IR laser treatment, enhancing cellular uptake of doxorubicin *via* photothermal and photodynamic mechanisms.

Clearly, a vast array of nanoparticle-based targeted drug delivery strategies have been developed, particularly in the field of chemotherapeutic delivery. Methodologies to impart targeting or delivery can be chosen from the toolbox of thoroughly investigated mechanism and stimuli and then tailored to specific cells or diseased sites, but little has been done in developing new mechanisms for targeting and delivery. This is problematic for conditions requiring immediate targeting and release of the drug, as few systems have been developed that result in immediate drug release at a target site without the need of an applied external stimuli. In treating thrombosis or severe bleeds, a targeted drug delivery

mechanism that can be efficacious immediately after administration would be extremely appealing, as treatment time is critical for these conditions.

2.2 Targeted Drug Delivery for Clot-Augmenting Therapies

Hemostasis is a complex system that exists on a continuum between pathologic bleeding (hemorrhage) and clotting (thrombosis). It involves platelets, red blood cells, and several plasma proteins and zymogens that function as cofactors and enzymes once activated. Due to the integral and complex nature of both platelet function (Appendix A) within clot formation and the coagulation cascade (Appendix B), genetic mutations (affecting coagulation proteins or platelet function), severe injury, or cardiovascular disease can have devastating effects that can result in life-threatening bleeding or clotting disorders (Appendix C).

2.2.1 Hemostasis Overview

Platelets are anucleate cell fragments of megakaryocytes with a diameter of 3.5 μm that are involved in several biological processes, but are integral in the clot formation process.[64] During primary hemostasis, circulating platelets adhere to sites of vascular injury through newly exposed matrix proteins. This adhesion event activates the platelet, resulting in further recruitment of circulating platelets, aggregation, and formation of a platelet-plug to initially stem bleeding.

During the formation of the platelet-plug, the coagulation cascade occurs wherein plasma zymogens and proteins operate in positive or negative feedback loops to promote coagulation or anticoagulation to achieve and maintain hemostasis. The main result of the

coagulation cascade is production of the enzyme thrombin, which cleaves fibrinogen into fibrin, enabling its self-assembly and polymerization. The fibrin network enhances the structural integrity of the clot to further stem bleeding.

Late-stage platelet recruitment and activation occurs when circulating platelets adhere to this fibrin network. Once activated, platelets exert a contractile force on this network, resulting in substantial clot contraction. This increases the stiffness of the clot to further increase its structural integrity as well as brings the injured vascular walls closer together to facilitate healing at later stages. Platelet contraction has been studied both on the bulk scale within the context of whole blood and platelet rich plasma clots and on the single-cell level.[64] Initial studies focused on bulk scale investigations measured the tension within a contracting clot, demonstrating a maximum contractile tension generated at ~15 minutes after calcium-induced activation.[65] Contraction of a whole blood clot results in a loss of roughly 80% of serum from within the clot, which decreases the clot to about 1/3 of its original size.[66,67]

Interestingly, single-cell studies have elucidated that the extent of platelet activation and the generated contractile force is highly variable between platelets even from the same patient sample, and can be heavily influenced by the stiffness of the substrate as well as the concentration of soluble clotting factors (*i.e.* thrombin). Average contractile forces of individual platelets measured *via* atomic force microscopy was determined to be 20 nN; however, the magnitude ranged from 1.5 to 79 nN per platelet.[68] To further investigate this large distribution in platelet biomechanical behavior, Qiu *et al.* elucidated the mechanosensing ability of platelets, demonstrating that platelet adhesion, spreading, and subsequent activation increased with increasing stiffness of the fibrinogen-coated

substrate to which the platelets were adhered.[69] This large range in platelet contraction was again demonstrated using a platelet-contraction cytometer and further showed that platelet contraction reached a maximum when the platelets were adhered onto a substrate exhibiting a stiffness of 75 kPa and exposed to 5 U/mL of thrombin.[67]

2.2.2 Targeted Drug Delivery Strategies

While systemic administration of pro-coagulants (plasma products or clotting factors) or thrombolytics and fibrinolytics remains the clinical standard to abate uncontrolled bleeding or treat thrombosis, respectively, there exist several drawbacks to currently used therapies including the need of large donor pools, storage of both frozen and freshly thawed plasma products, immunomodulatory response, bloodbourne disease, restricted administration time frames, and thrombotic or hemorrhagic side effects.[12,13,16-18,70,71] Targeted drug delivery systems have become a major focus of research in recent years because they have demonstrated a potential to lower the risk of side effects and increase efficacy for intravenously administered small molecule or biologic therapies by overcoming poor drug solubility, off target interactions with healthy tissues, altering pharmacokinetic profiles, and enabling longer half-lives. [2-8] As such, there have been several advances in the literature developing synthetic technologies to regulate the clotting process, thereby removing the need of human-derived products and decreasing the possibility of adverse side effects. Interestingly, several of these nanoparticle constructs act as the therapeutic itself and do not contain a "traditional" drug.

Several synthetic platelet strategies have been developed to stem bleeding that utilize nanoparticles decorated with ligands specific to clotting proteins or activated

platelets, thereby mimicking platelet adhesion and aggregation.[72-77] Shoffstall *et al.* developed polymeric nanoparticles fabricated from block copolymers, PLGA-*b*-PLL-*b*-PEG, decorated with the peptide GRGDS, which binds to platelet GPIIb/IIIa in order to increase platelet aggregation after a blunt trauma.[75] The investigators used a murine liver trauma model to demonstrate an increase in 1 hour survival using a scrambled peptide control from 45% to 92% with their optimized construct. SynthoPlate™, a liposomal nanoparticle, has been iteratively developed to display three targeting peptides specific for vWF (that is noncompetitive with the platelet binding domain), collagen, and a fibrinogen mimetic that binds to GPIIb/IIIa.[72-74] These nanoparticles bind to injury sites and platelets to increase adhesion and aggregation, contributing to enhanced primary and secondary hemostasis. To better recapitulate the physical properties of platelets, Anselmo *et al.* developed a flexible, discoid-shaped nanoparticle from layer-by-layer deposition of poly(allylamine hydrochloride) and bovine serum albumin onto a removable polystyrene core, which displayed the same targeting ligands as SynthoPlate™.[78] Their technology resulted in a 65% reduction in bleeding time compared to the control using a murine tail transection model. Brown *et al.* decorated ultra-low crosslinked poly(*N*-isopropylacrylamide-*co*-acrylic acid) microgels[79] with variable domain-like recognition motif specific to fibrin, H6, to create platelet-like particles.[77] The investigators showed in a rat femoral vein injury model that injection of these particles decreased bleeding time to a regime similar to what is seen with fVIIa, proposing a therapy with similar efficacy but with the potential of a lower risk of thrombotic side effects.

While targeted therapeutics to abate bleeding has heavily relied on specific ligand interactions to effect targeting, delivery of fibrinolytics to treat thrombosis spans a much

larger scope in the targeting technologies that have been developed. Ultrasound has been used both by Tiukinhoy-Laing *et al.* and Kawata *et al.* to deliver tissue plasminogen activator (tPA) from liposomes and gelatin constructs, respectively.[53,54] Voros *et al.* developed a magnetically targetable nanoparticle by encapsulating an iron oxide nanocube core with deposited BSA and tPA.[80] Magnetics were used to direct the construct and resulted in increased dissolution and at a faster rate using *in vitro* models.

Absar and co-workers utilized the c-terminal gamma chain of fibrinogen to target "camouflaged" tPA and liposomal tPA to clots.[81,82] While liposomal tPA utilized diffusion for delivery, "camouflaged" tPA exploited a thrombin-cleavable linker that protected tPA during circulation, but enabled full exposure of the enzyme in sites undergoing clotting. While the camouflaged construct resulted in lower efficacy than free tPA *in vitro*, the liposomal tPA resulted in decreased clot weight compared to free tPA *in vivo.*

The enhanced shear rate present in stenotic vascular environments was utilized by Korin *et al.* to effect targeted delivery of tPA.[83] PLGA nanoparticles fabricated from spray drying aggregate into microparticles due to their hydrophobic properties; however, these aggregates break apart in environments of high shear, like those experience in thrombotic environments (100 dyne/cm^2). These were decorated with tPA using biotin-streptavidin and were demonstrated to greatly enhance *in vivo* survival using a murine pulmonary embolism model, wherein all control mice died within 1 hour but >80% of the experimental cohort survived.

As erythrocytes and platelets are major components of blood clots, these blood cell populations are advantageously poised for targeted delivery of hemostatic or thrombolytic

drugs. Indeed, several innovative technologies have been developed using erythrocytes or platelets to deliver clot-augmenting therapeutics *via* cell surface display. For example, Murciano *et al.* conjugated tPA onto erythrocytes and showed a significant enhancement in circulation time and bioactivity of tPA-erythrocyte conjugates upon reinjection in comparison to free tPA.[19] Building upon this system, Zaitsev *et al.* coupled a complement receptor type-1 antibody to tPA, which allowed the tPA mutant to bind to erythrocytes upon injection, similarly showing enhancements of bioactivity, circulation time, and clot lysis without the need to harvest and re-inject cells.[20] Chen *et al.* developed a staphylokinase (a thrombolytic) mutant containing a RGD motif that enabled platelet binding and resulted in a decrease in clot lysis time compared to free staphylokinase.[84] A cell-nanoparticle construct was reported on by Chen *et al.* wherein heparin-poly-L-lysine nanoparticles adhered to red blood cells through electrostatic interactions.[85] While they detached in environments of high shear rates, the investigators showed a higher level of anti-fXa activity, which lasted for 100 hours in vivo compared to 20 hours for free heparin. This is likely due to the ability of nanoparticles adhered onto the red blood cells to avoid clearance systems.

Absar *et al.* attached tPA to platelets through a RGD motif, which binds to GPIIb/IIIa.[86] The RGD motif in their construct was linked to tPA through a heparin cleavable linker, thereby facilitating release of tPA when the platelets were in a thrombotic environment. Investigators showed an increase in clot lytic activity and a decrease in clot weight compared to free tPA.

Clearly, previously reported technologies that augment clotting span an extensive scope in the targeting and delivery methods that have been employed, including: ligand

specific peptides for targeting and adhesion, enzyme cleavable linkers, magnetic targeting or ultrasound-mediated release, enhanced shear rates, red blood cells, and platelets. An interesting behavior within the clotting process that has yet to be capitalized upon, however, is platelet's ability to exert a substantial contractile force during clot formation that results in a remarkable extent of clot contraction. The development of this drug delivery mechanism is herein described, which leverages the patient's own platelets to target drug encapsulating microcapsules to sites undergoing active bleeding and deliver the drug through contraction on the microcapsule, resulting in rupture and drug release. Utilizing the natural behavior of the patient's own cells as the sensor and actuator of targeted drug delivery is an empowering, elegant, and paradigm-shifting mechanism within the field.

CHAPTER 3. FEASIBILITY OF A PLATELET-MEDIATED TARGETED DRUG DELIVERY MECHANISM

3.1 Introduction

In order to conduct initial investigations into the feasibility of a platelet-mediated drug delivery system, a model drug delivery particle was required that: (1) was an established particle in the field of drug delivery, (2) could display fibrinogen on the surface of the particle to enable platelet adhesion and clot targeting, and (3) could be easily fabricated from well-established methods. As such, emulsion particles were initially used as the model drug delivery vehicle as they are an established particle for pharmaceutical and cosmetic formulations, [87-91] can use fibrinogen as the oil/water interface stabilizer, and can be easily fabricated from a variety of methods. Furthermore, due to the tunability of droplet stability *via* surfactant combinations, emulsification method, and suspension properties, we believed this would provide access to a variety of particles exhibiting different mechanical properties to thoroughly investigate a contractile-force mediated delivery mechanism.

3.1.1 Emulsions

Emulsions are nano- or micron-sized liquid droplet particles suspended in an insoluble liquid phase. An emulsion is formed when sufficient energy is introduced into a system of two insoluble liquids and surfactant (and in some cases, an additional co-surfactant). Common surfactants and co-surfactants include: synthetic compounds (*i.e.* Span 20® or Tween 85®),[92] nanoparticles (*i.e.* microgels or carbon nanotubes),[93,94] and

proteins (*i.e.* bovine serum albumin (BSA) or β-lactoglobulin).[95] The imparted energy brings the interfacial tension between the two phases to a sufficiently low level, which is further stabilized by the surfactant, creating a fluid-like interface. While all emulsions are kinetically stable initially after formation, nano-sized emulsions are additionally thermodynamically stable under certain conditions.[96,97] This makes them attractive formulation technologies for various fields (*i.e.* food sciences, cosmetics, and pharmaceutical sciences). The simplest, and by far, most common emulsion form is an oil-in-water (o/w) emulsion; however, various other architectures such as water-in-oil emulsions and water-in-oil-in-water double emulsions[51,96] have been developed for various applications.

3.1.2 Emulsions in Drug Delivery Systems

Due to their ease of fabrication from FDA approved compounds and facile manufacturing scale-up, emulsions have been heavily utilized in the field of pharmaceutical science for drug formulations. Their chemical composition and size are easily tunable, making them applicable for a variety of administration profiles including transdermal, subcutaneous, oral, and parenteral.[87-90]

Of particular pertinence to clot augmenting biotherapeutics are parenteral formulation strategies, as they are currently delivered intravenously to decrease the time for onset of action and maintain bioactivity. Substantial research has been conducted on nano-emulsions for intravenous delivery of a variety of lipophilic drugs. Indeed, the degree of lipophilicity of the encapsulated drug has been shown to affect the rate of diffusion out of the nano-emulsion.[98] Various investigations have shown this lipophilicity-mediated

controlled diffusive release *via* nano-emulsion encapsulation improves the circulation times for a variety of chemotherapeutics.[99-102] Ganta *et al.* encapsulated chlorambucil in a soybean oil emulsion using egg phosphatidylcholine and cholesterol as the surfactant mixture.[99] Not only was there a significant improvement in pharmacokinetics compared to the free drug when injected intravenously into C57 BL/6 mice, the growth rate of colon-38 adenocarcinoma was significantly suppressed. Zhang *et al.* modified the hydrophobic properties of doxorubicin by forming an oleic acid ionic complex to enhance encapsulation from 30% (unmodified doxorubicin) to 93%.[102] Not only were pharmacokinetics in mice similarly improved compared to the free doxorubicin, the concentration of doxorubicin found in the heart, lungs, and kidneys were lower.

Several strategies have been employed to modify the chemical and physical properties of the droplet surface to further enhance circulation or rapidly target them to diseased sites in order to avoid clearance by the liver or phagocytosis. PEGylation is by far the most widely employed method to enhance circulation time due to its non-fouling properties, imparting the structure it coats with a "stealth"-like property.[103,104] Alayoubi *et al.* conducted an interesting investigation wherein nano-emulsions (loaded with vitamin E as an anticancer agent against mammary adenocarcinoma cells) were either coated with poloxamer or PEG.[105] Poloxamer coated nano-emulsions showed increased plasma protein adsorption and a circulation half-life of 1.7 hours. Nano-emulsions coated with PEG demonstrated a substantially longer half-life of 12.3 hours. The authors attribute this increase in circulation time to the brush-like architecture of PEG on the droplet surface that enhances the steric repulsion of plasma protein adsorption onto the surface, thereby decreasing cellular uptake. Nano-emulsion targeting has been achieved through inclusion

of peptide targeting moieties onto the surface. Most notably by including an RGD peptide sequence onto the surface to target emulsions to tumors.[106]

Due to the substantial list of benefits seen in parenteral emulsion delivery of drugs, it is not surprising that several drugs are commercially available that use nano-emulsion formulations, including: Cleviprex® (clevidipine), Diazemuls® (Diazepam), and Diprivan® (propofol). Due to their established use in the field, ease of manufacturing over various methodologies, and facile tunability, we believe emulsions to be a pragmatic particle with which to conduct initial investigations into the feasibility of platelet-mediated drug delivery. As platelet contractile force-induced particle rupture is the mechanism that results in drug delivery in our proposed paradigm, it was essential that the emulsions demonstrated a fine-tuned stability: stabile enough to remain intact during storage and circulation, yet still allow for contractile force mediated rupture. As such, significant investigation was required into the parameters that influence emulsion stability.

3.1.3 Parameters Influencing Stability of Protein-Stabilized Emulsions

Stability of the o/w interface, and therefore ease of disruption, is in part dependent on the surfactant used. While most emulsions are thermodynamically unstable, interfacial tension can be decreased when stabilizing proteins approach the interface from the bulk solution, adsorb, alter their conformational structure (depending on the interface), and then partition their hydrophilic and hydrophobic regions into the respective phases.[107-109] Protein spreading causes interfacial tension to decrease and interfacial pressure to increase until it reaches a plateau, which imparts stability into the system. Proteins that are extremely fluid on the interface (*i.e.* β-casein) will transmit an imposed stress across the

interface with a homogenous dissipation and be more resistant to rupture.[110] Alternatively, globular proteins (*i.e.* β-lactoglobulin) impose a solid-like structure on the interface. Stress on the interface will consequently dissipate heterogeneously, leading to a localized failure in the protein layer and subsequent fracture leading to release of payload.[110]

System destabilization occurs through coalescence (droplets combining to decrease particle concentration and increase particle diameter), flocculation (droplet aggregation), creaming or sedimentation (droplets rising or sinking), and ripening (transfer of internal phase to a larger droplet demonstrated with an increase in diameter heterogeneity and minimal change in particle concentration) to ultimately achieve the energetically favored phase separation (Figure 3).[109]

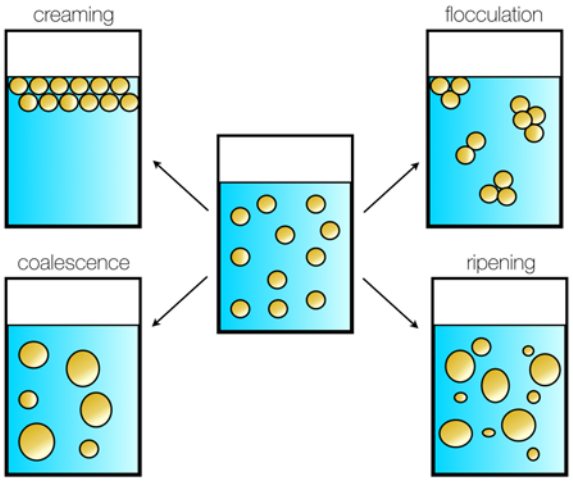

Figure 3. Destabilization pathways commonly taken by emulsion droplets before inevitable phase separation.

Because bioactive fibrinogen must be used as the surfactant to enable platelet adherence and clot targeting, this system is somewhat restricted in regards to surfactant choice, pH, and salt concentration. However, emulsion stability can be further adjusted through choice of emulsification method. A variety of methods exist to fabricate emulsions

with varying energetic input into the system from simple shaking to ultrasonication, membrane extrusion, high pressure homogenization, and microfluidic techniques. [95,111-115]

Formation of emulsions is most commonly achieved through vigorously shaking two insoluble phases, as often seen in food sciences (*i.e.* salad dressings). Due to the relatively low input of energy, droplet sizes are heterogeneous, macroscopic, and energetically unstable leading to phase separation within minutes or hours. For systems requiring greater stability and homogeneity, ultrasonication,[116] membrane extrusion,[117] and high pressure homogenization[118] are most commonly employed as they are easily scaled up for commercial manufacturing purposes. Particle sizes can reach the nanometer length scale, imparting substantial stability to the system. Microfluidic techniques include a variety of system designs including either polydimethyl siloxane (PDMS) and glass capillary based methods. Because the flow rates and channel geometries are precisely controlled for each emulsion droplet fabricated, these systems produce extremely homogenous particles in the micro- or nano- (if a commercial microfluidizer is used) size range.[114] While commercial microfluidizers can produce large quantities of emulsion particles at once, laboratory-scaled single-channel microfluidics that utilize single-droplet generation do not lend themselves to commercial scale up as they are resource and time intensive.[114]

In this chapter, fibrinogen stabilized emulsions were prepared via homogenization or capillary-based microfluidic fabrication methods in order to compare size and stability of the resultant particles during storage. A microfluidic device was then optimized in order to investigate platelet adhesion onto the emulsion surface and the effect of platelet-contractile force on the prepared fibrinogen stabilized emulsion droplets. Platelet-mediated droplet

rupture was qualitatively defined as significant morphological disruption and/or significant distortion of the interfacial surface layer of fibrinogen.

3.2 Experimental Approach

3.2.1 Materials

Dodecane, sudan black, and BSA were purchased from Sigma-Aldrich (St. Louis, MO). PBS, collagen type 1, CellMask Deep Red, CellMask Orange, fibrinogen-Alexa Fluor 488 conjugate, heparinated blood collection tubes, and 10% ACD blood collection tubes were purchased from Fisher Scientific (Pittsburgh, PA). PDMS (Sylgard 184) was purchased from Ellsworth Adhesive Systems (Germantown, WI).

3.2.2 Methods for Fibrinogen Emulsion Fabrication

Initial investigations using the following microfluidic emulsification method used BSA as a model protein instead of fibrinogen to optimize flow rates, as this was more cost-effective. Once conditions were optimized, a 1:1 mixture of fibrinogen and dextran was used in order to conserve fibrinogen. However, all dispersions contained 2 mg/mL surfactant in 10 mM PBS (ionic strength = 150 mM) as the continuous phase and dodecane dyed with sudan black as the oil phase. Images for confocal microscopy also contained 38 ng/mL fibrinogen-Alexa Fluor 488 conjugate and were polymerized with 0.8 U/mL of thrombin.

3.2.2.1 Capillary Microfluidic Fabrication

Emulsions fabricated with glass capillary-based microfluidic devices have been shown to produce extremely homogenous dispersions, as each emulsion is fabricated individually. Three different capillary devices were investigated (Figure 4). To construct the capillary devices, first two glass slides were conjoined by epoxying over two small pieces of glass. A square glass capillary with inner diameter of 1.0 mm is then secured on top of the glass slides with epoxy. A round glass capillary with outer diameter of 1.0 mm and inner diameter of 0.58 mm was pulled using a Sutter Instruments pipette puller to form two capillaries. The end of the pulled capillary was cut and placed inside the square capillary (on the left) for a simple capillary device (Figure 4A). For a capillary co-flow device (Figure 4B), an additional round capillary was placed inside the square capillary (on the right) so the ends of each capillary slightly overlap. For a capillary co-flow flow-focusing device (Figure 4C), the second capillary from the pulled capillary was cut so the

tip is larger than the first capillary and was placed inside the square capillary (on the right) where the tips are ~20-30 μm away from each other.

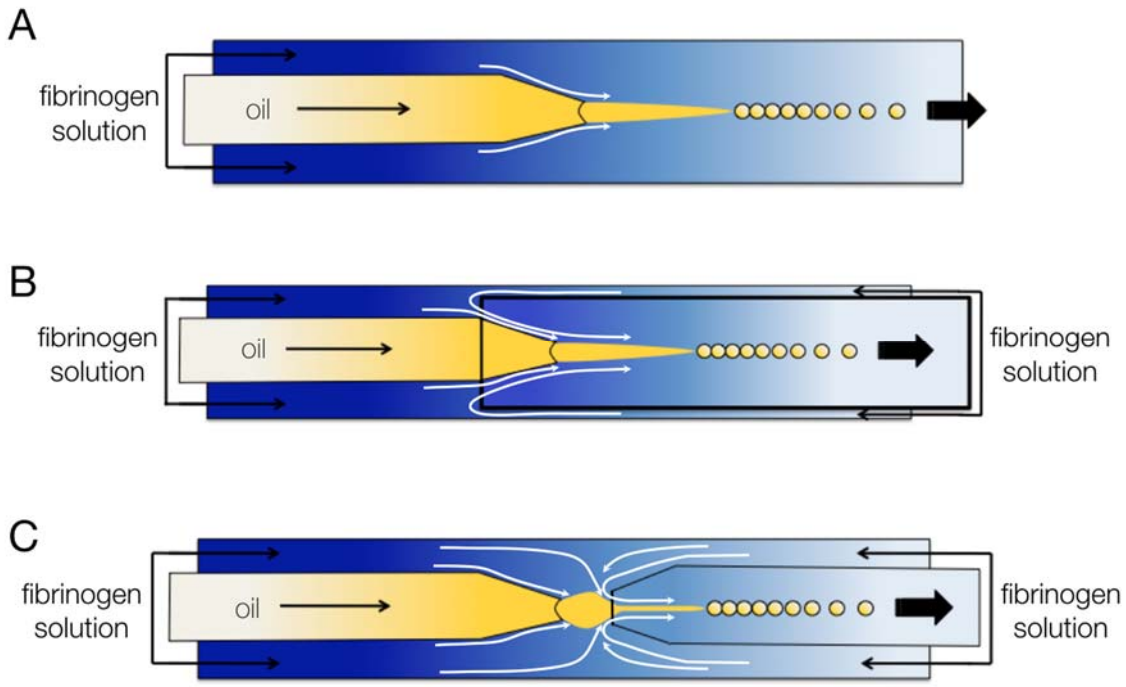

Figure 4. Representation of phase interactions in (A) capillary, (B) capillary co-flow, and (C) capillary co-flow flow-focusing microfluidic devices.

After all capillaries were in appropriate positions, they were glued to the glass with epoxy. Next, plastic short syringe tips were adjusted to fit over the capillaries at 3 to 4 positions (Figure 5): 1) over the left round capillary, 2) over the left round-square capillary junction, 3) over the square-right round capillary junction (for co-flow and co-flow flow-focusing), and 4) over the right round (exit) capillary. The syringe tips were fixed with epoxy, and the device was left to set overnight.

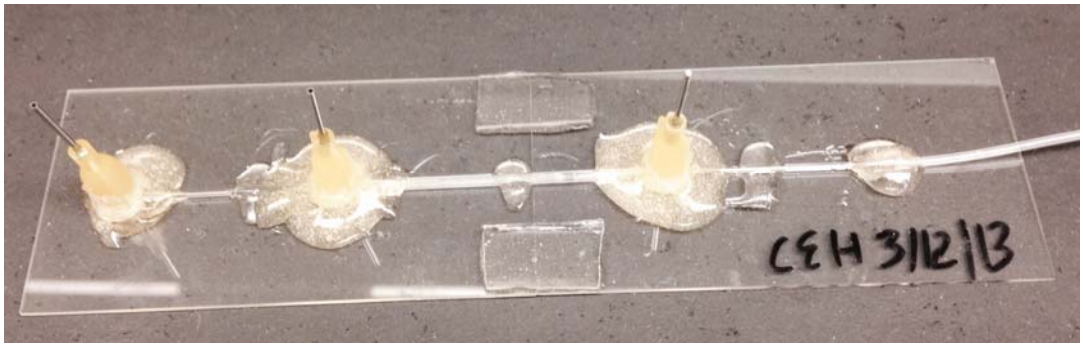

Figure 5. Image of a glass capillary-based co-flow microfluidic for emulsion fabrication.

Tubing was fitted to the device via syringe tips. The tubing was then attached to syringes loaded with each phase solution. The oil phase entered the device through the left round capillary from a 10 mL syringe. The continuous solution entered through the capillary junctions (30 mL syringe for the left and 5 mL syringe for the right), and the emulsions left through the right capillary, which goes to a collection vial. The syringes were placed in syringe pumps.

For the capillary microfluidic device, the left capillary tip diameter ~40 μm and flow rates for the continuous phase were 90 mL/hr and 6 mL/hr for the oil phase. For the co-flow device, capillary diameter was around ~40 μm, and flow rates for the left continuous phase was 10 mL/min, right continuous phase was 5 mL/hr, and oil was 5 mL/hr. For the co-flow flow-focusing device, the capillary diameters were ~40 and ~60 μm for the left and right tips, respectively. Flow rates were maintained at 8 mL/hr for the left continuous phase, 100 μL/hr for the right continuous phase, and 800 μL/hr for the oil.

3.2.2.2 Homogenization

For emulsions prepared via homogenization, both continuous and oil phases (10:3 continuous phase to oil volume ratio) were loaded into a culture tube. The sample was homogenized with an Omni International Tissue Master 50 at 15,000 rpm for 30 sec.

3.2.3 Washed Platelet Collection

Human blood was drawn according to IRB-approved protocols per the Declaration of Helsinki into 20% ACD. To isolate washed platelets, platelet-rich plasma (PRP) was first extracted from whole blood *via* centrifugation. Additional ACD was added to the PRP to make a 10% ACD solution before spinning down again to separate platelet-poor plasma (PPP) and platelets. The PPP was removed and platelets were resuspended to the desired concentration in Tyrode's buffer and stained with cell membrane stain (CellMask Deep Red).

3.2.4 Development of Microfluidic Assays

Microfluidic molds were fabricated *via* standard soft lithography techniques.[119] PDMS was poured into the mold and placed in a 60 °C oven overnight. The microfluidic was then cut out, entry and exit hole were punched into the channels, and then plasma bonded to a clean glass slide. Experiments using Y-channel and straight channel microfluidic devices were used without modification before the experiment. Significant modification of the device was required for the "Micro Thrombi" microfluidic experiments. First, the microfluidic walls are coated with 1 mg/mL collagen type 1 and washed with Tyrode's buffer. Heparinated whole blood with platelets stained with membrane stain (CellMask Orange) was perfused through to form platelet aggregates on the bottom and walls. The channel was then washed again with Tyrode's buffer, and

fibrinogen emulsions were then perfused through and device flipped 180°, which allowed the emulsion particles to adhere to the platelet aggregates. The channel was washed once more, and a round of concentrated platelets stained with a different membrane stain (CellMask Deep Red) suspended in Tyrode's buffer were perfused through with calcium (10 mM), magnesium (2 mM), and ADP. Experiments were monitored with confocal microscopy.

3.3 Results and Discussion

3.3.1 Investigation of Emulsion Fabrication Method

An emulsification method that produced a stable dispersion was investigated to fabricate fibrinogen emulsions. The emulsification methods investigated included homogenization and various glass-based capillary microfluidic devices. BSA was used as a model protein for these experiments as to not waste fibrinogen. The basic capillary microfluidic device (Figure 6A) is the simplest device to construct; however, extremely high flow rates are required consuming an enormous amount of material to produce emulsion droplets that are ~100 μm in diameter. This method was deemed unsuitable because of the amount of material required, and because the produced emulsions were too large and dilute.

A co-flow capillary device (Figure 6B) was next employed. The resulting emulsions were only slightly smaller, and flow rates remained too high to make the device feasible for fibrinogen-based emulsions. Finally, a co-flow flow-focusing device (Figure 6C) was used, which significantly reduced the required flow rates and droplet diameter (~50-80 μm in diameter). Because of the large volume of solution still required, 1:1

solutions of fibrinogen and dextran were used as a co-surfactant when fibrinogen emulsions were made in order to reduce the consumption of fibrinogen.

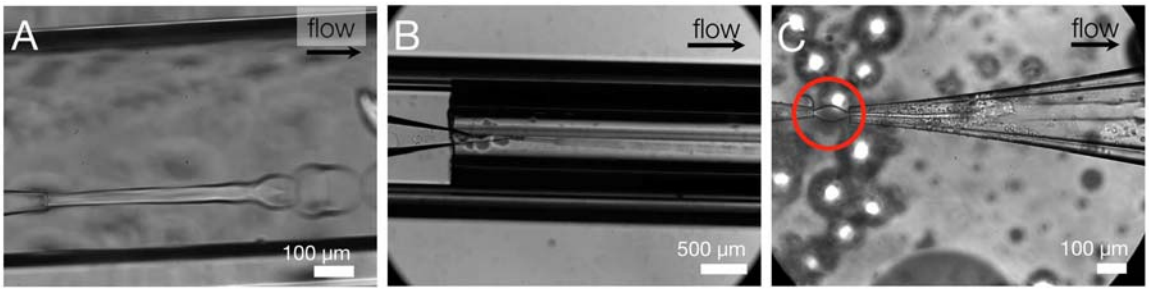

Figure 6. Brightfield micrographs of glass capillary-based fabrication of microemulsions. Images show (A) a standard glass capillary design, (B) a co-flow capillary design, and (C) a co-flow flow-focusing capillary design with the oil phase jet cone indicated with the red circle.

Stability studies were conducted comparing emulsions prepared with co-flow flow-focusing microfluidics and a tissue homogenizer (Figure 7). While microfluidic preparation gives a homogenous dispersion of large emulsions, homogenization gives a heterogeneous population but particles in the desired size range of ~10-50 µm in diameter. Samples from each method were left in the refrigerator at 4 °C for 6 days and compared again to determine if significant destabilization events occured. Clearly, both samples underwent coalescence. It also appears that some protein aggregation occurred in the homogenized sample, possibly due to the high-energy input from emulsification.

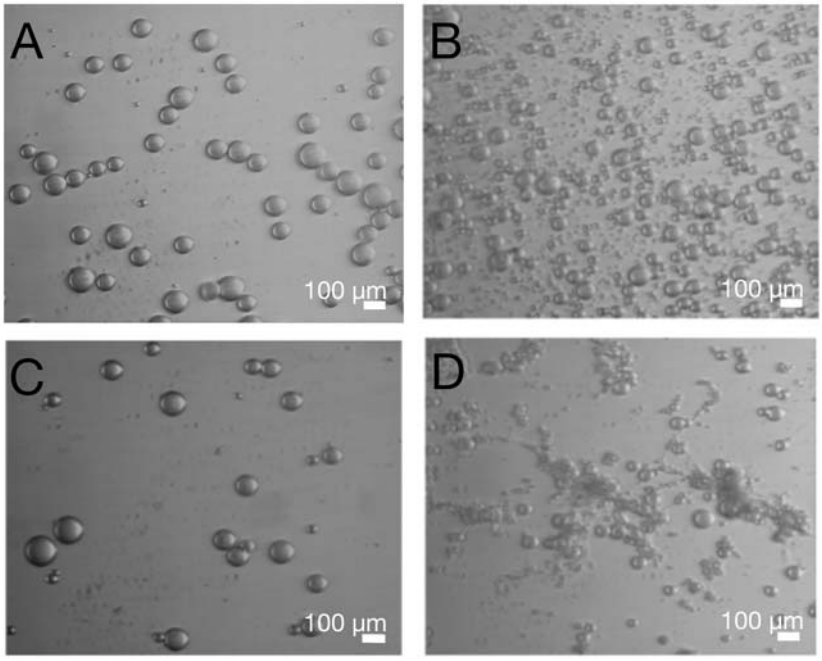

Figure 7. Emulsions fabricated from glass capillary microfluidics are more stable over time, but emulsions made from homogenization enable access to smaller sized droplets. Brightfield micrographs at 10x magnification show emulsions made of fibrinogen-dextran (1:1) stabilized solutions prepared with (a and c) co-flow flow-focusing microfluidics and (b and d) homogenization. Images taken (a and b) immediately after preparation and (c and d) after 6 days at 4 °C.

Due to desired particle size, material restraints, and logistical considerations, homogenization was chosen as the emulsification method for experiments involving platelet contraction. Emulsification and surface adsorption was not seen to affect protein structure in such a way as to interfere with thrombin cleavage and fibrin formation. Confocal images taken after thrombin addition clearly show fibrin fibers growing off the interface and incorporating emulsions (**Figure 6**).

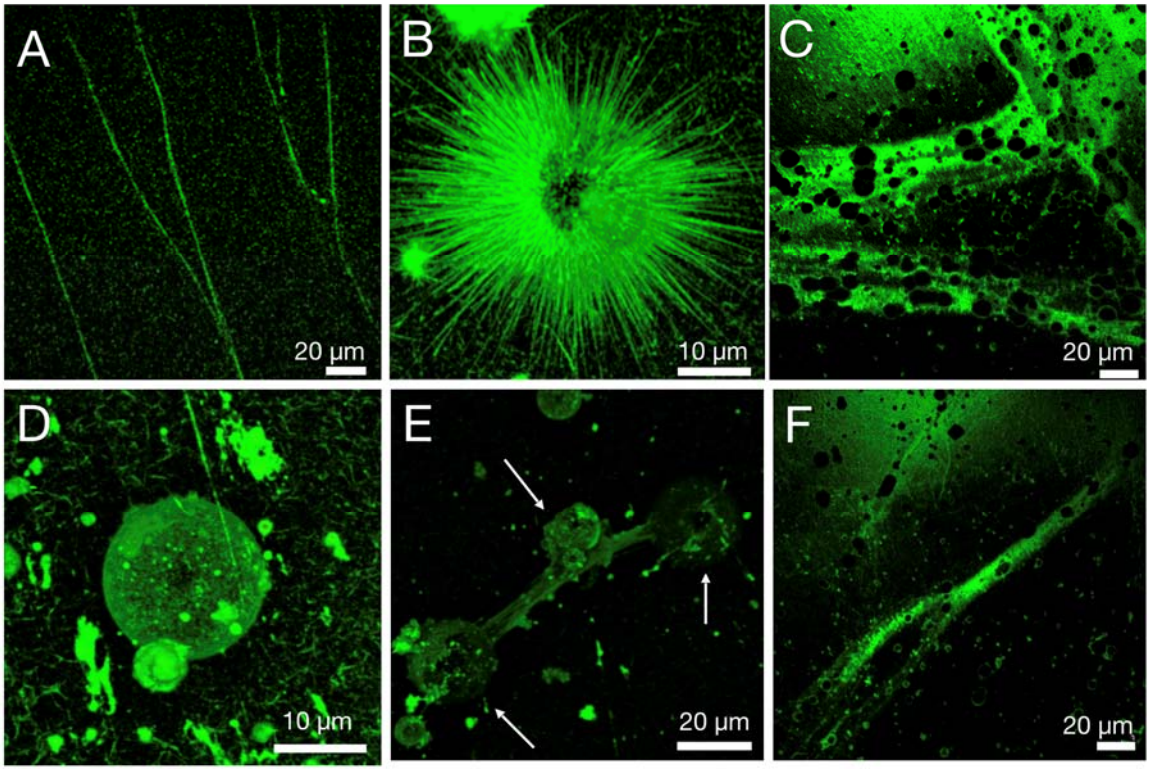

Figure 8. Interfacial fibrinogen enables droplet integration into fibrin networks. Confocal micrographs of (a) fibrin fibers, (b) a fibrinogen emulsion (no thrombin), (c and d) fibrin coated emulsions (thrombin added), and (e and f) emulsion encapsulated in fibrin fibers. Fibrin (green) labeled with fibrinogen-Alexa Fluor 488 conjugate.

3.3.2 Development of an Assay to Investigate the Effects of Platelet Contractile Force on Emulsion Particles

Several experimental designs were considered and attempted in order to achieve platelet adhesion to emulsion particles, platelet contraction, and visualization of emulsion disruption. Static macroscopic experiments were first attempted wherein platelets and fibrinogen emulsions were exposed to thrombin in a vial. It was hypothesized that the oil phase would leave the forming clot and rise to the top, indicating platelet-induced emulsion rupture had occurred. However, this was never observed possibly because the oil droplet would potentially get trapped in the forming clot and not separate out into a distinct phase.

Static microscopic experiments were then conducted wherein emulsions and platelets were subjected to thrombin in a cover well and observed with confocal microscopy. Several problems were uncovered at this stage: platelets were not always adhered to emulsions, contraction of the model clot did not always occur, and a significant density issue was realized where emulsions, being less dense than water, persisted at the top of the system and platelets, being denser, sank to the bottom. It is believed that the difference in densities was likely a factor in why platelets were not adhering to the emulsions in this experimental setup.

To create a more physiologic environment, microfluidics where then used to monitor platelet adhesion and contraction at the emulsion surface under flow. A Y-shaped microfluidic was first utilized in which washed platelets, fibrinogen (2 mg/mL), calcium (10 mM), magnesium (2 mM), and fibrinogen stabilized emulsions were perfused through the top channel, and thrombin (1 U/mL) was perfused through the bottom channel. While contraction of the clot formed at the Y-channel juncture can be seen, the channels were not wide enough to allow emulsions to flow through and the device clogged rapidly due to the fast fibrin formation and platelet aggregation (Figure 9A).

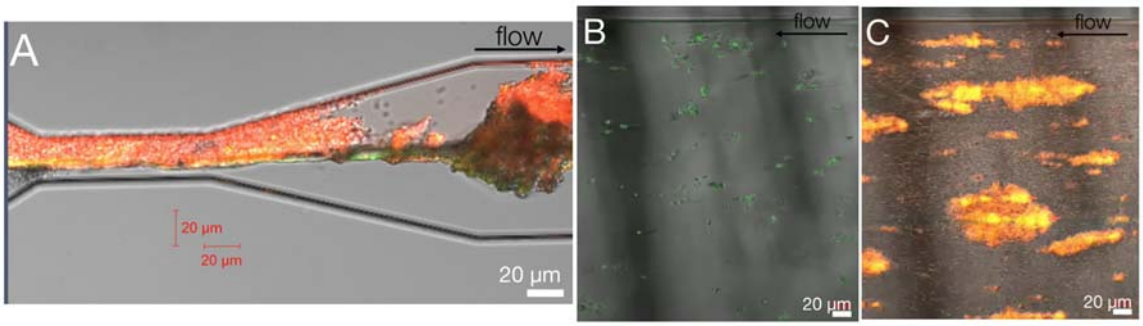

Figure 9. Confocal micrographs of microfluidic experiments investigating platelet adhesion and contraction on fibrinogen stabilized emulsions. A Y-channel device (A) was used in the presence of thrombin as well as a straight channel device in the presence of ADP. The immobilized emulsion droplets can be seen before perfusion of washed platelets (B) and after platelet aggregation onto the emulsion droplets (C). Fibrinogen can be seen in green (Alexa Fluor 488) and platelets can be seen in orange (membrane stain).

In order to address these issues, a microfluidic straight channel device was used with channels of 200 μm in diameter to ensure particle passage. Additionally, fibrinogen emulsions were perfused through before any activators or platelets, flipped over, and incubated on the glass. Before the experiment began, the device was flipped back over so the emulsions were adhered onto the glass slide on the bottom of the device (Figure 9B). ADP was perfused with washed platelets instead of thrombin in order to avoid device clogging.

Substantial platelet aggregation was seen on the immobilized emulsion droplets, creating tail-like aggregates throughout perfusion (Figure 9C). Platelet contraction of these aggregates was seen towards the end of the experiment; however, distinct emulsion disruption was still an elusive event. It was hypothesized that the experimental design was too reductionist in nature. The clotting environment is extremely dynamic wherein entrapped platelets are contracting in different times frames and to different extents due to the heterogeneity of substrate stiffness within a clot, concentration of soluble clotting activators, and time of adhesion and activation. The straight channel experimental design only enables platelet contractile force to be exerted in one direction relative to the emulsion particle. To utilize a design more aligned with physiologic conditions, a “micro thrombi” design was developed and implemented. This design allows for the emulsion particles to

adhere to a more physiologic substrate and for contraction to be exerted in two directions. These experiments used calcium and either thrombin or ADP as the platelet agonist.

In development of the "micro thrombi" assay, confirmation that micro thrombi could form *via* perfusion of heparinated whole blood through a collagen coated microfluidic channel as well as the ability of emulsion particles to adhere to immobilized micro thrombi was necessary. It is clear from qualitative analysis of the microfluidic device before perfusion of the second round of platelets that micro thrombi do form and fibrinogen stabilized emulsions do adhere to them (Figure 10).

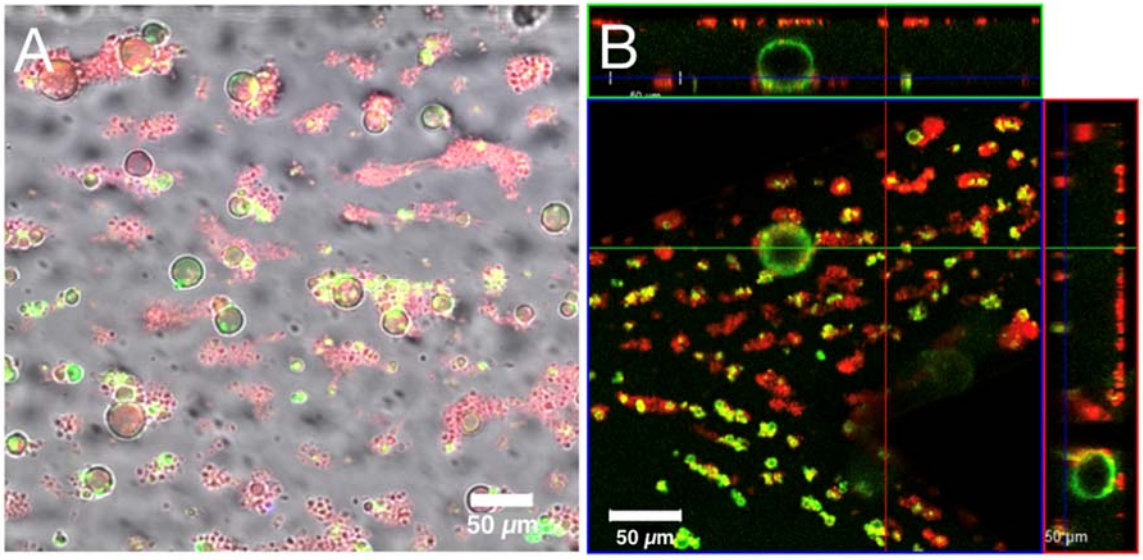

Figure 10. Confocal micrographs of "micro thrombi" assay device after fibrinogen (Alexa Fluor 488, green) emulsions were incubated onto the micro thrombi (platelets, cell membrane stain, red) demonstrate that droplets adhere to the platelet aggregates. (A) A micrograph showing the cross-section of only green and red channels are demonstrate emulsions adhere onto the micro thrombi in the Z direction. Micrograph of all channels merged (B) show numerous micro thrombi with adhered emulsions.

3.3.3 Platelet Contractile Force-Mediated Emulsion Disruption

After micro thrombi formation and targeted emulsion adherence was confirmed, the second round of washed platelets were perfused through the device along with platelet activators. Platelets clearly adhere to the fibrinogen coated surface, form large aggregates, and contraction can be seen throughout the aggregate (Figure 11). This contraction induces significant morphological disruption of the emulsion particle, changing its shape from circular to ovicular. Furthermore, the fibrinogen on the particle surface is ruptured resulting in a bare interfacial surface for half of the emulsion particle. These qualitative changes in the emulsion demonstrate that the contractile force of adhere platelets is substantial enough to invoke significant particle disruption.

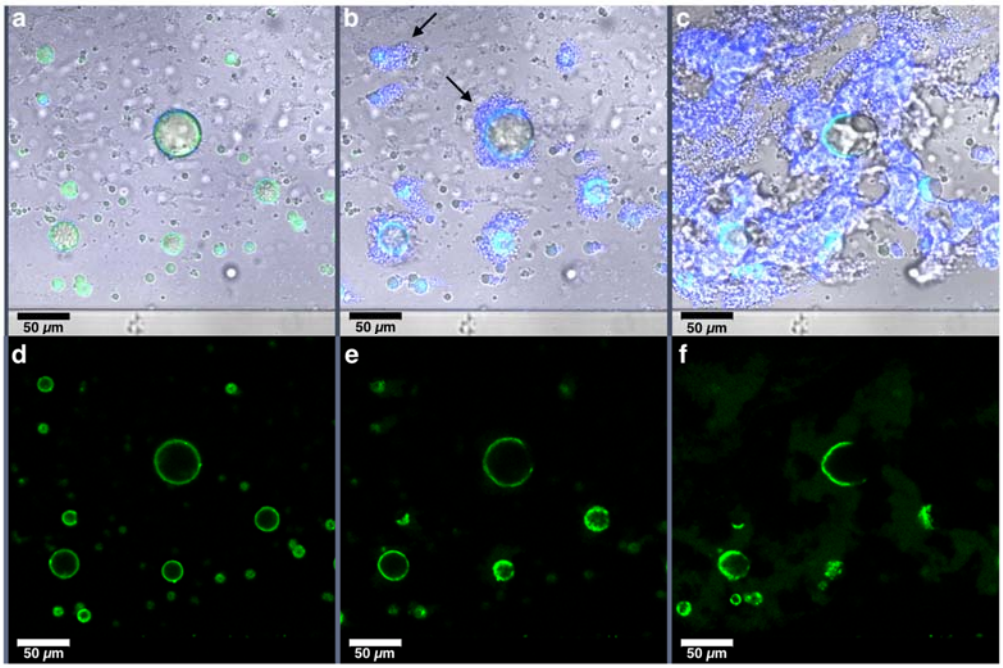

Figure 11. Perfusing platelets adhere to emulsion droplets, rupture the fibrinogen stabilizing layer, and deform droplet morphology. Progression of platelet aggregation (membrane stain, blue) on fibrinogen (Alexa Fluor 488, green) emulsions at (a and d) 0 minutes, (b and e) 10 minutes, and (c and f) 18 minutes using ADP as the platelet activator. Micrographs (a – c) show all channels merged and (d – f) show green channel only. Arrows indicate forming platelet aggregates.

This behavior was again seen in experiments using thrombin as the platelet activator (Figure 12). There is clear and significant destruction of the fibrinogen interfacial surface of the emulsion along with deformation of the emulsion droplet. As before, the contractile force of the platelet aggregated "pushed" the oil droplet away from the aggregate, but it does not get "released" from the fibrinogen/platelet aggregate.

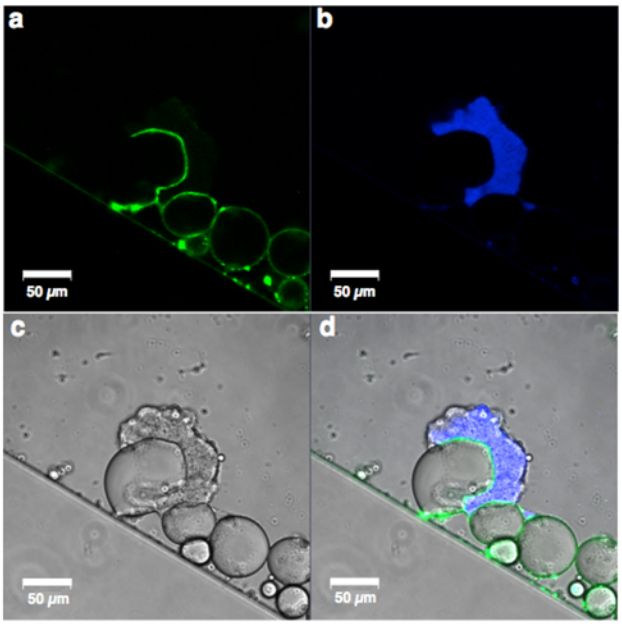

Figure 12. Only droplets with adhered platelets exhibit altered distribution of fibrinogen coating and morphological changes. Confocal micrographs of platelet (membrane stain, blue) induced fibrinogen (Alexa Fluor 488, green) emulsion droplet disruption using thrombin as the platelet activator. Micrographs show the split (a) green channel, (b) blue channel, (c) brightfield, and (d) all channel merged.

Upon further qualitative analysis, a difference in aggregation profiles can be seen depending on emulsion size; platelets aggregate behind small emulsions forming "tails" but in front of large emulsions forming "wings". This behavior is likely due to a larger dead zone in fluid flow in front of larger emulsions, allowing platelets to travel on the outskirts of the dead region and aggregate in the front (Figure 13). Presumably, smaller emulsions

would create smaller dead zones closer to the size scale of individual platelets, allowing them to pass over the emulsion. As they traverse the emulsion, the higher fluid velocity prevents them from adhering to the fibrinogen on the top, so they continue to slide along the surface until they are behind the emulsion where they can aggregate. A tail forms with continued aggregation as the platelets travel from emulsion surface to the back of the platelet aggregate.

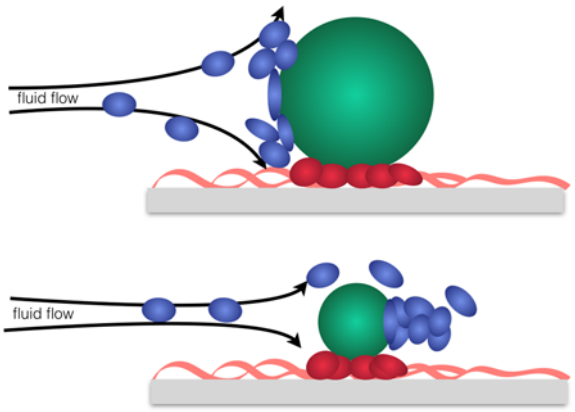

Figure 13. Illustration demonstrating the effects of emulsion size on fluid flow and platelet aggregation profile. Top – large dead zone allows platelets (blue) to adhere in front of the ~50 µm emulsion (green) and aggregate in a wing-like pattern. Bottom – smaller dead zone forces platelets to traverse over the ~10 µm emulsion and aggregate in the dead zone behind the emulsion in a tail-like pattern. Red platelets represent micro-thrombi adhered on a collagen layer (orange).

3.4 Conclusions

Fibrinogen stabilized emulsions can easily be fabricated via homogenization or capillary microfluidics without significant loss of bioactivity. While capillary microfluidics yields homogeneously sized emulsions, homogenization yields emulsions within a feasible size range for drug delivery. Fibrinogen stabilized emulsions fabricated *via*

homogenization were thus used to investigate the feasibility of platelet contractile force-mediated rupture as a drug delivery paradigm.

Several assay designs were developed to investigate this behavior on a qualitative level. Static co-incubation, Y-channel microfluidics, and straight channel microfluidics all exhibited deficiencies including density-mediated separation of platelets and emulsions and microchannel clogging. However, the "micro thrombi" assay was effective in demonstrating platelet adhesion and aggregation onto the emulsion surface, platelet aggregate contraction, and significant particle disruption in regards to the particle morphology and fibrinogen surface coverage. Because of the hydrophobic nature of emulsions, it is not possible to visualize a "release" of the interior phase because it is not soluble in the continuous phase (buffer).

From observations of experiments conducted with the "micro thrombi" assay, it can be concluded that: (1) platelets adhere to microparticles that display fibrinogen on their surface, and (2) that platelet contractile force is sufficient enough to rupture a microparticle surface. Thus, a platelet-mediated drug delivery paradigm that leverages the contractile force of activated platelets is feasible.

While emulsions were effective model particles to investigate the feasibility of this system, they do not lend themselves well to delivery of clot augmenting biotherapeutics. The majority of target drugs for clot augmenting applications are recombinant or plasma-derived proteins that are not soluble in oil phases. As such, the subsequent chapters investigate the development of a suitable drug carry nanoparticle for the application of this drug delivery paradigm for clot augmentation.

CHAPTER 4. MODIFICATION OF POLYELECTROLYTE MULTILAYER CAPSULES TO ENABLE PLATELET-MEDIATED RUPTURE

Results described in this chapter regarding development and characterization of the optimized PEM capsule have been reported in *ACS Nano*.[1]

4.1 Polyelectrolyte Multilayer Capsules

The layer-by-layer (LbL) deposition method was first reported by Iler *et al.* in 1966 for the fabrication of ultra-thin films using colloidal particles of opposite charge that were deposited onto glass in an alternating fashion and held together through electrostatic interactions.[120] Decher *et al.* expanded on the LbL assembly method using oppositely charged polyelectrolytes to fabricate polymer-based ultra-thin films.[121] Cationic polyelectrolytes that have been used in LbL assembly of ultra-thin films include poly(allylamine), poly(diallyldimethylammonium) (PDADMAC), and poly-L-lysine (PLL). Anionic polyelectrolytes that have been used include poly(styrene sulfonate), dextran sulfate, and poly-L-glutamic acid (PLG).

While initial investigations in the field focused on assembly onto planar substrates, polyelectrolyte LbL assembly has also been developed using colloidal particles as the substrate.[122-124] If a sacrificial colloidal substrate is used, it can be removed after the desired number of layers have been deposited such that the sacrificial colloidal substrate was used to template the assembly of a hollow PEM capsule typically in the size range of 1-10 μm in diameter. Such sacrificial cores can be organic or inorganic in composition and include

melamine formaldehyde, polystyrene, calcium carbonate, or mesoporous silica.[125-127] The cores can be dissolved by suspending the particles in an acidic solution, organic solvent, or solution containing a chelating agent (*i.e.* ethylenediaminetetraacetic acid (EDTA)).

A substantial advantage in utilizing the LbL assembly technique is the facile manner in which particle properties can be tuned. Polymer shell thickness can be most easily tuned by modulating the number of polyelectrolyte layers deposited and the solution conditions during the deposition step (*i.e.* salt concentration and pH).[128] Shell thickness not only affects the mechanical robustness of the particle (fewer layers yields a softer capsule), but also the diffusive release profile of a chemical species loaded within the capsule interior.[27,129,130] Changing the chemical composition of the polyelectrolytes used is another facile manner in which application specific modifications can be incorporated. For example, biocompatible polyelectrolytes can be used if the particle is being developed for biological applications (PDADMAC *versus* poly-L-arginine). Several commonly used polyelectrolytes can be covalently modified to include moieties (small molecules or peptide sequences) to target the PEM capsule to specific biological sites, functional groups to enable cross-linking between the polymer layers, and enhance drug retention.[131-133] Nanoparticles and proteins can also be non-covalently included within appropriate polyelectrolyte layers through their surface charge to effect particle targeting or additional behaviors.[52,134,135] Because of the facile and vast manners in which to tune PEM capsules for a specific application, these particles have been heavily investigated for applications as imaging agents,[136,137] sensing materials,[138] microreactors,[139] and of particular importance to this work, drug delivery.[140-142]

4.1.1 PEM Capsules for Drug Delivery

PEM capsules for the delivery of small molecules and proteins have been developed by loading the therapeutic into the interior of the capsule.[55,143-146] This can be accomplished through co-precipitation in the sacrificial templating core if calcium carbonate is used or *via* diffusion through the PEM capsule wall after fabrication and core removal.[26,147,148] Efficiency of encapsulation for the diffusion-based method is highly dependent on pH and salt concentration of the loading solution, as it has been shown that the permeability of the PEM capsule wall can be heavily influenced through protonation state, salt screening, and the charge of the loading molecule.[149]

As mentioned above, these particles have held particular interest for targeted drug delivery. Several strategies have been employed that require decoration of the surface with a targeting moiety (*i.e.* antibody, peptide, or magnetic nanoparticles). An antibody targeting mechanism was employed by Deo *et al.* by functionalizing the surface of poly-L-arginine and dextran sulfate microcapsules with Protein G *via* Biotin/Streptavidin.[150] Anti-collagen type IV or anti-fibronectin antibodies then readily adhered to the Protein G microcapsule surface, enabling antibody-specific targeting of collagen type IV or fibronectin coated substrates, respectively.

The well-established RGD peptide sequence was implemented for targeting of DQ-ovalbumin (model therapeutic cargo) encapsulated microcapsules by Costa *et al.*[151] Polyelectrolyte microcapsules fabricated from chitosan and elastin-like recombinamers that displayed either RGD or a scrambled RGD sequence (control) were co-incubated with human mesenchymal stem cells for 3 days. The investigators showed that, while cellular uptake for both microcapsules types were not significantly different, microcapsules displaying RGD resulted in higher intracellular bioavailability of DQ-ovalbumin.

Pavlov *et al.* included magnetite nanoparticles into the polyelectrolyte layer of microcapsules fabricated from LbL assembly of poly-L-arginine and dextran sulfate to enhance cell targeting for drug delivery in the presence of a magnetic field.[135] The authors investigated the intracellular delivery of luciferase enzyme and plasmid DNA into human embryonic kidney epithelial cell line 293T cells and showed 25 fold increase in enzyme activity and 3.4 fold increase in transfection compared to microcapsules without magnetite nanoparticles.

Once at the target site, a variety of mechanisms have been developed for release of the encapsulated therapeutic. These include application of ultrasound, redox responsivity, and enzymatic biodegradation to deliver the drugs more quickly than a diffusion-based mechanism would allow. Gao *et al.* embedded fluorescence carbon dots into the PEM wall of a poly(allylamine) and poly(styrene sulfonate) microcapsule *via* a hydrothermal reaction.[134] After application of ultrasound for 5 minutes, the authors demonstrated a 80% release of the fluorescent carbon dots from the PEM microcapsule.

To leverage the intracellular redox environment of cancer cells, a poly-L-arginine and dextran sulfate based microcapsule utilized a glutathione responsive disulfide crosslinker to conjugate doxorubicin directly to the poly-L-arginine in the PEM wall.[152] The investigators showed a higher therapeutic effect than free doxorubicin in HeLa cells due to sustained and site specific doxorubicin release.

In a later work, Timin *et al.* reported a triple responsive (UV, ultrasound, and enzyme sensitive) microcapsule for enhanced retention of encapsulated small molecule therapeutics in non-target areas.[55] These microcapsules were fabricated from poly-L-

arginine and dextran sulfate and employs a sol-gel approach to impart a SiO_2/TiO_2 coating on the microcapsule, which enhances small molecule retention and imparts UV light and ultrasound sensitivity. Release of encapsulated rhodamine B as a model small molecule was systematically investigated for each stimulus and compared to release without the stimulus. The investigators demonstrated a 60% increase in release for UV irradiated samples after 80 minutes, 80% increase in release after 180 seconds of sonication, and 30% increase in release after 27 hours of enzyme exposure.

Clearly, there is a large volume of work developing and tuning these constructs for drug delivery applications. While PEM microcapsules are easily optimized for a specific disease application, the targeting and delivery strategies that have been utilized, while well-established and well-characterized, are not novel in the field of drug delivery. In many cases, they are somewhat cumbersome as they require additional equipment or substantial time frames for delivery of the full dose. An increasing amount of research is being conducted on the integral role of the cellular biomechanical behavior in various diseases.[153,154] Leveraging the biomechanical behavior of cells presents as an elegant delivery method, wherein immediate delivery of a drug can be achieved at a target site without the need of external equipment.

4.1.2 Influence of Cellular Mechanics on PEM Capsules

A subset of research within the field investigating PEM microcapsules for drug delivery applications has focused on characterizing the deformability of these particles when subjected to an applied force.[27,130,155-158] Of particular importance to drug delivery, these studies have elucidated the forces necessary to result in release of an encapsulated

model therapeutic cargo for different microcapsule architectures.[158] Recently, these studies have been conducted to characterize the particle's response to applied force in order to avoid rupture and drug release during cellular uptake events, so the full dose of the encapsulated drug is delivered to the target site inside the cell.[27,130]

Delcea *et al.* investigated the force-induced deformation of PEM microcapsules fabricated from 4 double layers of PDADMAC and poly(styrene sulfonate) and subsequent release of encapsulated dextran-fluorescein isothiocyanate (FITC) molecules.[130] Microcapsule deformation and release was quantified after being loaded into Vero cells *via* electroporation, which was then correlated to deformation and release witnessed during atomic force microscopy colloidal probe experiments. The authors concluded that a force of at least 200 nN is applied to the PEM microcapsules during intracellular uptake, which resulted in nearly 75% release of encapsulated dextran-FITC due to roughly 20% total deformation of the particle.

Building upon this experiment, Palankar *et al.* investigated deformation of PEM microcapsules fabricated from non-biocompatible polyelectrolytes (poly(styrene sulfonate) and poly(allylamine) and microcapsules fabricated with varying layer number of biocompatible poly-L-arginine and dextran sulfate.[27] As in the previous investigation, an atomic force microscopy colloidal probe was used to ascertain mechanical stability of non-biocompatible and biocompatible PEM microcapsules. The non-biocompatible PEM microcapsules were mechanically more stable, exhibiting plastic deformation at 40% applied deformation compared to 20% for biocompatible PEM microcapsules, possibly due to stronger electrostatic interactions between PEM layers of the non-biocompatible polyelectrolytes. The authors then calculated force-deformation curves for biocompatible

PEM microcapsules fabricated with 4, 8, and 12 PEM layers. Microcapsules with 4 layers were the most deformable, exhibiting 30% deformation at an applied force of 200 nN. This was consistent with qualitative examination of PEM microcapsule deformation after cell internalization.

These investigations demonstrate that not only can the biochemical properties be readily tuned, but that the mechanical properties of PEM microcapsules can be modified to exhibit responsive behavior within a relevant range of forces exerted by cells. In developing a new paradigm that utilizes platelet biochemical and biomechanical behavior to sense vehicle targeting and actuate drug release, the ease in modification of these particle parameters make them extremely attractive while optimizing the system to display the desired functionalities. Moreover, as PEM capsules contain an aqueous core, these make them applicable to deliver clot-augmenting biotherapeutics. As such, PEM microcapsules were subsequently developed to (1) include fibrinogen to enable platelet-microcapsule hybridization and clot targeting, and (2) rupture and release the full drug cargo when hybridized and nearby platelets contract at sites requiring hemostatic augmentation.

4.2 Experimental

4.2.1 Materials

PLL hydrobromide (30-70 kDa), PLG sodium salt (50-100 kDa), dextran (70 kDa), MES, NaCl, dextran-fluorescein isothiocyanate (FITC) (70 kDa), dextran-rhodamine B isothiocyanate (RBITC) (70 kDa), EDTA, sodium bicarbonate, Sigmacote, calcium chloride, magnesium chloride, and sodium carbonate were purchased from Sigma-Aldrich (St. Louis, MO). PBS, human fibrinogen-AlexaFluor 488, CellMask Deep Red, collagen

type 1, rhodamine B isothiocyanate (RBITC), CD41a-APC, and acid citrate dextrose (ACD) blood collection tubes were purchased from Fisher Scientific (Pittsburgh, PA). Recombinant human alpha thrombin was purchased from Haematologic Technologies (Essex Junction, VT). Human fibrinogen was purchased from Enzyme Research Laboratories (South Bend, IN). Float-a-lyzer dialysis tubes (10 kDa MWCO) were purchased from Spectrum Labs (Rancho Dominguez, CA). PAC-1-FITC was purchased from BD Biosciences (San Jose, CA).

4.2.2 Washed Platelet (WP) Collection

Human blood was drawn according to IRB-approved protocols per the Declaration of Helsinki into 20% ACD. To isolate WPs, PRP was first extracted from whole blood *via* centrifugation. Additional ACD was added to the PRP to make a 10% ACD solution before spinning down again to separate PPP and platelets. The PPP was removed and platelets were resuspended to the desired concentration in Tyrode's buffer and stained with CellMask Deep Red.

4.2.3 PEM Capsule Fabrication

Calcium carbonate cores used to template the fabrication of PEM capsules were synthesized according to the literature by mixing equal volumes of 0.33 M calcium chloride and 0.33 M sodium carbonate for 30 seconds. Typically, 7 mL of each salt solution was added. Stir was then ceased, and the solution was left to stand for 10 minutes, followed by washing with DI water 3x and drying over vacuum using a Buchner funnel with fritted disc. A typical yield of 190-210 mg was achieved (83-91% yield). For cores loaded with dextran-RBITC, 5 mg of dextran-RBITC was added to the calcium chloride solution before

addition of sodium carbonate. For double cores with encapsulated dextran or dextran-FITC in the outer core layer, the above-fabricated cores were dissolved in DI water at 80 mg/mL. To the stirring core solution, 1 mL of 0.33 M sodium carbonate and 1 mL of 0.33 M calcium chloride with 5 mg dextran or dextran-FITC were simultaneously added. Stir was continued for 30 seconds, and then the solution was left to stand for 10 minutes. Cores were washed 3x with DI water and dried over vacuum. A typical yield of 93 mg (83%) was achieved.

To make the PEM capsules, 2 mg/mL solutions of PLL and PLG were made with 0.5 M NaCl, pH 6.25. Polyelectrolyte layers were deposited onto the cores with alternating charge in a LbL fashion. A 2% w/v solution of cores was dispersed in the PLL solution for 10 minutes. The cores were then pelleted at 200 x g for 5 minutes and washed 3 times with 0.5 M NaCl pH 6.25 before the next layer was deposited. When the desired number of layers was deposited, the cores were dispersed in a 0.2 M EDTA solution at pH 6.25 for 30 minutes to remove the calcium carbonate. The PEM capsules were then washed and pelleted several times (400 x g for 10 minutes, without acceleration or brake) with 5 mM MES pH 6.25 and stored at 4 °C until use. Synthesis resulted in 7-9 million particles/mL as determined *via* Beckman Coulter cell counter.

4.2.4 Zeta Potential

Samples were diluted with DI water at a 1:9 ratio. Each sample was measured 3 times at 20 runs for each measurement. Zeta potential of cores during polyelectrolyte deposition was measured with a Malvern Zetasizer Nano Series (Malvern, UK).

4.2.5 Platelet Activation

To coat the glass beads with fibrinogen, the LbL deposition technique was used to deposit a single PEM onto the glass beads consisting of PLL as the first layer and a 1:1 solution of PLG and fibrinogen as the outer layer. To fabricate the hybridized microparticles, 0.5 mL of a 1 million/mL solution of either PEM capsules or glass beads was added to 0.25 mL washed platelets (120 million/mL) stained with CellMask Deep Red. The solution was recalcified with 5 mM calcium and 2 mM magnesium and gently mixed for 10 minutes. Then 50 uL of Annexin V Alexa Fluor 488 or 100 uL of PAC-1-FITC was added before imaging. Images were taken *via* confocal laser scanning microscopy using a Zeiss LSM 700 system (Thornwood, NY). PAC-1-FITC and CellMask Deep Red intensities were determined in Image J.

4.2.6 "Clot-like" Gels

Static fibrin clot experiments were fabricated by mixing 2 mg/mL fibrinogen (pre-warmed), 1 U/mL thrombin, 10 mM calcium, 2 mM magnesium, washed platelets stained with CellMask Deep Red, and PEM capsules on a glass slides treated with Sigmacote. Clots were formed at 37 °C and 60% humidity and imaged *via* confocal laser scanning microscopy using a Zeiss LSM 710 NLO system (Thornwood, NY).

4.3 Results and Discussion

4.3.1 Platelet Adhesion onto PEM Capsules and Integration into Fibrin Networks

The polymers PLL and PLG were used as the positive and negative polyelectrolytes of the PEM microcapsule (Figure 14A). The polyelectrolytes are deposited onto calcium carbonate cores in a LbL fashion. Calcium carbonate was chosen as the sacrificial core due

to its relatively inert removal with EDTA (Figure 14B). As fibrinogen is deposited in a 1:1 ratio with PLG for the last polyelectrolyte layer, it was assumed an acid or organic solvent treatment to remove a mesoporous silica or polystyrene core would substantial lower the bioactivity of the protein.

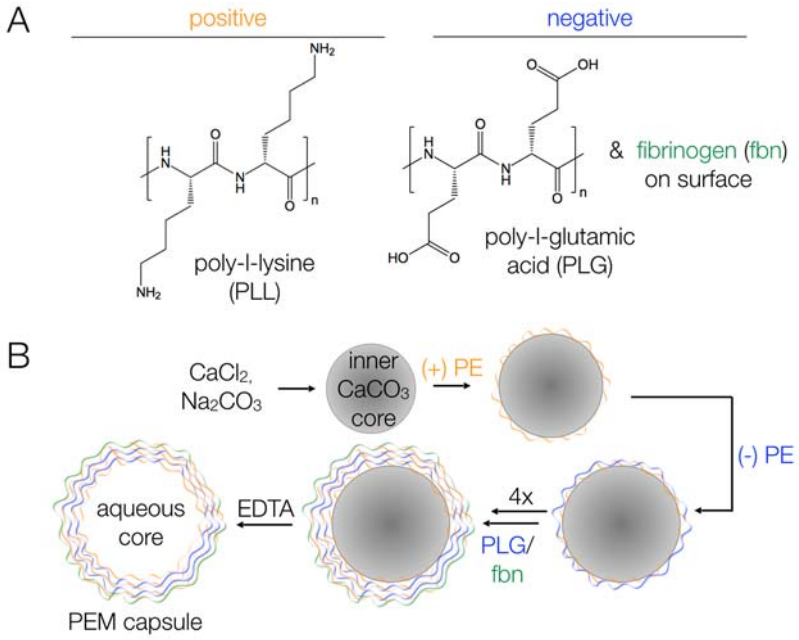

Figure 14. Schematic of LbL assembly of PEM capsules. (A) The polyelectrolytes poly-L-lysine (PLL) and poly-L-glutamic acid (PLG) were used to fabricate the PEM capsule. (B) Polyelectrolytes were deposited onto a calcium carbonate core, with the last layer consisting of 1:1 ratio of fibrinogen and PLG. The core is then removed with EDTA to yield capsules with an aqueous core and fibrinogen surface for platelet adhesion.

Calcium carbonate cores were fabricated *via* a precipitation reaction by rapidly mixing sodium carbonate and calcium chloride for 30 seconds, followed by 10 minutes of resting before washing over vacuum. Core size can be modified by adjusting stir speed (faster speeds yield smaller particles), the duration of time before stir is started after solutions are combined (longer durations yield larger particles), and salt concentration (higher concentration yields smaller particles).[159] The size of the final PEM microcapsule

is predominately determined by the size of the templating particle. Calcium carbonate cores used in these investigations were fabricated from 0.33 M calcium chloride and sodium carbonate at a stir speed of 600 rpm or 400 rpm to produce particles in the size range of 3 to 6.5 µm in diameter (Figure 15A,B), respectively.

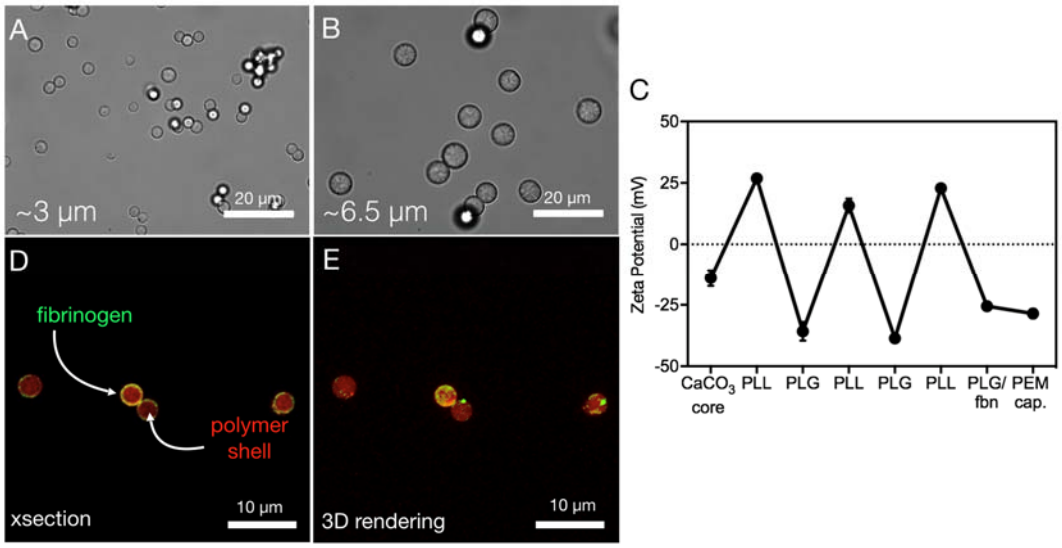

Figure 15. LbL assembly of polyelectrolytes onto calcium carbonate cores yields PEM capsules after core removal. (A,B) Brightfield micrographs of calcium carbonate cares are shown demonstrating variation of core size dependent on reaction conditions. Polyelectrolytes were deposited onto the calcium carbonate core in a LbL fashion, which can be confirmed through the zeta potential of the particle (C) after each deposition step (n = 3). Confocal micrographs of a cross section (D) and 3D rendering (E) of PEM capsules (red, PLL-RBITC) after fabrication show fibrinogen (green, Alexa Fluor 488) is localized to the exterior surface of the capsule.

To fabricate the PEM capsules, the polyelectrolytes are deposited onto the calcium carbonate templating core in an LbL fashion, beginning with the deposition of PLL. The zeta potential was taken throughout the fabrication process. The alternating charge of the particle after each deposition step suggest that the desired number of layers were, in fact, deposited onto the particle surface (Figure 15C). A total of 3 PEM bilayers were deposited as this (1) allows the fibrinogen to be on the exterior of the capsule (Figure 15D,E) as it

displays a negative charge at physiologic pH (thereby necessitating inclusion in the negative layer), and (2) imparts enough mechanical stability for processing. Particles with 2 PEM bilayers were initially investigated, but could not withstand the purification steps *via* centrifugation after the calcium carbonate template was removed with EDTA.

Once it was confirmed that fibrinogen was localized to the exterior of the capsule surface, the PEM capsules were mixed with washed human platelets and monitored with confocal microscopy to ascertain if the platelets adhered to the PEM capsule surface. Confocal images show that individual platelets do adhere to the surface of PEM capsules to form platelet-hybridized PEM capsules (HyPEMs) (Figure 16A). Furthermore, confocal images of "clot-like" gels fabricated from fibrinogen, washed human platelets, and thrombin show that platelet-HyPEMs also adhere to large platelets aggregates (Figure 16B) and integrate into fibrin networks (Figure 16B-D). This qualitative data suggests displaying fibrinogen on the exterior enables the "targeting" mechanism of this drug delivery paradigm through surface hybridization with platelets as well as polymerization into a fibrin network.

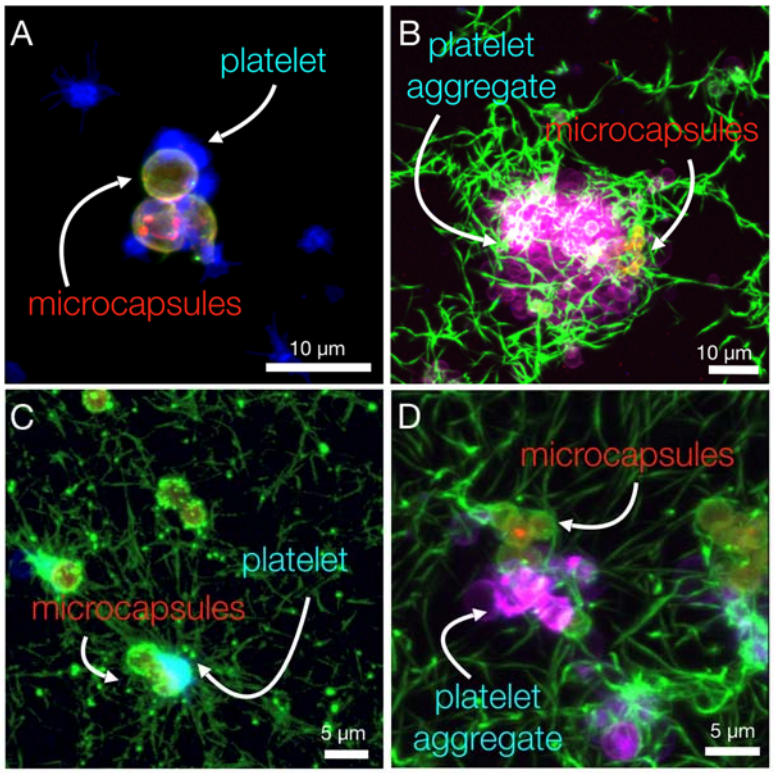

Figure 16. Fibrinogen on the surface of PEM capsules enables platelets to adhered to PEM capsule and polymerize into fibrin networks. Confocal micrographs show that platelets (blue, cell membrane stain) adhere to the surface of PEM capsules (red and green, PLL-RBITC and fibrinogen Alexa Fluor 488) to form platelet-hybridized PEM capsules (HyPEMs) (A). Furthermore, these constructs adhere to platelet aggregates (B) and polymerize into fibrin (green, Alexa Fluor 488) networks (B-D).

While it is not surprising that no PEM capsule rupture can be seen in Figure 16A in the absence of platelet agonists, it is surprising that no PEM capsule disruption can be seen in Figure 16B-D, in which thrombin is present. This experiment was repeated several times at various platelet and fibrinogen concentration; however, little PEM capsule disruption was qualitatively witnessed. Loss of circularity was occasionally seen (Figure 17A); however, this could not be considered conclusive rupture. Additional evidence supporting the potential of PEM capsules to rupture due to platelet contractile forces is seen in the confocal micrographs in Figure 17B,C. It appears the contraction of the

opposing platelets tethered to the PEM capsule *via* fibrin fibers Figure 17B tore the bottom capsule open. Similarly, in Figure 17C, disruption of the PEM layer can be seen due to several contracting platelets around two PEM capsules. While this was not a commonly viewed event, this does support the hypothesis that platelet contractile force is sufficient to physically rupture PEM capsules.

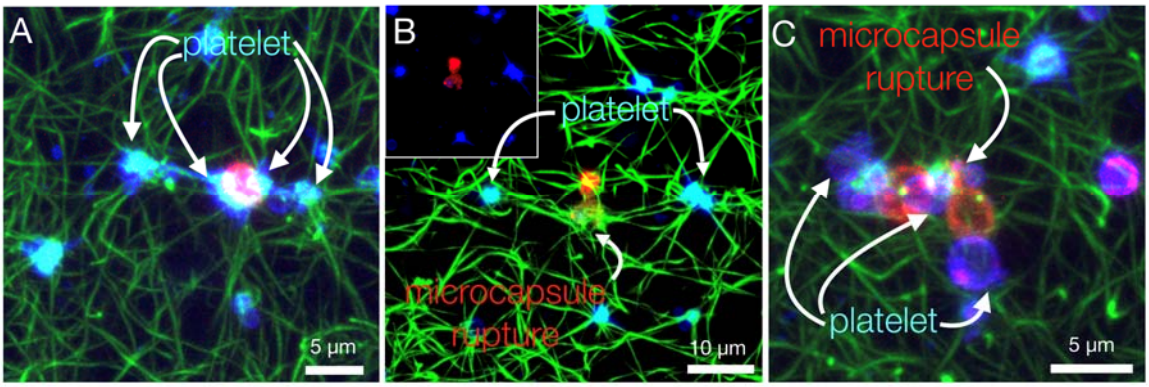

Figure 17. Evidence of morphological disruption of PEM microcapsules in "clot-like" gels. Confocal micrographs showing (A) morphological change from circular to ovicular of PEM capsules (red, PLL-RBITC) being contracted upon by two hybridized platelets (blue, cell membrane stain) within a fibrin (green, Alexa Fluor 488) network. Rupture of PEM capsules can also be seen between two opposing, contracting platelets that are tethered to the capsules (B). This can more clearly be seen in the inset with the green channel removed. Morphological disruption and possible rupture can also be seen due to hybridized platelet contraction (C).

These experiments were repeated, but PEM capsules loaded with fluorescently-tagged dextran were used instead of empty PEM capsules. It was hypothesized that, perhaps, rupture may be occurring but may not always result in an obvious perturbation of the capsule morphology to such an extent that it can be detected through qualitative analysis with confocal microscopy. If rupture is occurring with dextran loaded capsules, it was hypothesized that it would result in release of the fluorescent dextran, which will be easier to detect *via* confocal microscopy.

Dextran was encapsulated into the calcium carbonate cores by including dextran-FITC into the calcium chloride solution during the precipitation step. After polyelectrolyte deposition and core removal, dextran-FITC is retained in the capsule interior. The PEM capsules were mixed with fibrinogen, human washed platelets, and thrombin as before. While there was not an overwhelming amount of dextran release, there were events providing additional qualitative support for utilization of PEM capsules for this drug delivery paradigm. The confocal micrograph in Figure 18A shows that a portion of the PEM capsule walls is getting essentially pulled off of the capsule *via* contracting fibrin fibers. More compelling evidence is seen in Figure 18B, wherein a platelet is contracting on the PEM capsule and release of the dextran can be seen out of the "back" of the capsule.

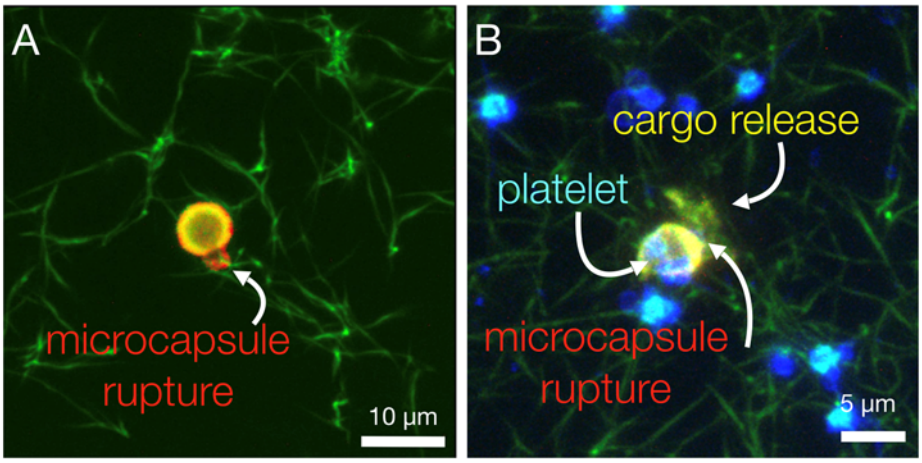

Figure 18. Release of encapsulated dextran from PEM capsules in "clot-like" gels. Confocal micrographs demonstrate rupture of PEM capsules (red, PLL-RBITC) loaded with dextran (green, FITC) *via* (A) contracting fibrin (green, Alexa Fluor 488) and (B) hybridized platelets (blue, cell membrane stain). (B) Dextran can be seen release from the rupture PEM capsule due to platelet contractile force.

While the dextran loaded PEM capsules resulted in more compelling evidence than the empty PEM capsules that they can be ruptured with platelet contractile forces, the number of rupture or release events was still slim – approximately 2-4 events every 200 uL

of gel. At this point, it was hypothesized that the highly charged characteristic property of the polyelectrolytes themselves could be interfering with release of an encapsulated cargo if the PEM capsule was ruptured.

4.3.2 Structural Modification of PEM Capsule to Enable Platelet-Contraction Mediated Release

To separate the highly-charged PEM wall from the encapsulated cargo and mitigate electrostatic interactions between the two, a layer of dextran was included into the PEM capsule between the PEM wall and encapsulated cargo. This was accomplished by employing a double core strategy wherein the calcium carbonate cores were fabricated as before (empty or with encapsulated cargo) but then used again as a seed particle for a second precipitation reaction with the inclusion of dextran (Figure 19).[1] After LbL assembly and EDTA removal of the core, dextran is retained as a thin layer separating the core cargo from the PEM wall.

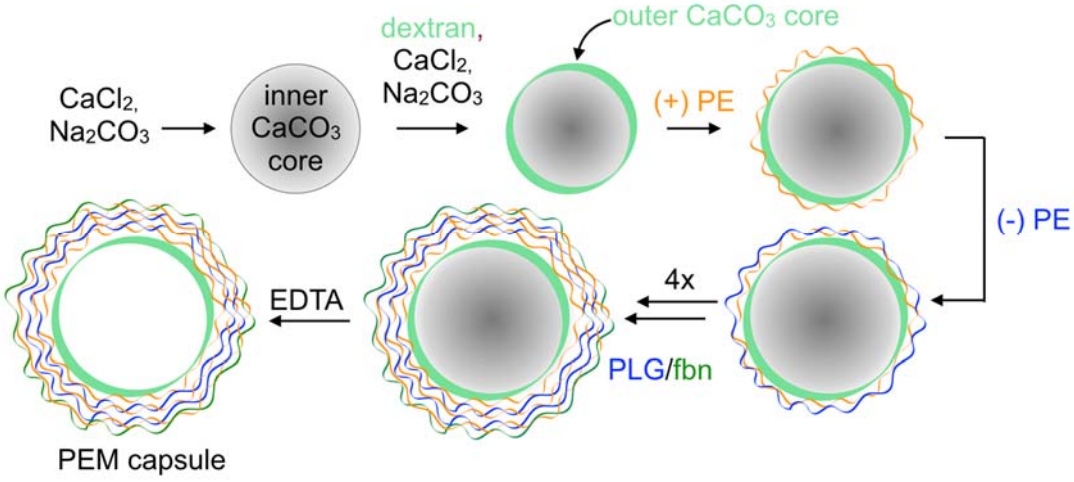

Figure 19. The double core strategy enables inclusion of a dextran layer to separate the encapsulated cargo from the PEM wall. An initial calcium carbonate core is made and then used as a seed particle for a second precipitation reaction to include dextran

in an outer layer of the core. LbL deposition of polyelectrolytes proceeds as in the previous method to fabricate PEM capsules with an internal dextran layer.

Dextran-RBITC was encapsulated in the inner core region while dextran-FITC was encapsulated in the outer core region (Figure 20A,B). The inner calcium carbonate core is 3.9 ± 0.4 μm in diameter (calculated *via* Image J, n=102) and increases to 4.7 ± 0.4 μm (calculated *via* Image J, n=101) when the outer calcium carbonate layer with encapsulated dextran was deposited.[1] After core removal, the dextran is retained as a thin layer in between the PEM wall and encapsulated cargo (Figure 20C,D) without mixing, further suggesting there exists a certain degree of non-covalent interaction between the PEM wall and molecules adjacent to it within the aqueous core. After deposition of 6 polyelectrolyte layers (3 PEM bilayers), PEM capsules exhibited a diameter of 5.1 ± 0.4 μm (calculated *via* Image J, n=105) after chelation of the calcium carbonate core.[1]

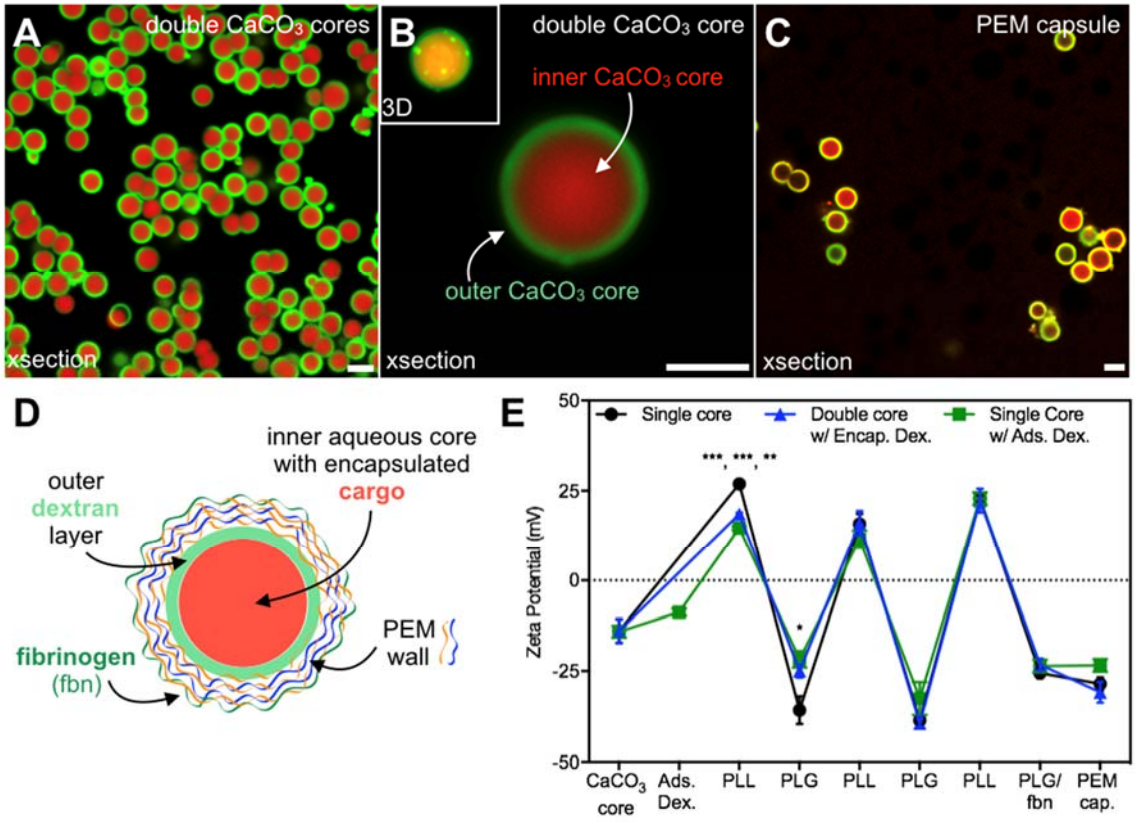

Figure 20. Utilizing double calcium carbonate cores as templating particles enables inclusion of a dextran layer to shield the encapsulated biotherapeutic payload from the highly charged PEM. Confocal micrographs (A,B) show morphology of the double calcium carbonate core with dextran-RBITC (red) loaded in the inner core region and dextran-FITC (green) loaded in the outer region. A 3D rendering of a single double core is shown in the inset of B. The final PEM capsules retain dextran both from the inner and outer core regions in their respective areas (C,D). All scale bars = 5 μm. The zeta potential (E) was ascertained throughout the fabrication process, demonstrating a statistically significant difference in charge after the first layer is deposited between single core and double core ($p<0.001$), single core and adsorbed dextran ($p<0.001$), and double core and adsorbed dextran ($p<0.05$). Additionally, there is a significant difference in charge after the second layer is deposited between using a single core and adsorbed dextran ($p<0.05$), n = 3. Statistical significance: * $p<0.05$, *** $p<0.001$.

The zeta potential was again determined to ascertain if inclusion of dextran altered deposition of polyelectrolyte layers (Figure 20E) throughout the fabrication process by altering the surface charge of the calcium carbonate core particles. Double cores with encapsulated dextran in the outer layer and single cores with adsorbed dextran (as an additional method) were compared to single cores used previously. Adsorbing dextran onto the core surface decreases the absolute value of the zeta potential while encapsulating it in the outer core results in roughly the same zeta potential as the single core. After deposition of the first polyelectrolyte layer (PLL), the zeta potential of both the double core and adsorbed core were significantly lower than the single core ($p<0.001$), and the adsorbed core was significantly lower than the double core ($p<0.05$). This suggests that inclusion of dextran does decrease the amount of PLL deposited onto the core surface; however, this is mitigated by including it in the outer core region compared to adsorbing it onto the surface. This conclusion is reinforced by comparing the zeta potentials after the next layer of polyelectrolyte (PLG) is deposited. While both dextran conditions are again lower than the single core, only the absolute magnitude of adsorbed dextran is significantly lower than the

single core ($p<0.05$). As such, dextran was encapsulated in the outer core for subsequent experiments.

The amount of fibrinogen deposited in the last layer on the exterior of the particle was quantified. A total of 6.3 ± 0.2 μg/mL fibrinogen was deposited onto the PEM capsule surface as determined by fluorescence intensity of a PEM capsule with fluorescent fibrinogen deposited onto the surface (Figure 21A).[1] As before, washed human platelets adhere to the surface of the PEM capsule to form the platelet-HyPEMs (Figure 21B) without inducing rupture of the PEM wall.

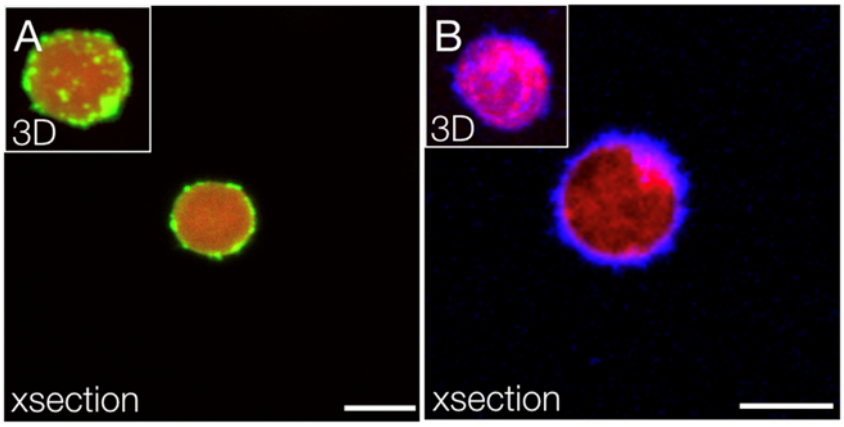

Figure 21. Fibrinogen on the surface of PEM capsules fabricated from double cores enable platelet hybridization. Fibrinogen (green, Alexa Fluor 488) is localized to the exterior of the PEM capsule (red, PLL-RBITC) as seen in a cross section (A) and 3D rendering of the same in the inset. Platelets (blue, cell membrane stain) adhere to the PEM capsules (B), as seen in a cross section of a single platelet-HyPEM and 3D rendering of the same in the inset. Scale bars = 5 μm.

While stiff substrates coated with fibrinogen have been shown to cause platelet activation upon binding *via* activation of the $\alpha_{IIb}\beta_3$ integrin, this suggests that PEM capsules are soft enough to prevent any substantial platelet activation during the hybridization event.[160] To confirm this, hybridized platelet activation was investigated using an Annexin

V-Alexa Fluor 488 conjugate stain and a PAC-1-FITC conjugate stain. Annexin V is specific for phosphatidylserine (PS) exposure, which is associated with platelet activation, and PAC-1 is specific for activated integrin $\alpha_{IIb}\beta_3$ and is therefore a marker of platelet activation.[69,160] Platelets hybridized onto PEM capsules (Figure 22A) were compared to platelets adhered onto fibrinogen coated glass beads (diameter = 3 μm) as a positive control (Figure 22B) as they represent a substantially stiffer substrate than the PEM capsules. Annexin V intensity was normalized to platelet intensity (Figure 22C), which shows statistically significant lower PS exposure on platelets hybridized to PEM capsules compared to platelets adhered onto fibrinogen coated glass beads (0.29 ± 0.03 and 0.35 ± 0.01, respectively).[1]

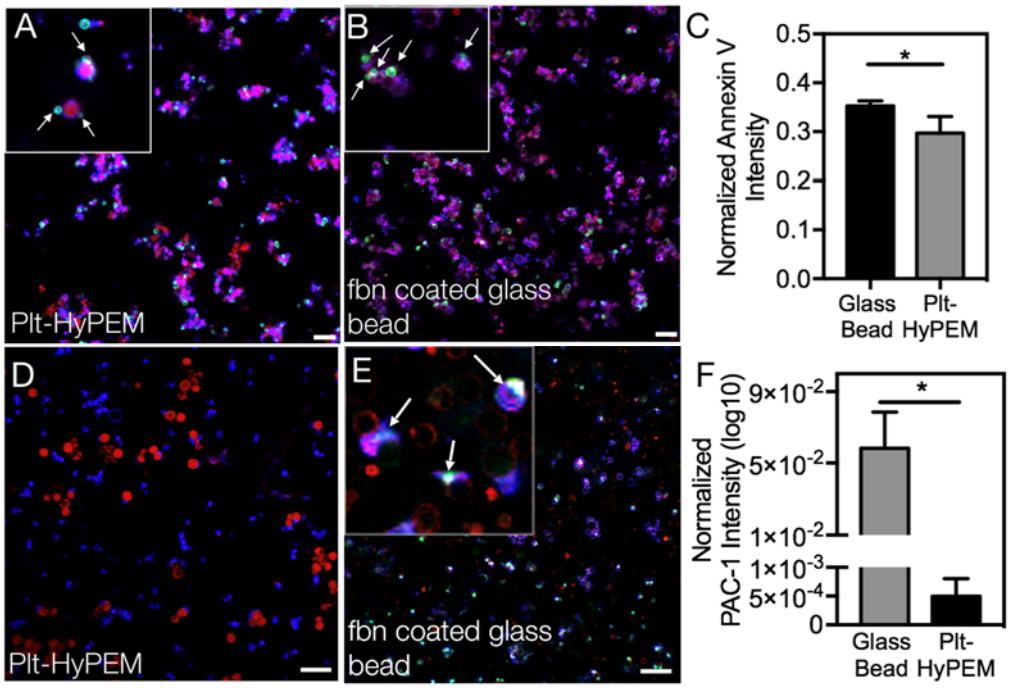

Figure 22. Hybridized platelets remain quiescent due to the softness of PEM capsules. Activation of platelets (indicated by arrows in inset) hybridized to PEM capsules (red, PLL-RBITC) (A,D) or fibrinogen coated glass beads (B,E) was quantified using phosphatidylserine exposure (green, Annexin V-Alexa Fluor 488) (A-C) or PAC-1

(green, FTIC) (D-F). Results are represented by the mean ± SD, n = 3-4. Statistical significance: * p<0.05. Scale bars = 20 µm.

Similarly, PAC-1 intensity was normalized to platelet intensity to quantify platelet activation (Figure 22F), which shows that activation of $\alpha_{IIb}\beta_3$ integrin is two orders of magnitude less when platelets are adhered onto PEM capsules (0.0005 ± 0.0003) compared to the fibrinogen coated glass beads (0.06 ± 0.02).[1] These results confirm that the PEM capsules are biochemically suited to enable platelet adhesion to surface fibrinogen and mechanically tuned (by leveraging the mechanosensing ability of platelets) to mitigate fibrinogen-induced activation.

4.3.3 "Burst" Release of an Encapsulated Cargo

While it is ideal that hybridized platelets remain quiescent and do not perturb the morphology or structure of PEM capsules in non-target environments, it is essential that they rupture the PEM capsules once activated and contracting. To evaluate if the PEM capsules are susceptible to platelet contraction-induced rupture, the PEM capsules were loaded with a model payload (dextran-RBITC) and monitored while in a clot-like gel. The PEM capsules were mixed with fibrinogen, washed platelets, and clotting activators (2 mM magnesium, 10 mM calcium, and 1 U/mL thrombin) to polymerize the fibrinogen into fibrin and activate the platelets.

PEM capsule rupture induced by activated, hybridized platelets and release of dextran-RBITC can clearly be seen in Figure 23. Both activated hybridized platelets and platelet aggregates are shown breaching (Figure 23A), fracturing (Figure 23B), and fully collapsing the PEM capsule (Figure 23C).[1] This significant and severe disruption in PEM capsule morphology resulted in the release of the model payload, dextran-RBITC (Figure

23B-D and Figure 24).[1] The structurally damaging effects of the force generated by contracting, hybridized platelets is shown in Figure 23D, where the platelet has contracted on top of the PEM capsule with such force that material failure of the PEM capsule occurred, resulting in the formation of a hole through PEM capsule wall to enable the "burst" release of the model payload.

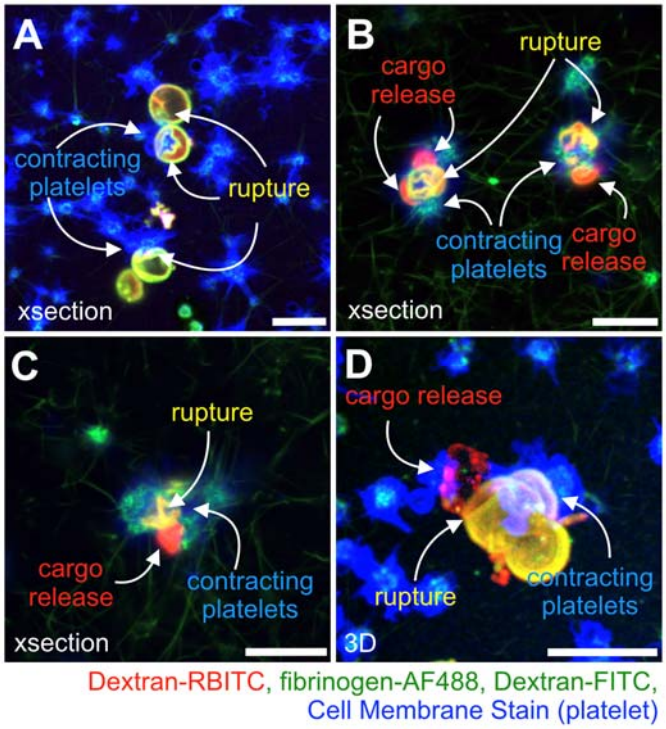

Figure 23. Platelet contractile force is sufficient to rupture PEM capsules in "clot-like" gels to release a model biotherapeutic payload. PEM capsules (outer dextran-FITC, green) with an encapsulated model payload (dextran-RBITC, red) were immobilized in clot-like gel consisting of fibrin (fibrinogen-AF488, green) and activated platelets (membrane dye, blue). Platelets adhered on the surface of PEM capsules are seen rupturing the capsule wall (A-D), resulting in release of the inner model payload (B-D). Contracting, adhered platelets are seen "popping" open a PEM capsule (D), enabling release of the inner model payload. Due to differences in intensity between dextran-FITC and fibrinogen-AF488, fibrin may be extremely faint in order to avoid oversaturation of the PEM capsule fluorescent channel. All scale bars = 10 µm.

It is important to note that the dextran-FITC from the outer core is retained in the PEM capsule, indicating the outer dextran layer is non-covalently interacting with the highly-charged PEM wall, inhibiting its release into the fibrin matrix despite PEM capsule rupture. In fact, PEM capsules without the dextran layer do not show any burst release of model payload during platelet contraction as seen in the initial investigations of this chapter, suggesting its presence in the PEM capsule formulation is necessary to facilitate a full, "burst" release following a rupture event.

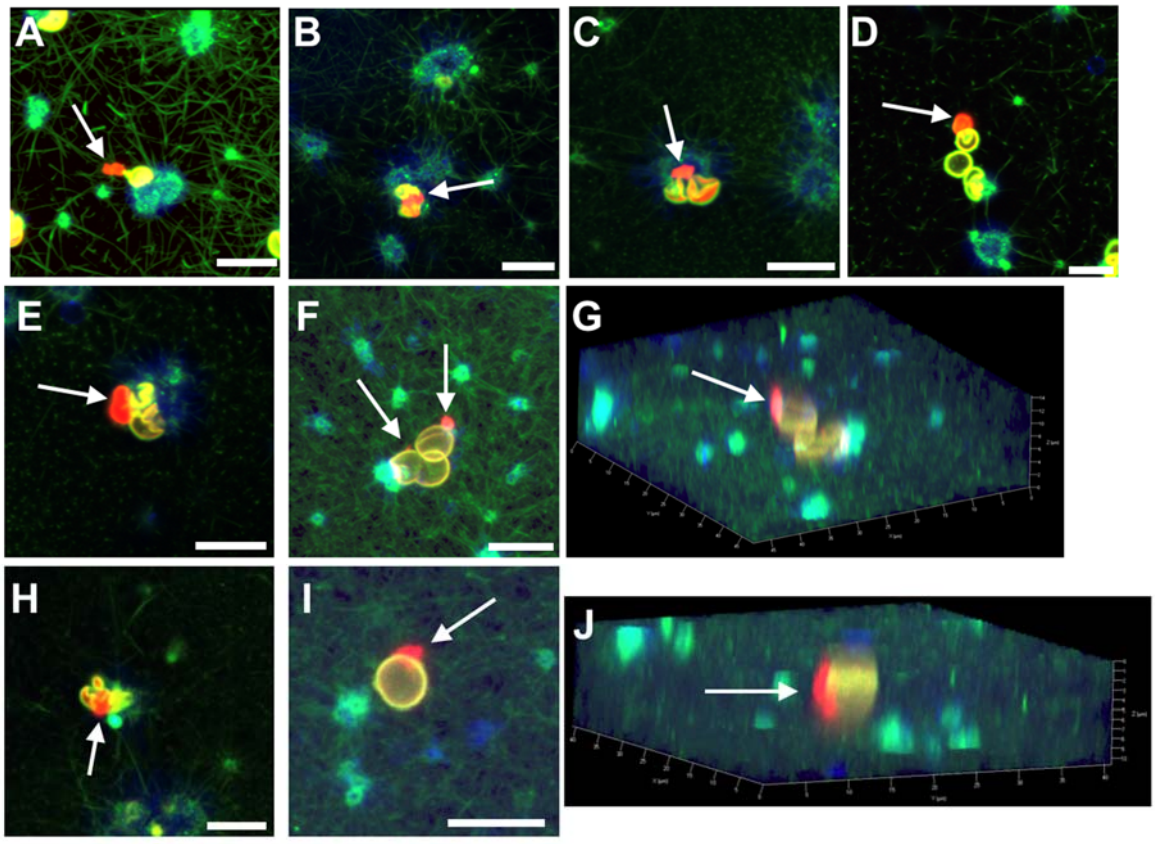

Figure 24. Platelet contractile force-mediated rupture enables "burst" delivery of the encapsulated model biotherapeutic in "clot-like" gels. PEM capsules (outer dextran-FITC, green) with an encapsulated model payload (dextran-RBITC, red) were immobilized in a clot-like gel consisting of fibrin (fibrinogen-AF488, green) and activated platelets (membrane dye, blue). Platelets adhered on the surface of PEM capsules are seen rupturing or collapsing their capsule walls (A-J), resulting in release of the payload. Panels G and J represent Z-stack images of panels F and I, which show

release of the payload out of the interior of the PEM capsule due to nearby platelet contraction. Due to differences in intensity between dextran-FITC and fibrinogen-AF488, fibrin appears faint in order to avoid oversaturation of the PEM capsule fluorescent channel. All scale bars = 10 µm.

4.4 Conclusions

These results indicate that not only do the PEM capsules comprise the appropriate biochemical cues to facilitate platelet hybridization without substantial activation, they also possess suitable mechanical and structural properties to enable platelet contractile force-mediated rupture of the PEM capsule followed by "burst" release of the encapsulated payload. These features are due to the fibrinogen on the surface of the PEM capsule as well as the dextran layer that separates the encapsulated model payload from non-covalently interacting with the highly-charged PEM wall. While the studies in this chapter utilized fluorescently tagged dextran as the model cargo, to more definitely determine its potential as a drug delivery paradigm, *in vitro* studies ascertaining its effects on efficacy of an already known biotherapeutic are required. As this paradigm utilizes the patient's own platelets as the sensor and actuator of targeted delivery, using this formulation to deliver clot augmenting drugs to a thrombus or vascular injury site would be an appropriate application. Delivery of fVIII to treat bleeds in hemophilia A patients was therefore chosen with the particular challenge of delivery in the presence of anti-fVIII inhibitory antibodies.

CHAPTER 5. PLATELET-MEDIATED TARGETED DELIVERY OF FACTOR VIII *IN VITRO*

Results described in this chapter regarding development and characterization of the optimized PEM capsule have been reported in *ACS Nano*.[1]

5.1 Hemophilia A

Congenital hemophilia A is a recessive X-linked genetic bleeding disorder that affects approximately 20,000 patients in the United States. It is caused by mutations in the F8 gene (~1,300 have been identified) that adversely affects the activity or production of the plasma protein, fVIII, for which it encodes.[161,162] As this protein is necessary in the clotting cascade, these mutations result in an inability of the patient to form a blood clot, giving them a very high risk of hemorrhage after minor injury. Hemophilia A is further characterized by severity, which is correlated to the severity of the genetic mutation in the F8 gene.[163] Roughly 25% of hemophilia A patients have mild hemophilia, which is characterized by plasma fVIII activity levels ranging from 6-30% of a healthy person. Plasma fVIII activity levels ranging from 1-5% is identified as moderate hemophilia (15% of patients), and a patient with less than 1% is considered to have severe hemophilia (60% of patients).

In order to prevent or treat bleeds, there are several clinically available treatment options. For patients with mild hemophilia A, desmopressin is commonly used. This can be administered intravenously, subcutaneously, or intranasally and exhibits a half-life of

5-8 hours. While the mechanism is not clearly understood, it can increase fVIII activity level 2 to 6-fold over the patient's baseline value.[164]

Patients with moderate and severe hemophilia A typically use fVIII replacement therapy in which they intravenously inject either plasma-derived or recombinant fVIII, resulting in systemic exposure of the biotherapeutics to the patient.[28,29] These are administered according to one of two dosing schedules depending on the severity and frequency of breakthrough bleeding events a patient experiences. For patients that experience few breakthrough bleeds (mild and moderate hemophilia), an on-demand schedule may be used wherein intravenous administrations only occur to treat an active bleeding event. Several injections may be required to abate a single bleed depending on severity. This dosing schedule is less expensive and generally less intrusive into the patient's life if adequate.

A prophylactic administration is used for patients with severe hemophilia or patients that experience several breakthrough bleeding events. Here, fVIII is administered several times a week as the half-life of recombinant fVIII range from approximately 8-19 hours.[165] This ensures a baseline plasma fVIII activity level is maintained in order to prevent breakthrough bleeding events. These patients often still experience breakthrough bleeds, though they are less frequent, requiring additional on-demand injections of fVIII or another pro-clotting biotherapeutic.[166]

5.1.1 Hemophilia A with Inhibitory Antibodies

While prophylactic administration of fVIII enables successful management of bleeds for the majority of severe hemophilia patients, this treatment does not work for about 30% of severe hemophilia patients (~3,000 to 4,000 patients in the US) because they develop

anti-fVIII inhibitory antibodies.[30] These antibodies bind to active domains within fVIII that partially or fully inactive the protein. Spontaneous development of these inhibitors to endogenous fVIII in a patient without hemophilia A is identified as acquired hemophilia A. This can occur in both genders, and while the exact cause is unknown, development is typically associated with the presentation of another disease or condition and is not always permanent.[167,168] These antibodies are termed autoantibodies, which bind to either the A2 or C2 domain (but not both).[169,170] Binding to the A2 domain interferes with fVIII binding to factor IXa, and inhibitor binding to the C2 domain interferes with fVIII binding to platelet phospholipid, vWF, and cleavage by factor Xa and thrombin.

However, acquired hemophilia A is rare, and the majority of hemophilia A patients with inhibitory antibodies are those with congenital hemophilia A that develop them to exogenous replacement fVIII. These patients typically have a polyclonal response, developing inhibitors to both the A2 and C2 domains.[170] Inhibitors developed by congenital hemophilia patients are termed alloantibodies and result in complete inhibition of the fVIII replacement therapy.[169,170]

Development of inhibitors for congenital hemophilia A patients typically occurs within the first 150 exposures with the median development occurring between the 10th and 15th exposure, and as such, initially affect the patient while in the pediatric stage.[171] Development of inhibitors is correlated to the type of F8 mutation responsible for the patient's hemophilia.[172] Thus, risk of inhibitor development increases with a family history of inhibitors – 48% compared to 15% risk of development, respectively.[173]

5.1.2 Clinically Available Treatment Options for Hemophilia A Patients with Inhibitors

The presence of inhibitors severely limits the effective treatment options for these patients towards abating bleeds. There are three main treatment options that are currently clinically available for congenital hemophilia patients, which include immune tolerance induction (ITI) therapy or the use of bypassing agents like activated factor VII (fVIIa) or activated prothrombin complex concentrate (*i.e.* FEIBA®).[174] Patients undergoing ITI therapy receive regular administration of fVIII multiple times per week for a prolonged duration to achieve peripheral tolerance. ITI therapy has a success rate of ~70%; however, it is not appropriate for all patients as there are several drawbacks. The age in which a patient develops inhibitors, the baseline titer level, and peak titer level can preclude patients from ITI therapy as poor candidates to achieve tolerance. Generally, patients should be put on ITI therapy within two years of inhibitor development. Initiation of treatment can be delayed until the patient's titer is below 10 BU/mL; however, recent investigations have shown some high-titer patients and those of older age can achieve tolerance.[175,176] Treatment can also make treating breakthrough bleeds problematic, as bypassing agents cannot be used if the inhibitor titer is greater than 10 BU/mL due to the risk of catheter-associated thrombosis.[177] Furthermore, as the treatment requires several injections per week over a period of several months or years, this necessitates large financial resources as well as time investment into the treatment.

Use of a bypassing agent for patients that do not qualify for ITI therapy or are adverse to the treatment plan is an alternative though there exists shortcomings for each specific therapeutic option.[31] Recombinant fVIIa (NovoSeven®) activates coagulation through the extrinsic pathway, thereby circumventing the need for fVIII replacement therapy. While extremely effective, it has an extremely low half-life (~1-2 hours), requiring daily

injections if dosing on a prophylactic schedule.[34] Therefore, the clinical utility of this treatment falls heavily in an on-demand dosing schedule. Furthermore, NovoSeven® has been shown to cause thrombotic side effects in otherwise healthy patients experiencing hemorrhage, and while hemophilia patients are not at high risk for this side effect, it nonetheless remains a risk, especially if in combination with another pro-coagulant.[32,33] Activated prothrombin complex concentrates similarly bypasses the need for fVIII by directly supplying the activated clotting factors that depend on fVIII's functional presence. While these therapies exhibit longer half-lives, the volume that must be infused is much larger, which requires longer infusion times and may require visits to the clinic. Interestingly, patients using bypassing agents prophylactically see more breakthrough bleeds than patients on replacement factor with the same severity, indicating its suboptimal efficacy.[174]

Obizur® is recombinant porcine fVIII and has recently received FDA approval for acquired hemophilia A patients. Their phase II/III clinical trial data on 28 patients showed that bleeds were positively controlled (bleed abatement or substantially decreased) in all patients within 24 hours despite the fact that 10 of those patients exhibited some level of anti-porcine fVIII inhibitors.[178] Furthermore, bleeds were successfully controlled in 24 out of the 28 patients at longer time points.

5.1.3 Treatment Options Undergoing Development

Two promising biotherapeutic candidates are currently undergoing clinical trials for haemophilia with inhibitors: emicizumab (ACE910) and Fitusiran. ACE910 is a recombinant bispecific antibody that mimics fVIII's cofactor function in the clotting

cascade by binding to both activated factor IX and activated factor X. It has an impressive half-life and can be administered subcutaneously once weekly, but it does not completely prevent breakthrough bleeds.[179] This has been problematic in their phase III trial, as treatment with a bypassing agent has caused several thrombotic side effects in trial patients and one associated death due to rectal hemorrhage.[180,181] Fitusiran is a subcutaneously administered biotherapeutic that can be administered once a month. It is a RNAi that lowers antithrombin levels, which decreases the negative feedback loop in the coagulation cascade, thereby promoting coagulation. No thrombotic side effects have been reported in their phase I clinical trial for hemophilia with inhibitors, but breakthrough bleeds have been reported that can successfully be manged with bypassing agents without thrombotic side effects.[182] 56% of the patients in the cohort were bleed free while 69% did not experience spontaneous bleeding events.

Recently, research on PEGylating fVIII[183,184] or formulating fVIII with nanoparticles[185,186] in order to mitigate inhibitor interactions has been reported. However, neither strategy is ideal, as PEGylation has been shown to only prevent some inhibitor species from binding to fVIII[184] while association with nanoparticles limits the bioavailability of the fVIII dose. PEGylated fVIII (Adynovate®) did receive FDA approval due to the longer exhibited half-life. Interestingly, a PEGylated nanoparticle construct was shown to adversely increase inhibitor titer in a hemophilia mouse model, which could possibly be due to the suggested immunogenic properties of PEG.[187,188] We propose that the herein reported platelet-HyPEMs can shield fVIII from the patient's inhibitors and provide a "burst" release of the full fVIII dose, enabling rapid rescue hemostasis for these patients.

5.2 Experimental

5.2.1 Materials

PLL hydrobromide (30-70 kDa), PLG sodium salt (50-100 kDa), dextran (70 kDa), MES, NaCl, EDTA, sodium bicarbonate, calcium chloride, magnesium chloride, sodium carbonate, and human coagulation fVIII concentrate were purchased from Sigma-Aldrich (St. Louis, MO). PBS, collagen type 1, rhodamine B isothiocyanate (RBITC), Alexa Fluor 488 Protein Labeling kit, CD41a-APC, and 3.2% buffered sodium citrate blood collection tube, were purchased from Fisher Scientific (Pittsburgh, PA). Float-A-Lyzer G2 dialysis tubes (MWCO 100 kDa) were purchased from Spectrum Labs. Tissue factor (TF) and activated factor VII (fVIIa) was purchased from Haematologic Technologies (Essex Junction, VT). ADVATE (antihemophilia factor (recombinant), Shire) and mAb 2-76 were provided by Dr. Shannon Meeks. The mAb 59D8 was kindly provided by Dr. Shawn Jobe's lab at the Blood Center of Wisconsin. Chromogenix Coamatic factor VIII Assay Kit was purchased from Diapharma (West Chester, Ohio). PDMS (Sylgard 184) was purchased from Ellsworth Adhesive Systems (Germantown, WI). 3M silicone adhesive transfer tape (50 μm thickness) was purchased from APDMRO (Ontario, CA).

5.2.2 Whole Blood (WB) and Platelet Poor Plasma (PPP)

Human blood was drawn according to IRB-approved protocols per the Declaration of Helsinki into 3.2% sodium citrate for WB and PPP isolations. To obtain PPP, WB was spun down to separate platelet rich plasma (PRP) from red blood cells and the buffy coat. PRP was spun down a second time to separate and isolate PPP from platelets.

5.2.3 Loading PEM Capsules with fVIII

To load PEM capsules with fVIII via inclusion into the calcium carbonate core, 5 mg of fVIII from human plasma concentrate was added to 7 mL 0.33 M calcium chloride solution before addition of 7 mL 0.33 M sodium carbonate. Core fabrication and removal proceeded as previously described. To load fVIII into the PEM capsules after their fabrication via diffusion, 50 μg/mL of fVIII was incubated with the PEM capsules at a particle density of 1 million/mL for 1 hour in pH 6.25 MES buffer (137 mM ionic strength). The microcapsules were then washed and pelleted several times with pH 6.25 MES buffer (5 mM ionic strength) (400 x g for 10 minutes, no acceleration or brake) to remove any unloaded fVIII.

5.2.4 Protein Labeling

To a solution of 10 mg/mL fVIII from plasma concentrate in sodium bicarbonate buffer (pH 9), 150 μL of a 10 mg/mL solution of RBITC in DMF was added. The solution was stirred for 1 h at room temperature in the dark. To purify, the solution was either dialyzed against PBS (100 kDa MWCO) or run through a Bio-Rad BioGel P-30 purification column. PLL was labeled in the same manner, but purified via dialysis (10 kDa MWCO) in the dark. Monoclonal antibody 59D8 was labeled and purified with AF488 using an Alexa Fluor 488 Protein Labeling Kit. A degree of labeling between 5 and 7 was typically achieved.

5.2.5 fVIII Diffusive Release

Experiments measuring the diffusive release of fVIII-RBITC out of capsules were conducted in PPP at 37 °C and under 40 rpm agitation. At time = 0, 100 uL of each sample was removed and incubated in 10 mM HCl for 30 minutes to dissolve the PEM capsules, allowing for quantitation of fVIII loading. At appropriate time points, PEM capsules were pelleted and an aliquot of the supernatant was removed to measure diffusive release of fVIII-RBITC. A PPP aliquot of the same volume was added back to the PEM capsule solution to preserve sample volume. Fluorescence intensity of the supernatant was measured and compared to a standard curve to calculate concentration of released fVIII-RBITC in the supernatant and then compared to the t=0 concentration to calculate the percent of fVIII diffusion out of the PEM capsule. All fluorescent measurements were taken on a Cytation 5 Imaging Reader by BioTek (Winooski, VT) and were conducted in triplicate.

5.2.6 fVIII Activity in PPP

The activity of stock fVIII (ADVATE) and fVIII (ADVATE) loaded PEM capsules (*via* supernatant during the fVIII loading procedure) was first determined with the Chromogenix Coamatic Factor VIII Assay Kit. An amount of 2 U/mL of fVIII was then added to PPP with 0.92 mg/mL mAb 2-76. Samples were incubated at 37 °C and under 40 rpm agitation for six hours. FVIII plasma activity was determined with the Chromogenix Coamatic Factor VIII Assay Kit at every hour.

5.2.7 In Vitro Microfluidic Vascular Injury Model

Fabrication of the microfluidic followed a previously reported method with modifications (Figure 25).[1] To form the perpendicular collagen/TF patch in the center of

the microfluidic channel, a PDMS-based straight channel with a width of 2 mm was vacuum-bonded to a clean glass slide. Collagen (0.5 mg/mL) and TF (4 nM) in 10 mM acetic acid was perfused through the channel and incubated at room temperature for 1.5 hours. The PDMS straight-channel was removed and slide was rinsed with DI water and dried with nitrogen. A straight channel was cut into 3M silicone transfer adhesive at a width of 1.2 mm with a Silhouette CAMEO craft cutter (Lindon, Utah). One side of the adhesive was then adhered to a piece of clean PDMS. Holes were punched for channel inlets and outlets. The remaining side was then adhered to the glass slide containing the collagen/TF strip. The adhesive was aligned such that the collagen/TF strip was perpendicular to and in the middle of the adhesive straight channel. After adherence to the coverslip, the glass was blocked with 5% BSA for 1 hour.

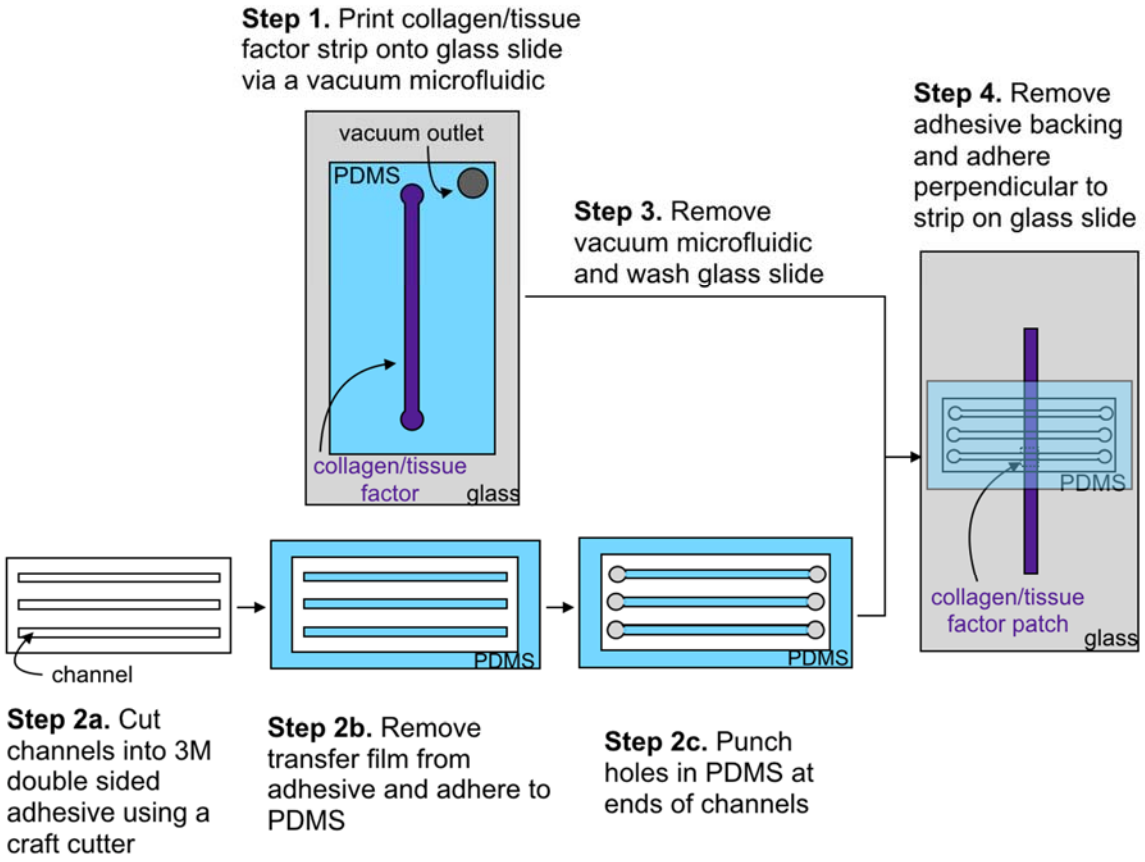

Figure 25. Schematic of protocol for in vitro microfluidic vascular injury model.

WB was perfused at 5 μL/min for 10 minutes followed by PPP at 5 μL/min for 30 minutes (healthy sample) or 50 minutes (fVIII-inhibited samples) using a Harvard Apparatus Elite Syringe Pump (Holliston, Massacheusetts). Both WB and PPP was recalcified to 5 mM Ca and contained 2 mM Mg, CD41a-APC, 59D8-AF488, 0.92 mg/mL mAb 2-76 inhibitory antibody for fVIII-inhibited samples, and experiment condition. All samples were kept at the same total volume and contained the same WB or PPP volumes.

The collagen patch was monitored over time *via* confocal laser scanning microscopy using a Zeiss LSM 700 system (Thornwood, NY). Tile scans were taken of the entire patch after the experiment ended and used to measure fluorescence intensity of fibrin, platelets, and fVIII on the patch *via* Image J.

5.2.8 In Vitro Clot Formation Time

Citrated whole blood was mixed with 0.92 mg/mL mAb 2-76 inhibitory antibody for 30 minutes followed by addition of 5 mM Ca, 2 mM Mg, and 12 pM TF. Samples with blebbistatin were incubated with 10 μM blebbistatin for 1 hour before addition of clotting actiavtors. ADVATE or PEM capsules loaded with ADVATE were added at the appropriate concentration and incubated for an additional 10 minutes. ADVATE activity was confirmed immediately before addition using the Chromogenix Coamatic Factor VIII Assay Kit. Samples (50 uL) were loaded into wells and washed with PBS to remove soluble blood products at appropriate time points until the wash solution was clear. Samples were considered clotted when the clot covered the bottom of well and remained unchanged between time points.

5.2.9 Statistical Analysis

All data was reported as the mean ± standard deviation of at least 3 experiments and calculated on GraphPad Prism 7.0 (San Diego, CA) using one-way analysis of variance (ANOVA) with Dunnett's correction or student's t test with Welch's correction.

5.3 Results and Discussion

5.3.1 Encapsulation of fVIII and Diffusive Release

The biotherapeutic payload is contained in the inner core and was either encapsulated in the core during calcium carbonate core fabrication or *via* diffusion after core chelation and PEM capsule purification.[26,147,149] Encapsulation efficiency of fVIII in calcium carbonate cores is 79.8 ± 11.3%, yielding a loading efficiency of 40.0 ± 14% after core removal.[1] The loading efficiency of fVIII *via* diffusion varied with loading concentration; however, a loading concentration of 50 µg/mL was chosen that yielded a 51.2 ± 2.6% loading efficiency (Figure 26).[1]

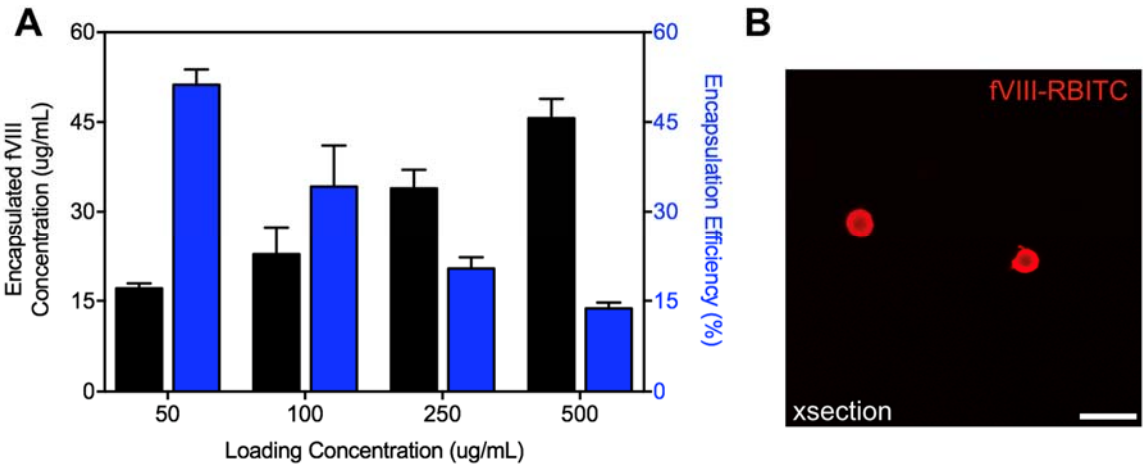

Figure 26. Characterization of fVIII loading via diffusion into the PEM capsules. The encapsulated concentration and encapsulation efficiency was characterized for various loading concentrations of fVIII (A). A confocal micrograph cross section (B) shows encapsulated fVIII (fVIII-RBITC, red) is completely distributed throughout the PEM capsule interior. Results are represented by the mean ± SD. Scale bar = 10 µm.

PEM capsules have been reported in the literature to be porous depending on the chemical characteristics of polyelectrolytes used, number of PEMs deposited, and medium in which they are dispersed (*i.e.* pH and ionic strength).[189,190] The porosity and its effects on fVIII diffusion out of the PEM capsule during circulation in blood are of particular concern. To investigate the extent of diffusion, PEM capsules were loaded with fVIII tagged with RBITC (encapsulated during calcium carbonate core formation) and incubated in platelet poor plasma (PPP) at 37 °C for 1 week to simulate circulation in non-target, healthy vascular environments. Fluorescence of the supernatant was measured at specific time points and compared to a standard curve to determine the amount of diffused fVIII.

PEM capsule formulations with and without dextran in the outer core region were investigated to ensure the dextran layer did not adversely affect the porosity of the PEM capsule. Both formulations show the same trend, with 56 ± 2% and 48 ± 3% of fVIII diffusing out of PEM capsules with and without dextran, respectively, after 6 hours incubation (Figure 27A).[1] Within 24 hours, 70 ± 1% and 69 ± 2% of fVIII diffuses out of the PEM capsules, which plateaus to just below 80% for both formulations after 2 days incubation (Figure 27B). Ideally, all of the encapsulated fVIII would be retained in the PEM capsules during circulation for this type of delivery system; however, because the delivery system is designed to quickly abate bleeding, the PEM capsules should target and deliver fVIII within the first few hours after administration. Approximately 70% fVIII is

retained in the PEM capsules after the first two hours, enabling it to be a viable system under clinically relevant time frames to treat bleeding complications in hemophilia patients.

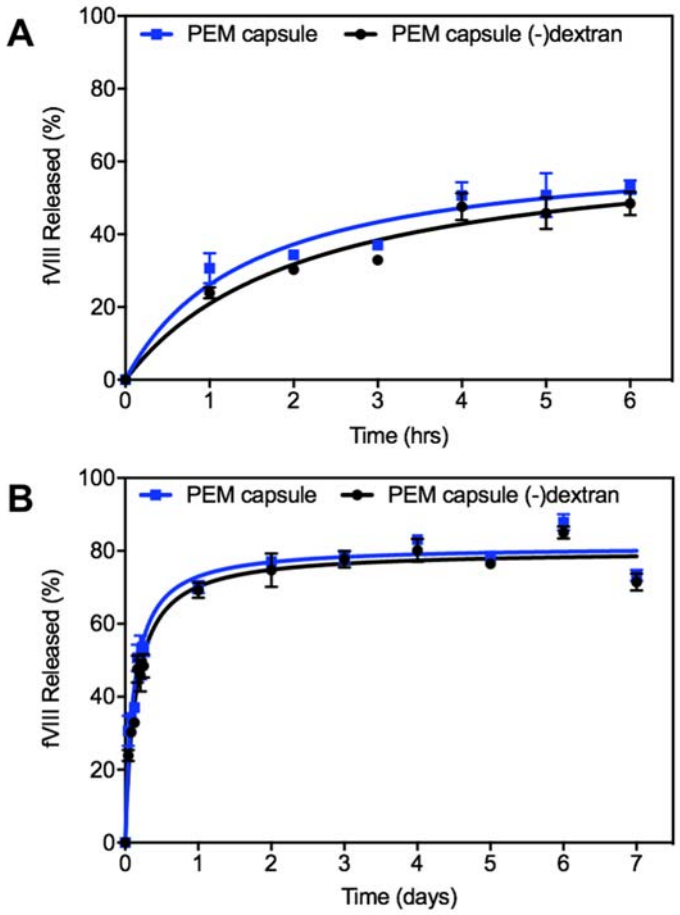

Figure 27. Characterization of fVIII diffusion. PEM capsules were incubated in platelet poor plasma (PPP) for 1 week at 37ºC to simulate circulation in non-target areas. The extent of fVIII diffusion out of the PEM capsules during the initial 6 h (A) and 1 week (B) of incubation are shown. Results are represented by the mean ± SD, n=3.

To further verify the applicability in clinically relevant time frames, we monitored the activity of free fVIII in PPP containing a potent fVIII inhibitory antibody (mAb 2-76)[191] to mimic acquired hemophilia. PEM capsules loaded with fVIII or fVIII delivered

systemically were added to PPP samples at 2 U/mL and incubated at 37 °C. The activity of free fVIII in the plasma was measured every hour over a six hour period with a two-stage chromogenic assay and normalized to the initial fVIII activity level of each sample (Figure 28A).[1]

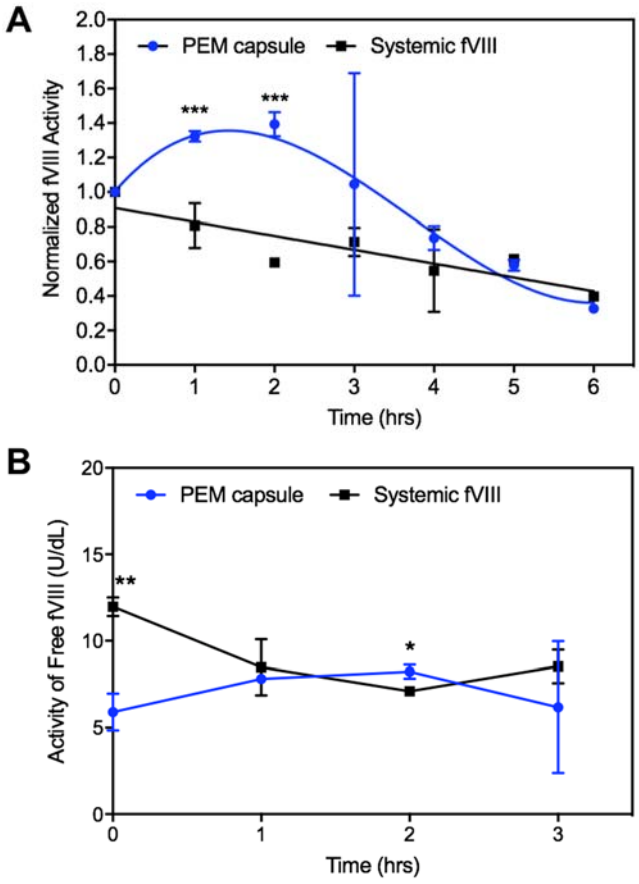

Figure 28. Characterization of fVIII activity in platelet poor plasma (PPP). Factor VIII loaded PEM capsules or free fVIII were incubated in PPP in the presence of inhibitory antibodies at 37 ºC for 6 hours. The activity of fVIII in the plasma was determined using a two-stage chromogenic assay at one hour intervals. Activity normalized to initial activity (A) and absolute activity (B) are shown. Results are represented by the mean ± SD, n = 3-6 experiments. Statistical significance: * p<0.05, ** p<0.01, and *** p<0.001.

While the activity of systemically delivered fVIII gradually decreases over time, the activity of fVIII delivered *via* PEM capsules significantly increases in the first two hours

compared to the initial activity. This is likely due to the fact that fVIII measured by the activity assay in the PEM capsule samples is fVIII that has diffused out of the PEM capsules. Thus, the recently diffused fVIII experiences a brief period between its diffusion and binding with an inhibitory antibody in which it retains activity. This is further supported by comparing the absolute activity values of fVIII delivered *via* PEM capsules and systemic exposure (Figure 28B).[1] While the activity of free fVIII is significantly higher at t = 0 hours for systemic delivery, the activity of fVIII in the plasma from the PEM capsule samples is significantly higher at t = 2 hours. While the full dose of fVIII is immediately exposed in the systemic case, only 30% of encapsulated fVIII has been diffused through the PEM capsule at t = 2 hours. Its higher activity at t = 2 hours despite the lower concentration of free fVIII suggests some of the diffused fVIII has yet to interact with inhibitory antibodies at the time the activity assay was conducted. While diffusion is not the primary mode of delivery for this platelet-contraction mediate delivery mechanism, the fact that the fVIII plasma activity at t = 2 hours is higher at only 30% of the dosage relative to systemically delivered fVIII further demonstrates the clinical utility of fVIII loaded PEM capsules for patients with inhibitors in the context of on-demand time frames to treat breakthrough bleeds.

5.3.2 FVIII-Loaded HyPEMs Result in Increased Fibrin Production Compared to Systemic fVIII in a Microfluidic Vascular Injury Model Using fVIII-Inhibited Blood

Efficacy of the system was first evaluated by assessing the extent of fibrin formation (the final product of the coagulation cascade) utilizing a microfluidic vasculature model previously reported in the literature with several modifications.[192] The microfluidic device contains a collagen/tissue factor patch in the middle of the channel to enable a defined

region for coagulation for image quantitation. First, a vacuum-bound microfluidic was used in the reported device to both print the collagen/tissue factor patch as well as to form the perpendicular channels during sample perfusion over the patch. For simplicity, an adhesive-bound microfluidic was used in this work to form the perpendicular channels during sample perfusion. Second, the reported device used 4 μg/mL corn trypsin inhibitor (CTI) as the sole anticoagulant and perfused whole blood through the 20 minute experiment. The use of CTI was attempted in this work, which occasionally worked (Figure 29A); however, it resulted in passive platelet aggregation in the tubing, which perfused into the channel causing massive artificial aggregation on the patch, and in several cases, caused the forming clot to rip off of the patch (Figure 29B,C). Varying CTI concentrations (4 and 8 μg/mL), calcium concentrations (5, 8, and 10 mM), shear rates (100, 500, and 1,000 s^{-1}), and perfusion durations (10, 15, and 20 minutes) were tried in the presence of CTI, seldom with positive outcomes (*i.e.* coagulation without artificial platelet aggregation). CTI in the presence of citrate and heparin reversed by protamine sulfate were tried as alternative anticoagulants, but yielded results similar to CTI alone or did not enable fibrin formation. As such, citrated whole blood (recalcified) was perfused over the patch for 10 minutes in order for platelets to sufficiently adhere to the patch. This was followed by perfusion of citrated PPP (recalcified) to enable fibrin formation. Removing platelets effectively removed the problem of artificial aggregation and false positive effects in fibrin formation enhancement.

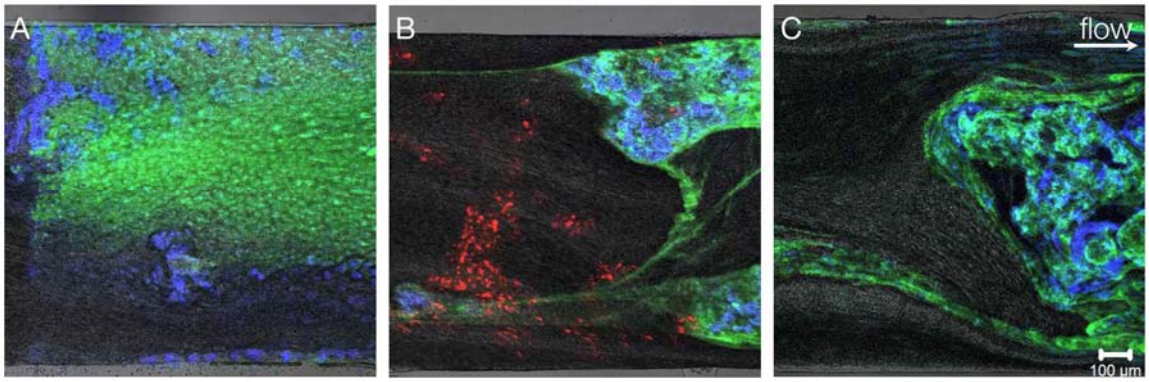

Figure 29. Confocal micrographs of the left side of the collagen and tissue factor patch show inconsistent fibrin and platelet formation during perfusion of whole blood utilizing corn trypsin inhibitor as the anticoagulant. Images were taken during perfusion wherein (A) normal platelet aggregation and fibrin formation was occasionally seen on the patch area. However, the majority of the time platelet aggregates perfusing out of the tube (B) ripped the forming clot off of the patch or (C) adhered onto the patch resulting in an inaccurate increase in platelet aggregation and fibrin formation. Platelets were stained with CD41a-APC (blue), fibrin with 59D8-AF488 (green), and fVIII loaded PEM capsules with fVIII-RBITC (red).

This optimized device enables fluorescence-based quantitation of platelet adherence to and fibrin formation on a patch of collagen and tissue factor printed in the middle of the microfluidic channel (Figure 30A).[1] Healthy patient samples were used to investigate the effects that different components of the PEM capsule formulation had on efficacy. It was hypothesized that the dextran layer was required for "burst" release of fVIII, fibrinogen was required for platelet hybridization and patch targeting, and fVIII was required for efficacy. PEM capsules were loaded with fVIII *via* encapsulation into the calcium carbonate core. Fibrin intensity on the patch (determined using the fibrin-specific antibody, mAb 59D8-AF488)[193] normalized to patch area and platelet density was used as a downstream indicator of fVIII efficacy (Figure 30B).[1]

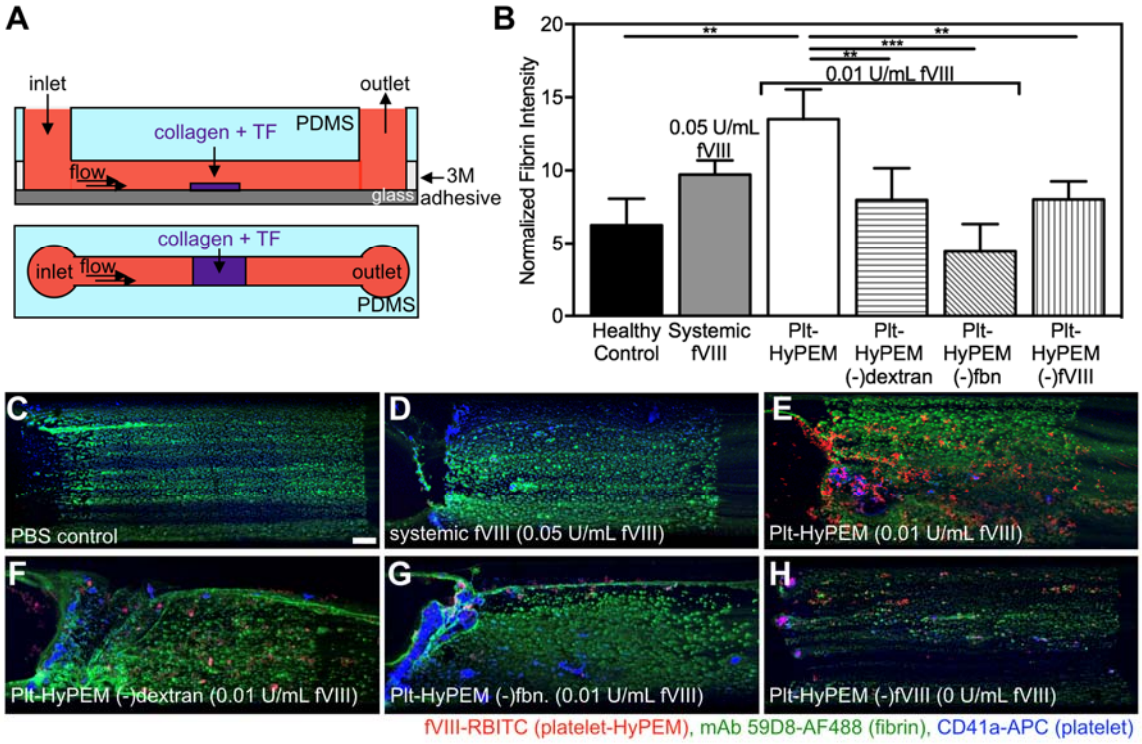

Figure 30. Microfluidic vascular injury model using healthy samples show fVIII loaded platelet-HyPEM result in increased fibrin formation. (A) A schematic of the microfluidic showing cross sectional (top) and top-down (bottom) perspectives with the collagen/tissue factor patch in the middle of the channel in purple shown. Quantitative analysis was performed by normalizing fibrin intensity to platelet intensity and patch area (B). Tiled confocal micrographs of the patch are shown for the healthy control condition (C), 0.05 U/mL systemic fVIII (D), and 0.01 U/mL fVIII loaded platelet-HyPEMs: in the full formulation (E), without dextran (F), without fibrinogen (G), and without fVIII (0 U/mL fVIII) (H). Fibrin, platelets, fVIII loaded platelet-HyPEMs, and empty platelet-HyPEMs were labeled with mAb 59D8-AF488 (green), CD41a-APC (blue), fVIII-RBITC (red), and PLL-RBITC (red), respectively. Results are represented by the mean ± SD, n = 3-4. Statistical significance: **p<0.01 and ***p<0.001 compared to 0.01 U/mL fVIII loaded platelet-HyPEM. A total of 8 donors were used. Scale bar = 200 µm.

Both the healthy control (Figure 30C) and systemic fVIII (Figure 5D) expectedly result in less fibrin formation, normalized fibrin intensity of 6.3 ± 1.8 and 9.7 ± 1.0, respectively, compared to the full platelet-HyPEM formulation, 13.5 ± 2.0 (Figure 30E).[1] All platelet-HyPEMs missing one component of the full formulation also produce less fibrin than the full platelet-HyPEM formulation. Platelet-HyPEMs without dextran (Figure

30F), without fibrinogen (Figure 30G), and without fVIII (Figure 30H) result in a normalized fibrin intensity of 8.0 ± 2.2, 4.4 ± 1.9, and 8.0 ± 1.2 respectively.[1] This data suggests that all components of the platelet-HyPEM formulation (dextran layer, fibrinogen, and of course loaded fVIII) are necessary for the operational drug delivery system.

The efficacy of platelet-HyPEMs was then investigated using fVIII-inhibited blood by adding the fVIII inhibitory antibody (mAb 2-76)[191] to the samples in order to mimic the conditions of hemophilia A with inhibitors. The PPP perfusion time was increased to 50 minutes to allow sufficient fibrin formation for quantitative comparison (Figure 30A). Two concentrations of systemic fVIII (0.05 U/mL and 0.5 U/mL) were investigated that represent 5% and 50% normal plasma activity levels, respectively (Figure 30B,C). The normalized fibrin intensity of 0.05 U/mL systemic fVIII is 0.1 ± 0.05, which increased to 0.5 ± 0.3 when the fVIII systemic concentration increased to 0.5 U/mL fVIII.[1] When platelet-HyPEMs loaded with 0.01 U/mL fVIII (Figure 30D) were used, the normalized fibrin intensity increases to 1.9 ± 0.6, which is a 3.8x increase compared to 0.5 U/mL systemic fVIII.[1] Notably, this significant increase occurs even though the fVIII concentration used in the platelet-HyPEMs was over an order of magnitude less than the fVIII concentration used for systemic exposure.

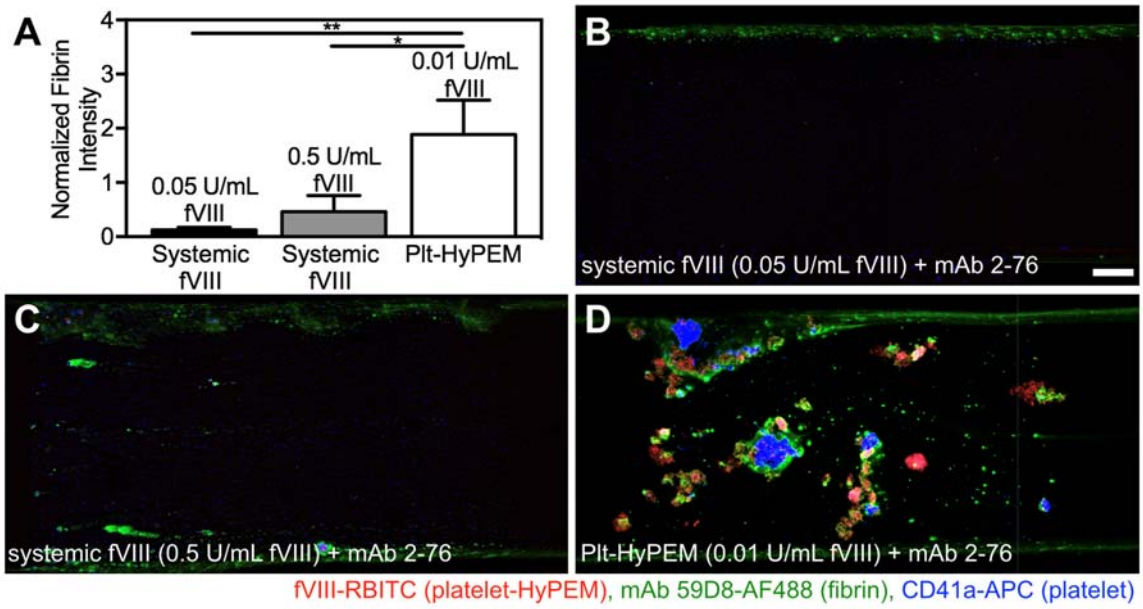

Figure 31. Microfluidic vascular injury model using fVIII-inhibited samples showed platelet-HyPEMs increased fibrin formation by a factor of 3.8. Quantitative analysis was performed by normalizing fibrin intensity to platelet intensity and patch area (A). Tiled confocal micrographs of the patch are shown for 0.05 U/mL systemic fVIII (B), 0.5 U/mL systemic fVIII (C), and 0.01 U/mL fVIII loaded platelet-HyPEMs (D). Fibrin, platelets, and fVIII loaded platelet-HyPEMs were labeled with mAb 59D8-AF488 (green), CD41a-APC (blue), and fVIII-RBITC (red), respectively. Results are represented by the mean ± SD, n = 3. Statistical significance: *p<0.05 and **p<0.01 compared to 0.01 U/mL fVIII loaded platelet-HyPEM. A total of 5 donors were used. Scale bar = 200 µm.

For comparison to clinically used treatments, addition of systemic fVIIa as the pro-coagulant was investigated with fVIII-inhibited blood in the same microfluidic design. During the first 10 minutes wherein whole blood was perfused, significant deposition of single platelets as well as platelet aggregates could be seen. Fibrin formation during the last couple of minutes of whole blood perfusion was also witnessed. As this was not witnessed during whole blood perfusion for the healthy patient sample conditions, this indicated a substantial pro-coagulant environment, especially within the context of a bleeding disorder. At the end of the 10-minute perfusion, the platelets in the front (left side) of the patch had aggregated into one vast aggregate, such that all the platelets in that region

of the patch were consolidated into the aggregate to occlude the entire width of the microfluidic channel (1 mm) (Figure 32). While this experimental condition was the only conducted once, the initial *in vitro* results substantiate concerns of using fVIIa in the clinic for potential risk of thrombotic side effects.

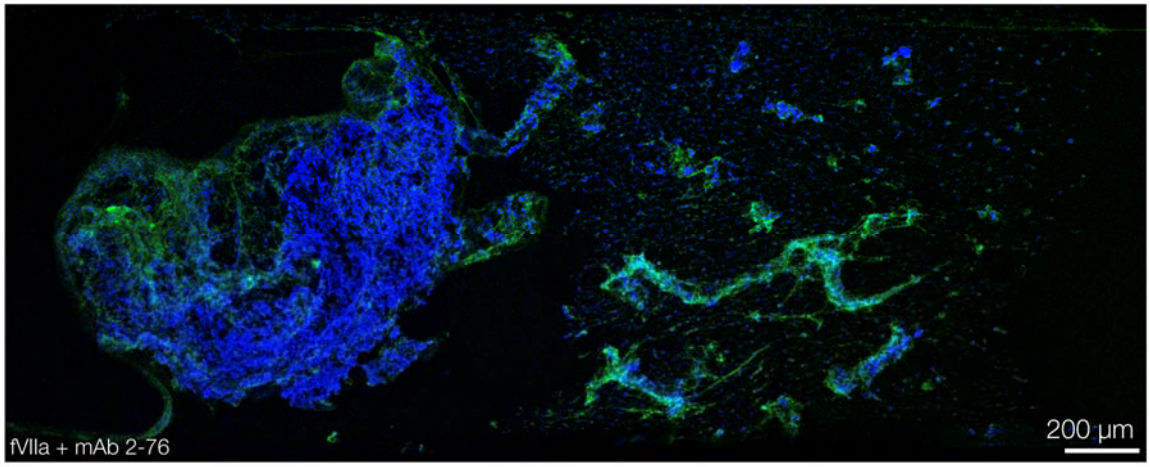

Figure 32. Microfluidic vascular injury model demonstrates the thrombotic risk of using activated factor VII (fVIIa) as the pro-coagulant in fVIII-inhibited blood. A tiled confocal image shows substantial thrombosis and microchannel occlusion seen after perfusion of fVIII-inhibited blood with fVIIa for 10 minutes over the collagen-tissue factor patch. Platelets (CD41a-APC) and fibrin (59D8-AF488) are seen in blue and green, respectively.

5.3.3 FVIII-Loaded HyPEMs Shortened Clot Formation Time in the Presence of fVIII Inhibitors Compared to Systemic fVIII

While the microfluidic model demonstrated fVIII loaded HyPEMs increased fibrin formation in the presence of fVIII inhibitors compared to systemic controls, there are limitations correlating fibrin formation with formation of a stable clot. To that end, we monitored clot formation on the bulk scale using a previously reported well plate assay to determine the clot formation time for various conditions.[194] PEM capsules were loaded with commercially available recombinant fVIII (ADVATE) *via* diffusion. Wells were

loaded with WB and were washed at specific time intervals, leaving insoluble blood clot products behind. A stable clot was considered formed when the bottom of the well was completely covered with insoluble blood clot products. Utilizing this method, we determined the clotting times of two control conditions (healthy and mAb 2-76 fVIII-inhibited) and several conditions in the presence of mAb 2-76 fVIII inhibitor: 0.5 U/mL systemic fVIII, 0.25 U/mL fVIII loaded platelet-HyPEMs, 0.5 U/mL fVIII loaded platelet-HyPEMs, and 0.5 U/mL fVIII loaded platelet-HyPEMs with 10 μM blebbistatin (Figure 33).

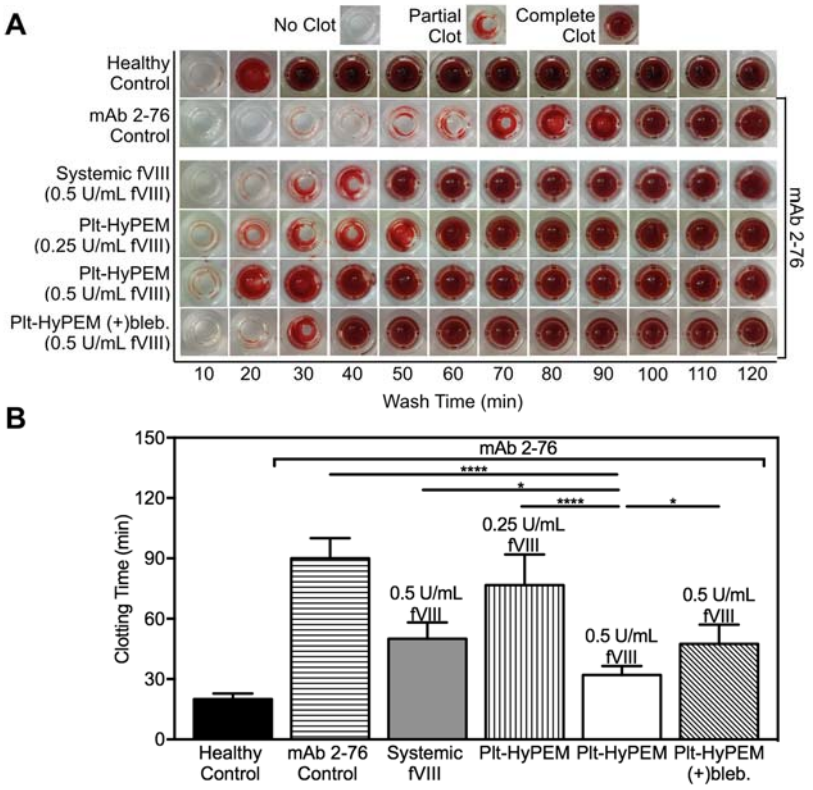

Figure 33. Clot formation analysis showed 0.5 U/mL fVIII loaded platelet-HyPEMs approached clotting time of healthy samples. Images of individual wells that were washed at 10-minute intervals showing progression of clot formation are shown (A). Average clotting times were calculated (B) for healthy control and mAb 2-76 inhibited conditions: control, 0.5 U/mL systemic fVIII, 0.25 U/mL fVIII loaded platelet-HyPEMs, 0.5 U/mL fVIII loaded platelet-HyPEMs, and 0.5 U/mL fVIII loaded

platelet-HyPEMs in the presence of blebbistatin (bleb.). Results are represented by the mean ± SD of clotting times, n = 3-5. Statistical significance: *p<0.05 and ****p<0.0001 compared to 0.5 U/mL fVIII loaded platelet-HyPEMs. A total of 6 donors were used.

The average clotting time of fVIII-inhibited samples with 0.5 U/mL fVIII loaded platelet-HyPEMs is 32 ± 4 minutes.[1] This is 58 minutes faster than mAb 2-76 inhibited control conditions (90 ± 10 minutes) and 18 minutes faster than 0.5 U/mL systemic fVIII condition (50 ± 8 minutes).[1] Wells loaded with 0.25 U/mL fVIII loaded platelet-HyPEMs only decrease clotting time slightly to 76 ± 15 minutes, indicating the higher dose of 0.5 U/mL fVIII is necessary to overcome fVIII inhibition in static conditions.[1]

To further confirm that platelet contraction is necessary for delivery of fVIII from the platelet-HyPEMs, 10 μM blebbistatin (a myosin inhibitor that prevents platelet contraction but not adhesion to fibrinogen)[69] was added along with 0.5 U/mL fVIII loaded platelet-HyPEMs in the presence of fVIII inhibitor. Addition of blebbistatin results in a statistically significant increase in clotting time (48 ± 10 minutes, $p<0.05$) compared to the condition of fVIII loaded platelet-HyPEMs without blebbistatin, indicating platelet contraction is necessary for the full therapeutic release of fVIII.[1] Furthermore, there is no statistically significant difference between the clotting time of 0.5 U/mL systemic fVIII and 0.5 U/mL fVIII loaded platelet-HyPEMs with blebbistatin, suggesting the decrease in clotting time compared to the mAb 2-76 control is due to the fVIII that had diffused out of the platelet-HyPEM during the assay, mimicking systemic exposure, and not a "burst" release of the full encapsulated fVIII payload.

5.4 Conclusions

In summary, I have developed PEM capsules that are biochemically, mechanically, and structurally tuned to enable platelet-mediated controlled delivery. Fibrinogen is effectively displayed on the PEM capsule exterior and enables platelet adherence and formation of the platelet-HyPEMs. The LbL fabrication provides a facile manner in which to tune the mechanical properties through the number of deposited polyelectrolyte layers, mitigating platelet activation upon hybridization and facilitating PEM capsule rupture upon activated platelet contraction. Finally, incorporating the dextran layer adapts the structural properties to facilitate the "burst" release of the encapsulated biotherapeutic payload, fVIII, after rupture. It should be noted, however, that the LbL fabrication process is very time consuming and requires substantial material resources, and as such, may not translate well to the manufacturing scale-up necessary for commercial production. Significant development in manufacturing process of PEM capsules is thus required to develop a method that imparts the same mechanical and biochemical properties of the construct while using less material and is automated to both reduce human labor and minimize batch-to-batch variation.

I have shown that platelet-HyPEMs loaded with fVIII increase fibrin formation in both healthy and fVIII-inhibited blood compared to systemic delivery of fVIII. Furthermore, fVIII loaded platelet-HyPEMs decrease clotting time for fVIII-inhibited samples towards the clotting time regime of a healthy patient. Our *in vitro* results suggest that platelet-HyPEMs loaded with fVIII have potential to be developed into an efficacious treatment method for hemophilia A patients with inhibitors because the encapsulated fVIII is protected from inhibitor binding, enabling a targeted "burst" release of fVIII to quickly rescue hemostasis. The targeted "burst" release enabled by activated platelet contractile

forces provides an advantage over other nanoparticle-based delivery systems for fVIII in the presence of inhibitors. While it was reported that adsorbing fVIII onto soy phosphatidylinositol (PI)-containing lipid nanoparticles decreased the ability of fVIII inhibitors to bind to the fVIII protein (fVIII antibody binding domains are thought to be protected in the lipid layer), release of full fVIII dose is reliant upon desorption of the protein and redistribution between the PI nanoparticles, vWF, inhibitor, and its free form.[186] This prevents the full dose from being effectively available immediately after administration. Moreover, the PI-nanoparticles do not include a targeting moiety, which results in fVIII desorbing in non-target areas without the ability to significantly accumulate at a target area. In contrast, our targeted system protects the full, encapsulated fVIII protein from inhibitor binding during circulation and can theoretically deliver 70% of the initial fVIII dose upon activated platelet contraction at the injured site within 2 hours after administration.

Development of a targeted drug delivery system that leverages platelet contractile force as the delivery mechanism represents a paradigm shift for targeted drug delivery systems. In this system, platelets are used as "smart micromachines" enabling sensing of the target site when exposed to soluble platelet activators and then delivery upon mechanical contraction. This is a more active approach to targeted drug delivery because it enables immediate delivery of high, localized dosages to quickly augment hemostasis, especially when compared to other targeted systems that rely on diffusive release, chemical or enzymatic dissolution, or the use of external equipment (*i.e.* lasers or magnets). While this was a clearly useful drug delivery system for fVIII in the presence of inhibitors, we believe this can further be applied to deliver other pro-clotting agents, thrombolytics,

oncolytic agents, and therapies to combat infection as platelets are involved in mediating thrombosis, cancer, and immunity as well.

CHAPTER 6. FUTURE WORK

6.1 Scalable Manufacturing Method for PEM capsules

While the LbL self-assembly fabrication method for PEM capsules enables substantial tunability on the mechanical, biochemical, and architectural properties, it does not lend itself well to large-scale manufacturing because it is extremely time intensive, requires a large amount of excess materials, and the human involvement for every step imparts the opportunity for substantial batch-to-batch variability. Therefore, development of a scalable manufacturing method is critical in for the translational potential of this technology into the clinic in terms of the feasibility as a potential acquisition for a large pharmaceutical company and meeting stringent design and quality guidelines for the FDA.

Microfluidics offer a promising strategy to fabricate microcapsules with high fidelity and yield. For this sub-milestone, we will develop a microfluidics-based reactor to provide a scalable manufacturing process that yields homogenous PEM microcapsules. The chip will consist of reactors for each layer deposition and will be connected with microfluidic channels that separate the microcapsules from polyelectrolyte solution in between layer deposition steps to prevent aggregation (Figure 34). Several devices in the literature have shown microfluidic channels can be constructed to separate blood cells based on size.[195-197] We plan to use these designs to purify the forming microcapsules from the polyelectrolyte solution between each reactor (layer deposition).

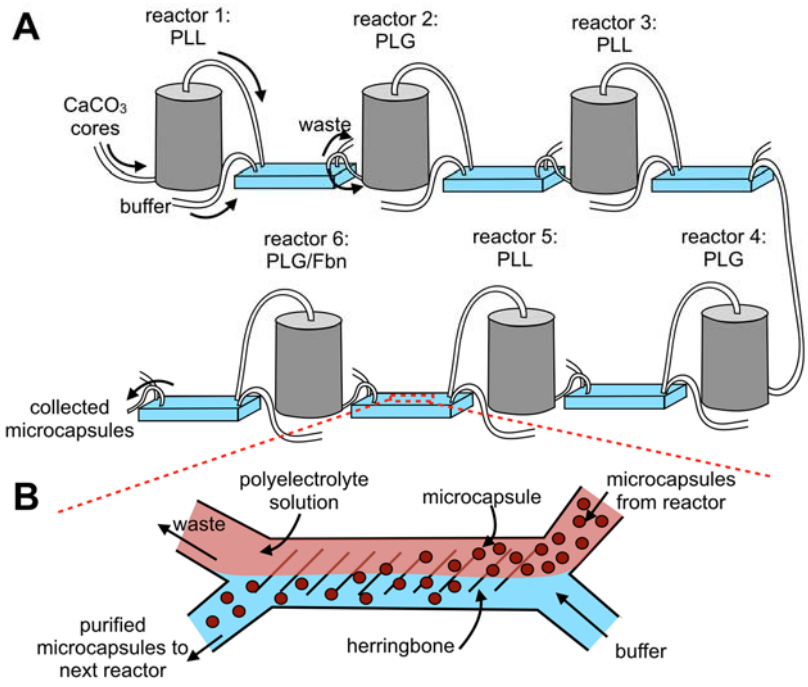

Figure 34. Schematic of a continuous-flow microreactor for PEM capsule fabrication. (A) Calcium carbonate cores are perfused into the microreactors where the polyelectrolyte layer is deposited. (B) The particles then continue to perfuse into the separation microfluidic to replace the polyelectrolyte solution with fresh buffer. This is repeated in a continuous fashion until the desired number of layers have been deposited.

The flow rates, calcium carbonate core concentration, and polyelectrolyte concentrations will be optimized to yield microcapsules that exhibit properties similar to those fabricated via LbL deposition. Of particular concern is the amount of fibrinogen deposited onto the microcapsule and thickness of the polyelectrolyte wall as these biochemical and physical parameters directly affect platelet adhesion onto the microcapsule and their ability to rupture the microcapsule wall once activated and contracting. To investigate the amount of deposited fibrinogen, we will use fluorescent fibrinogen and determine the fluorescence intensity of the PEM microcapsule solution after fabrication. To determine polyelectrolyte wall thickness, we will use fluorescent poly-l-

lysine and measure wall thickness using a super resolution confocal microscope. SEM and AFM will be used as additional methods to super resolution confocal microscopy to measure wall thickness.

A potential pitfall for this strategy is if the calcium carbonate core or forming microcapsules adhere to the reactor or microfluidic channels during flow and fabrication due to their substantial charge. Not only would this block flow in the device, but also aggregation will result in large PEM microcapsules that are heterogeneously formed. Solutions to this problem include incorporating surfactant into the PDMS channels (i.e. pluronic) and constructing the reactors out of materials with either minimal charge or like charge of the polyelectrolyte solution being deposited.

6.2 *In Vivo* Delivery of fVIII in Hemophilia A Mouse Models with Inhibitors

Genetically engineered hemophilia mice are the gold standard animal model in evaluating pro-clotting drugs for hemophilia. Specifically, evaluating efficacy of pro-clotting drugs in the tail-clip model has shown excellent correlation to performance in humans.[198,199] Furthermore, these mice can be conditioned with repetitive exposure of fVIII to produce fVIII inhibitory antibodies with inhibition behavior similar to human antibodies.[191,200,201] This model will be used to investigate safety and preliminary efficacy of our system in comparison to the current clinically used treatment options (i.e. heavy dosing of fVIII and fVIIa). These studies will be conducted in collaboration with Dr. Shannon Meeks at Emory University, who not only has vast experience in these models, but is also a leader in the fields of fVIII inhibitors and development of recombinant fVIII therapies.

The first area of investigation using the mouse model will be initial safety of the PEM microcapsules after intravenous administration. As the PEM microcapsules are on the size-scale of individual blood cells and are loaded with a pro-clotting drug, thrombotic side effects due to microvascular occlusion are a concern. An experimental condition injecting empty PEM microcapsule will first be investigated to ensure the size of the PEM microcapsules will not cause occlusive or thrombotic events. PEM capsules at 100,000 or 50,000 particles/mL will be injected into the mice once weekly for 4 weeks, followed by an off week and a double dose injection on the 6^{th} week. Mice will be monitored for physical signs of distress throughout the 6 weeks. At the end of the 6 weeks, mice will be sacrificed and blood will be collected (*via* cardiac puncture) for complete blood cell counts and measurement of thrombin-antithrombin complex concentration. Once it is established that PEM microcapsules do not cause vascular blockage, mice will be anesthetized and injected with fVIII-loaded PEM microcapsules. Again, safety of the construct will first be investigated before efficacy in any injury models.

After safety of the microcapsules has been established, preliminary efficacy will be investigated using a tail-clip model. Several controls will needed to be used here to evaluate potential for clinical utility and superiority. These controls include: fVIIa (NovoSeven®), FEIBA ®, and porcine fVIII (Obizur®). After efficacious dosages have been identified, investigations to determine pharmacokinetics, pharmacodynamics, and full investigation of platelet hybridization (activation of platelets and persistence of the construct) will be conducted.

A possible pitfall is if the PEM microcapsules occlude any blood vessel and result in thrombotic symptoms. If this occurs, we will investigate using smaller PEM microcapsules

in the size range of 100-500 nm. These can be easily achieved by using polystyrene cores instead of calcium carbonate cores to template fabrication, which can be removed in a similar manner as the calcium carbonate cores (organic solvents or acid treatment). Similarly, unilamellar liposomes decorated with fibrinogen can be investigated as an alternative drug-carrying vehicle as they are a common drug delivery vehicle and have achieved FDA approval in several drug formulations. Platelet adhesion and rupture will need to be confirmed for these smaller alternative architectures if this route is necessary.

6.3 Delivery of Thrombolytic Biotherapeutics to Treat Pulmonary Embolism

Heart disease is a leading cause of mortality in Western countries. Therapies that breakup blood clots that have caused myocardial infarction, pulmonary embolism, deep vein thrombosis, or stroke are either small molecules (i.e. warfarin) or biotherapeutics (i.e. tissue plasminogen activator (tPA) or streptokinase) that are delivered systemically.[11,14] While many of the small molecules are prescribed prophylactically to prevent recurring thrombosis, large doses of the biotherapeutics are required immediately after a thrombotic event. Because of the potential hemorrhagic side effects that are associated with tPA, there exists a fairly restrictive time frame (3 hours for stroke and 12 hours for heart attack) in which it can be administered in large doses.[15] Furthermore, streptokinase, which exhibits a longer half-life (biphasic half-life of 18 and 83 minutes compared to 5 minutes of tPA), has been shown to cause immunomodulatory response, limiting its clinical utility.[202]

Initial *in vitro* experiments determining its fibrinolytic potential using static gel model have been conducted (Figure 35). Fibrinogen, low-melting point agar, and thrombin were mixed together in TRIS buffer and poured into petri dishes. The gels were incubated

at 37 °C for 2 hours to make the fibrin-agar gel then cooled to room temperature. Holes were punched into the gel and loaded with PRP, 5 mM calcium, 2 mM magnesium, 12 pM tissue factor, and the experimental condition (PBS as a control, 500 ng/mL free tPA, and PEM capsules loaded with 500 ng/mL tPA via diffusion). The gels were then incubated at 37 °C overnight. The area of each well was determined via ImageJ. Fibrinolysis resulted in increase of the well area due to degradation of peripheral fibrin in the gel around the well.

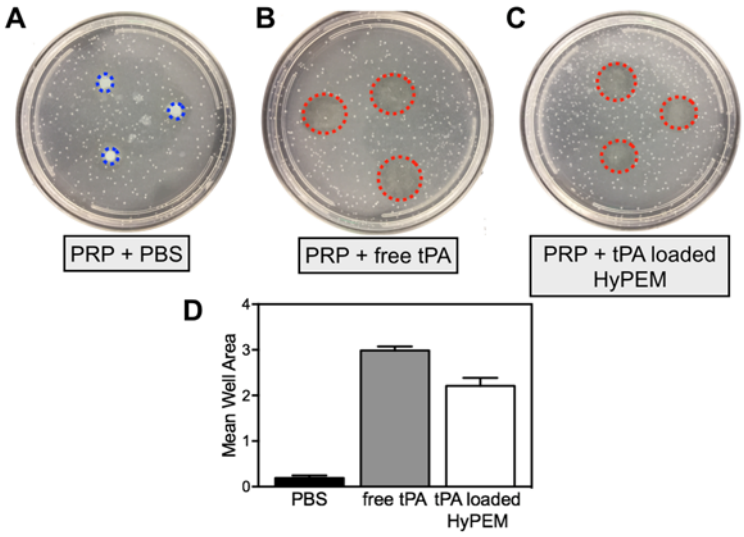

Figure 35. Fibrinolysis in fibrin-agar gels demonstrate fibrinolytic activity of tissue plasminogen activator (tPA). Wells were punched in fibrin-agar gels and loaded with (A) platelet rich plasma (PRP) with PBS, (B) PRP with 500 ng/mL free tPA, and (C) PRP with 500 ng/mL tPA loaded HyPEMs. Gels were then incubated overnight, and (D) the mean area of the wells was determined to evaluate the extent of tPA-induced fibrinolysis.

Significant fibrinolysis can be seen for both free tPA and tPA loaded PEM capsules, though there is more fibrinolysis with the free tPA condition, as evidenced by the higher mean well area. Despite that tPA loaded PEM capsules do not perform as well as the free tPA in this assay, these are motivating initial results encouraging further studies into this

application. While efficacy might not be as high for tPA, it may extend half-life of the therapeutic, decrease potential hemorrhagic side effects, and possible modulate adverse immune response seen in streptokinase. Further studies determining lysis time of whole blood clots and extent of clot lysis in microfluidic experimental setups should be conducted.

APPENDICES

Appendix A: Primary Hemostasis

Platelets marginate to the blood vessel wall during circulation due to their size, which facilitates their function as the "first responders" to an injury on the vascular wall. Platelets are recruited to the site of injury through several mechanisms: adhesion to the newly exposed sub-endothelial matrix proteins, adhesion to the platelet plug, or adhesion to fibrin of a nascent clot. Once a vascular injury occurs, sub-endothelial matrix proteins are exposed (*i.e.* collagen, vWF, and fibronectin), enabling platelet adhesion through specific glycoproteins (GP) and integrins on the platelet surface. GPIa/IIa, also known as integrin $\alpha_2\beta_1$, and GPVI adhere to collagen. GPIc/IIa ($\alpha_5\beta_1$), and GPIIb/IIIa ($\alpha_{IIb}\beta_3$) bind fibronectin while GPIIb/IIIa ($\alpha_{IIb}\beta_3$) and $\alpha_5\beta_3$ bind fibrinogen. GPIb, $\alpha_5\beta_3$, and GPIIb/IIIa ($\alpha_{IIb}\beta_3$) bind to vWF. Receptor binding to these proteins initiates a contact-mediated outside-in pathway of platelet activation by inducing a conformational change in the receptor. Platelets spread into irregular shapes through multiple pseudopods as a downstream result of this activation.

Their activation also results in secretion of dense granules (serotonin, calcium, ADP, ATP, and CD63) and alpha granules (mixture of adhesive proteins, procoagulants, anticoagulants, anti-lytic factors, anti-heparins, and growth-promoting factors).[64] The proteins and compounds released in these granules serve to induce vasoconstriction, mediate the clotting response, promote tissue healing pathways, and further recruit activated platelets to the injury site. Inside-out signaling can occur when platelets are

exposed to soluble clotting factors (*i.e.* ADP or thrombin, a procoagulant enzyme produced in the coagulation cascade), which bind to their respective receptors on the platelet membrane surface. The transmission of binding events through the cytoplasm results in the conformational change in the $\alpha_{IIb}\beta_3$ integrin and subsequent platelet activation. Importantly, these platelets are then allowed to bind fibrinogen and vWF to their respective receptors, which act as ligands to adhere to adjacent platelets, thereby facilitating platelet aggregation at the injury site to form a platelet plug that initially functions to stem bleeding.

During the formation of the platelet plug, the coagulation cascade begins, resulting in the production of thrombin to polymerize fibrinogen into fibrin, which is integral to clot porosity and stiffness.[64] Red blood cells and platelets adhere to the forming fibrin network, which enhances the integrity of the clot structure. Platelets can additionally be activated through this binding event, as fibrin binds to the $\alpha_{IIb}\beta_3$ integrin. An additional response of platelet activation is platelet contraction on the fibrin fibers of which they are adhered. This occurs when the platelet's myosin light chain is phosphorylated, which induces a contractile force through the myosin heavy chain to actin filaments. This contractile force is transmitted from inside the cell to outside the cell and propagates through fibrin network because the actin filaments are attached to the $\alpha_{IIb}\beta_3$ integrin, which are adhered to fibrin fibers in the clot. Clot contraction enhances the mechanical robustness of the clot by further increasing stiffness and decreasing porosity. It also brings the vascular walls closer together to further stem bleeding and enhance tissue regrowth and wound healing at later time points.

Appendix B: The Coagulation Cascade

The coagulation cascade is a complex response mechanism wherein plasma zymogens are converted into their enzymes, towards the end result of producing thrombin to cleave fibrinogen and form the fibrin network within the clot structure. Several steps within the clotting cascade require interaction of a negatively charged phospholipid membrane (*i.e.* as seen on activated platelets or endothelial cells) and activated co-factors. There are traditionally two coagulation pathways which merge at the critical thrombin production step: the extrinsic and intrinsic pathways.

The extrinsic pathway is initiated when damaged endothelial cells express the membrane glycoprotein, tissue factor, which acts as a cofactor to activated factor VII (fVIIa).[64] Tissue factor binds fVIIa to fully expose its activation site, which enhances its enzymatic activity to produce more fVIIa, as well as activation of factor X and factor IX. Production of fXa and fIXa enables the conversion of prothrombin to thrombin. While the concentration of thrombin produced is not sufficient enough to maintain hemostasis due to the negative feedback of tissue factor pathway inhibitor (secreted by endothelial cells and activated platelets), it is sufficient enough to initiate the intrinsic pathway. An additional negative feedback loop exists for the extrinsic pathway wherein circulating antithrombin covalently binds to the active sites of fXa and thrombin, resulting in its deactivation and clearance.

The classical intrinsic pathway begins when thrombin produced from the extrinsic pathway cleaves fXI to fXIa, which then activates fIX to fIXa. In addition, thrombin also activates the cofactors fVIII (requiring first dissociation from vWF with which it circulates) and fV to their activated forms, fVIIIa and fVa.[64] The tenase complex is then formed when fVIIIa, fIXa, and calcium associate on a phospholipid surface. This complex activates fX

to fXa, which then associates with fVa and calcium on a phospholipid surface to form prothrombinase. This activated complex then converts prothrombin into thrombin, which cleaves the fibrinopeptides A and B off of the fibrinogen Aα and β chains, thus enabling fibrin formation through its self-assembly. Along with several additional positive feedback loops, thrombin cleaves fXIII to fXIIIa, which covalently crosslinks the fibrin fibers to enhance its stability. Thrombin also initiates negative feedback loops that block fVIII and fV activation through active protein C, to modulate the hemostatic response and prevent thrombosis.

Fibrinolysis is another mechanism within the hemostatic response that modulates clot formation to avoid pathologic clotting.[64] Tissue plasminogen activator (tPA) and urokinase-type plasminogen activator are enzymes that cleave the zymogen plasminogen into plasmin, which then activates matrix metalloproteins that dissolve the fibrin network. Both tPA and plasminogen have a binding affinity to fibrin, resulting in enhanced plasmin generation. Of course, there exist fibrinolysis inhibitors that function to prevent the cleavage of plasminogen into plasmin (plasminogen activator inhibitors 1 and 2), decrease the binding affinity of plasminogen and tPA to fibrin (thrombin-activatable fibrinolysis inhibitor (TAFI)), and inhibit unbound plasmin directly (α2-antiplasmin).

The contact pathway also plays a role in activation of the intrinsic pathway, although it is believed to be a relatively minor role for *in vivo* hemostatic response.[64] Interestingly, *in vitro* behavior of this pathway is drastically different, progressing through a slightly different pathway (relying on fXII) and resulting in a major activation response in coagulation assays compared to *in vivo* behavior. *In vivo,* the contact activation pathway

occurs when high molecular weight kininogen binds to cell-surface receptors, enabling association of prekallikrein and fXI. Cell-surface proteases then activate prekallikrein to kallikrein and fXI to fXIa. While fXIIa is not required, it is believed its presence may enhance the activation rate.

Appendix C: Bleeding and Clotting Disorders

Due to the integral and complex nature of both platelet function within clot formation and the coagulation cascade, genetic mutations affecting coagulation proteins or platelet function can have devastating effects that can result in life-threatening bleeding or clotting disorders. There are several known congenital diseases that result in dysfunctions in platelet function. Bernard-Soulier Syndrome occurs when platelets have defects in GPIb, causing interference in platelet binding to vWF, which results in prolonged bleeding times.[64] Glanzmann thrombathenia is characterized by dysfunctional or absent GPIIb/IIIa on platelets, severely affecting platelet aggregation and contraction. When transmembrane migration of phospholipids is defective, it is called Scott Syndrome and substantially decreases the ability for the tenase and prothrombinase components to assemble in the coagulation cascade. Wiscott-Aldrich syndrome occurs when defects in actin cytoskeleton exists, interfering with platelet's ability to form pseudopodia after adhering onto a substrate.

Several coagulation disorders exist due to congenital mutations in genes that encode for hemostatic proteins.[64] These include fXI deficiency, fX deficiency, fVII deficiency, fV deficiency, and prothrombin deficiency and all result in bleeding tendencies of varying severity. Infusion of donor plasma is typically the first option in treating severe bleeds for

these patients. Of particular note are fVIII, fIX, and von Willebrand deficiencies, which cause hemophilia A, hemophilia B, and von Willebrand disease, respectively. Infusion of plasma-derived or recombinant replacement factor is the standard of care for these patients; however, if the patient has developed inhibitory antibodies to the replacement factor, the treatment regime can become substantially more complicated and intense. On the opposite end of the spectrum, there are several congenital thrombophilias like antithrombin deficiency, protein C deficiency, and protein S deficiency that results in higher risks of venous thrombosis, which can cause myocardial infarction or stroke. If patients presenting signs of heart attack or stroke are diagnosed within a required time frame, they are intravenously administered a bolus dose of an antithrombotic (*i.e.* recombinant tPA) and are typically put on a less potent anticoagulant prophylactically (*i.e.* warfarin).

REFERENCES

(1) Hansen, C. E.; Myers, D. R.; Baldwin, W. H.; Sakurai, Y.; Meeks, S. L.; Lyon, L. A.; Lam, W. A. Platelet-Microcapsule Hybrids Leverage Contractile Force for Targeted Delivery of Hemostatic Agents. *ACS Nano* **2017**, *11*, 5579–5589.

(2) Deng, Z. J.; Morton, S. W.; Ben-Akiva, E.; Dreaden, E. C.; Shopsowitz, K. E.; Hammond, P. T. Layer-by-Layer Nanoparticles for Systemic Codelivery of an Anticancer Drug and siRNA for Potential Triple-Negative Breast Cancer Treatment. *ACS Nano* **2013**, *7*, 9571–9584.

(3) Tabernero, J.; Shapiro, G. I.; LoRusso, P. M.; Cervantes, A.; Schwartz, G. K.; Weiss, G. J.; Paz-Ares, L.; Cho, D. C.; Infante, J. R.; Alsina, M.; *et al.* First-in-Humans Trial of an RNA Interference Therapeutic Targeting VEGF and KSP in Cancer Patients with Liver Involvement. *Cancer Discov.* **2013**, *3*, 406–417.

(4) Seymour, L. W.; Ferry, D. R.; Anderson, D.; Hesslewood, S.; Julyan, P. J.; Poyner, R.; Doran, J.; Young, A. M.; Burtles, S.; Kerr, D. J. Hepatic Drug Targeting: Phase I Evaluation of Polymer-Bound Doxorubicin. *J. Clin. Oncol.* **2002**, *20*, 1668–1676.

(5) Li, S.-D.; Howell, S. B. CD44-Targeted Microparticles for Delivery of Cisplatin to Peritoneal Metastases. *Mol. Pharm.* **2010**, *7*, 280–290.

(6) Meng, H.; Xue, M.; Xia, T.; Ji, Z.; Tarn, D. Y.; Zink, J. I.; Nel, A. E. Use of Size and a Copolymer Design Feature to Improve the Biodistribution and the Enhanced Permeability and Retention Effect of Doxorubicin-Loaded Mesoporous Silica Nanoparticles in a Murine Xenograft Tumor Model. *ACS Nano* **2011**, *5*, 4131–4144.

(7) Xiong, X.-B.; Lavasanifar, A. Traceable Multifunctional Micellar Nanocarriers for Cancer-Targeted Co-Delivery of MDR-1 siRNA and Doxorubicin. *ACS Nano* **2011**, *5*, 5202–5213.

(8) Allen, T. M.; Cullis, P. R. Drug Delivery Systems: Entering the Mainstream. *Science* **2004**, *303*, 1818–1822.

(9) Bobo, D.; Robinson, K. J.; Islam, J.; Thurecht, K. J.; Corrie, S. R. Nanoparticle-Based Medicines: a Review of FDA-Approved Materials and Clinical Trials to Date. *Pharm. Res.* **2016**, *33*, 2373–2387.

(10) Ulbrich, K.; Holá, K.; Šubr, V.; Bakandritsos, A.; Tuček, J.; Zbořil, R. Targeted Drug Delivery with Polymers and Magnetic Nanoparticles: Covalent and Noncovalent Approaches, Release Control, and Clinical Studies. *Chem. Rev.* **2016**, *116*, 5338–5431.

(11) The National Institute of Neurological Disorders and Stroke rt-PA Stroke Study Group. Tissue Plasminogen Activator for Acute Ischemic Stroke. *N. Engl. J. Med.* **1995**, *333*, 1581–1588.

(12) Reynolds, P. S.; Michael, M. J.; Cochran, E. D.; Wegelin, J. A.; Spiess, B. D. Prehospital Use of Plasma in Traumatic Hemorrhage (the PUPTH Trial): Study Protocol for a Randomised Controlled Trial. *Trials* **2015**, *16*, 1693.

(13) Mitra, B.; Cameron, P. A.; Parr, M. J.; Phillips, L. Recombinant Factor VIIa in Trauma Patients with the "Triad of Death." *Injury* **2012**, *43*, 1409–1414.

(14) Plosker, G. L.; Lyseng-Williamson, K. A. Clopidogrel. *Drugs* **2007**, *67*, 613–646.
(15) Hacke, W.; Kaste, M.; Bluhmki, E.; Brozman, M.; Dávalos, A.; Guidetti, D.; Larrue, V.; Lees, K. R.; Medeghri, Z.; Machnig, T.; *et al.* Thrombolysis with Alteplase 3 to 4.5 Hours After Acute Ischemic Stroke. *N. Engl. J. Med.* **2008**, *359*, 1317–1329.
(16) Witmer, C. M.; Huang, Y.-S.; Lynch, K.; Raffini, L. J.; Shah, S. S. Off-Label Recombinant Factor VIIa Use and Thrombosis in Children: a Multi-Center Cohort Study. *J. Pediatr.* **2011**, *158*, 820–825.e821.
(17) Khan, S.; Allard, S.; Weaver, A.; Barber, C.; Davenport, R.; Brohi, K. A Major Haemorrhage Protocol Improves the Delivery of Blood Component Therapy and Reduces Waste in Trauma Massive Transfusion. *Injury 44*, 587–592.
(18) Jackman, R. P. Immunomodulation in Transfused Trauma Patients. *Curr. Opin. Anaesthesiol.* **2013**, *26*, 196–203.
(19) Murciano, J.-C.; Medinilla, S.; Eslin, D.; Atochina, E.; Cines, D. B.; Muzykantov, V. R. Prophylactic Fibrinolysis Through Selective Dissolution of Nascent Clots by tPA-Carrying Erythrocytes. *Nat. Biotech.* **2003**, *21*, 891–896.
(20) Zaitsev, S. Human Complement Receptor Type 1-Directed Loading of Tissue Plasminogen Activator on Circulating Erythrocytes for Prophylactic Fibrinolysis. *Blood* **2006**, *108*, 1895–1902.
(21) Absar, S.; Kwon, Y. M.; Ahsan, F. Bio-Responsive Delivery of Tissue Plasminogen Activator for Localized Thrombolysis. *J. Control. Release* **2014**, *177*, 42–50.
(22) Cherniakov, I.; Domb, A. J.; Hoffman, A. Self-Nano-Emulsifying Drug Delivery Systems: An Update of the Biopharmaceutical Aspects. *Expert Opin. Drug Deliv.* **2015**, *12*, 1121–1133.
(23) Becker, A. L.; Johnston, A. P. R.; Caruso, F. Layer-by-Layer-Assembled Capsules and Films for Therapeutic Delivery. *Small* **2010**, *6*, 1836–1852.
(24) Delcea, M.; Möhwald, H.; Skirtach, A. G. Stimuli-Responsive LbL Capsules and Nanoshells for Drug Delivery. *Adv. Drug Deliv. Rev.* **2011**, *63*, 730–747.
(25) Volodkin, D. V.; Petrov, A. I.; Prevot, M.; Sukhorukov, G. B. Matrix Polyelectrolyte Microcapsules: New System for Macromolecule Encapsulation. *Langmuir* **2004**, *20*, 3398–3406.
(26) Petrov, A. I.; Volodkin, D. V.; Sukhorukov, G. B. Protein-Calcium Carbonate Coprecipitation: A Tool for Protein Encapsulation. *Biotechnol. Prog.* **2008**, *21*, 918–925.
(27) Palankar, R.; Pinchasik, B.-E.; Schmidt, S.; De Geest, B. G.; Fery, A.; Möhwald, H.; Skirtach, A. G.; Delcea, M. Mechanical Strength and Intracellular Uptake of $CaCO_3$-Templated LbL Capsules Composed of Biodegradable Polyelectrolytes: The Influence of the Number of Layers. *J. Mater. Chem. B* **2013**, *1*, 1175–1181.
(28) Bray, G. L.; Gomperts, E. D.; Courter, S.; Gruppo, R.; Gordon, E. M.; Manco-Johnson, M.; Shapiro, A.; Scheibel, E.; White, G. 3.; Lee, M. A Multicenter Study of Recombinant Factor VIII (Recombinate): Safety, Efficacy, and Inhibitor Risk in Previously Untreated Patients with Hemophilia a. the Recombinate Study Group. *Blood* **1994**, *83*, 2428.

(29) Peyvandi, F.; Garagiola, I.; Young, G. The Past and Future of Haemophilia: Diagnosis, Treatments, and Its Complications. *Lancet* **2016**, *388*, 187–197.
(30) Scharrer, I.; Bray, G. L.; Neutzling, O. Incidence of Inhibitors in Haemophilia a Patients - a Review of Recent Studies of Recombinant and Plasma-Derived Factor VIII Concentrates. *Haemophilia* **1999**, *5*, 145–154.
(31) Astermark, J.; Donfield, S. M.; DiMichele, D. M.; Gringeri, A.; Gilbert, S. A.; Waters, J.; Berntorp, E. A Randomized Comparison of Bypassing Agents in Hemophilia Complicated by an Inhibitor: the FEIBA NovoSeven Comparative (FENOC) Study. *Blood* **2007**, *109*, 546–551.
(32) Ng, H. J.; Loh, Y. S. M.; Tan, D. C. L.; Lee, L. H. Thrombosis Associated with the Use of Recombinant Activated Factor VII: Profiling Two Events. *Thromb. Haemost.* **2004**, *92*, 1448–1449.
(33) Aledort, L. M. Comparative Thrombotic Event Incidence After Infusion of Recombinant Factor VIIa Versus Factor VIII Inhibitor Bypass Activity. *J. Thromb. Haemost.* **2004**, *2*, 1700–1708.
(34) Mathijssen, N. C. J.; Masereeuw, R.; Holme, P. A.; van Kraaij, M. G. J.; Laros-van Gorkom, B. A. P.; Peyvandi, F.; van Heerde, W. L. Increased Volume of Distribution for Recombinant Activated Factor VII and Longer Plasma-Derived Factor VII Half-Life May Explain Their Long Lasting Prophylactic Effect. *Thromb. Res.* **2013**, *132*, 256–262.
(35) Zhou, Z.-Y.; Koerper, M. A.; Johnson, K. A.; Riske, B.; Baker, J. R.; Ullman, M.; Curtis, R. G.; Poon, J.-L.; Lou, M.; Nichol, M. B. Burden of Illness: Direct and Indirect Costs Among Persons with Hemophilia a in the United States. *J. Med. Econ.* **2015**.
(36) Saenko, E. L.; Ananyeva, N. M.; Kouiavskaia, D. V.; Khrenov, A. V.; Anderson, J. A. M.; Shima, M.; Qian, J.; Scott, D. Haemophilia a: Effects of Inhibitory Antibodies on Factor VIII Functional Interactions and Approaches to Prevent Their Action. *Haemophilia* **2002**, *8*, 1–11.
(37) Torchilin, V. P. Passive and Active Drug Targeting: Drug Delivery to Tumors as an Example. In *Drug Delivery*; Handbook of Experimental Pharmacology; Springer Berlin Heidelberg: Berlin, Heidelberg, 2010; Vol. 197, pp. 3–53.
(38) Danhier, F.; Feron, O.; Préat, V. To Exploit the Tumor Microenvironment: Passive and Active Tumor Targeting of Nanocarriers for Anti-Cancer Drug Delivery. *J. Control. Release* **2010**, *148*, 135–146.
(39) Maeda, H.; Bharate, G. Y.; Daruwalla, J. Polymeric Drugs for Efficient Tumor-Targeted Drug Delivery Based on EPR-Effect. *Engineered polymers in controlled drug delivery and targeting* **2009**, *71*, 409–419.
(40) Upponi, J. R.; Torchilin, V. P. Passive vs. Active Targeting: an Update of the EPR Role in Drug Delivery to Tumors. In *Nano-Oncologicals*; Advances in Delivery Science and Technology; Springer International Publishing: Cham, 2014; pp. 3–45.
(41) Kim, I.-Y.; Kang, Y.-S.; Lee, D. S.; Park, H.-J.; Choi, E.-K.; Oh, Y.-K.; Son, H.-J.; Kim, J.-S. Antitumor Activity of EGFR Targeted pH-Sensitive Immunoliposomes Encapsulating Gemcitabine in A549 Xenograft Nude Mice. *J. Control. Release* **2009**, *140*, 55–60.
(42) Gao, J.; Zhong, W.; He, J.; Li, H.; Zhang, H.; Zhou, G.; Li, B.; Lu, Y.; Zou, H.;

Kou, G.; *et al.* Tumor-Targeted PE38KDEL Delivery via PEGylated Anti-HER2 Immunoliposomes. *Int. J. Pharm.* **2009**, *374*, 145–152.
(43) Gabizon, A.; Shmeeda, H.; Horowitz, A. T.; Zalipsky, S. Tumor Cell Targeting of Liposome-Entrapped Drugs with Phospholipid-Anchored Folic Acid–PEG Conjugates. *Adv. Drug Deliv. Rev.* **2004**, *56*, 1177–1192.
(44) Zhu, L.; Huo, Z.; Wang, L.; Tong, X.; Xiao, Y.; Ni, K. Targeted Delivery of Methotrexate to Skeletal Muscular Tissue by Thermosensitive Magnetoliposomes. *Int. J. Pharm.* **2009**, *370*, 136–143.
(45) Sawant, R. M.; Sawant, R. R.; Gultepe, E.; Nagesha, D.; Papahadjopoulos-Sternberg, B.; Sridhar, S.; Torchilin, V. P. Nanosized Cancer Cell-Targeted Polymeric Immunomicelles Loaded with Superparamagnetic Iron Oxide Nanoparticles. *J Nanopart Res* **2009**, *11*, 1777–1785.
(46) Su, Y.; Xie, Z.; Kim, G. B.; Dong, C.; Yang, J. Design Strategies and Applications of Circulating Cell-Mediated Drug Delivery Systems. *ACS Biomater. Sci. Eng.* **2015**, *1*, 201–217.
(47) Torchilin, V. P. Multifunctional, Stimuli-Sensitive Nanoparticulate Systems for Drug Delivery. *Nat Rev Drug Discov* **2014**, *13*, 813–827.
(48) Sawant, R. R.; Torchilin, V. P. Challenges in Development of Targeted Liposomal Therapeutics. *AAPS J.* **2012**, *14*, 303–315.
(49) Goldenbogen, B. R.; Brodersen, N.; Gramatica, A.; Loew, M.; Liebscher, J. R.; Herrmann, A.; Egger, H.; Budde, B.; Arbuzova, A. Reduction-Sensitive Liposomes From a Multifunctional Lipid Conjugate and Natural Phospholipids: Reduction and Release Kinetics and Cellular Uptake. *Langmuir* **2011**, *27*, 10820–10829.
(50) Xiong, M.-H.; Li, Y.-J.; Bao, Y.; Yang, X.-Z.; Hu, B.; Wang, J. Bacteria-Responsive Multifunctional Nanogel for Targeted Antibiotic Delivery. *Adv. Mater.* **2012**, *24*, 6175–6180.
(51) Lee, Y.-H.; Ma, Y.-T. Synthesis, Characterization, and Biological Verification of Anti-HER2 Indocyanine Green–Doxorubicin-Loaded Polyethyleneimine-Coated Perfluorocarbon Double Nanoemulsions for Targeted Photochemotherapy of Breast Cancer Cells. *Journal of Nanobiotechnology* **2017**, *15*, 41.
(52) Huang, F.; Liao, W.-C.; Sohn, Y. S.; Nechushtai, R.; Lu, C.-H.; Willner, I. Light-Responsive and pH-Responsive DNA Microcapsules for Controlled Release of Loads. *J. Am. Chem. Soc.* **2016**, *138*, 8936–8945.
(53) Tiukinhoy-Laing, S. D.; Huang, S.; Klegerman, M.; Holland, C. K.; McPherson, D. D. Ultrasound-Facilitated Thrombolysis Using Tissue-Plasminogen Activator-Loaded Echogenic Liposomes. *Thromb. Res.* **2007**, *119*, 777–784.
(54) Kawata, H.; Uesugi, Y.; Soeda, T.; Takemoto, Y.; Sung, J.-H.; Umaki, K.; Kato, K.; Ogiwara, K.; Nogami, K.; Ishigami, K.; *et al.* A New Drug Delivery System for Intravenous Coronary Thrombolysis with Thrombus Targeting and Stealth Activity Recoverable by Ultrasound. *Journal of the American College of Cardiology* **2012**, *60*, 2550–2557.
(55) Timin, A. S.; Muslimov, A. R.; Lepik, K. V.; Saprykina, N. N.; Sergeev, V. S.; Afanasyev, B. V.; Vilesov, A. D.; Sukhorukov, G. B. Triple-Responsive

Inorganic–Organic Hybrid Microcapsules as a Biocompatible Smart Platform for the Delivery of Small Molecules. *J. Mater. Chem. B* **2016**, *4*, 7270–7282.
(56) Ruan, S.; Cao, X.; Cun, X.; Hu, G.; Zhou, Y.; Zhang, Y.; Lu, L.; He, Q.; Gao, H. Matrix Metalloproteinase-Sensitive Size-Shrinkable Nanoparticles for Deep Tumor Penetration and pH Triggered Doxorubicin Release. *Biomaterials* **2015**, *60*, 100–110.
(57) Sanhai, W. R.; Sakamoto, J. H.; Canady, R.; Ferrari, M. Seven Challenges for Nanomedicine. *Nat Nano* **2008**, *3*, 242–244.
(58) Anselmo, A. C.; Gilbert, J. B.; Kumar, S.; Gupta, V.; Cohen, R. E.; Rubner, M. F.; Mitragotri, S. Monocyte-Mediated Delivery of Polymeric Backpacks to Inflamed Tissues: a Generalized Strategy to Deliver Drugs to Treat Inflammation. *J. Control. Release* **2015**, *199 IS* -, 29–36.
(59) Murdoch, C. Mechanisms Regulating the Recruitment of Macrophages Into Hypoxic Areas of Tumors and Other Ischemic Tissues. *Blood* **2004**, *104*, 2224–2234.
(60) Choi, K. Y.; Saravanakumar, G.; Park, J. H.; Park, K. Hyaluronic Acid-Based Nanocarriers for Intracellular Targeting: Interfacial Interactions with Proteins in Cancer. *Colloids Surf., B* **2012**, *99 IS* -, 82–94.
(61) Chen, H.; Kim, S.; He, W.; Wang, H.; Low, P. S.; Park, K.; Cheng, J.-X. Fast Release of Lipophilic Agents From Circulating PEG-PDLLA Micelles Revealed by In Vivo Forster Resonance Energy Transfer Imaging. *Langmuir* **2008**, *24*, 5213–5217.
(62) Han, H. S.; Choi, K. Y.; Ko, H.; Jeon, J.; Saravanakumar, G.; Suh, Y. D.; Lee, D. S.; Park, J. H. Bioreducible Core-Crosslinked Hyaluronic Acid Micelle for Targeted Cancer Therapy. *J. Control. Release* **2015**, *200*, 158–166.
(63) Gao, Y.; Xie, X.; Li, F.; Lu, Y.; Li, T.; Lian, S.; Zhang, Y.; Zhang, H.; Mei, H.; Jia, L. A Novel Nanomissile Targeting Two Biomarkers and Accurately Bombing CTCs with Doxorubicin. *Nanoscale* **2017**, *9*, 5624–5640.
(64) Israels, L.; Israels, E. *Mechanisms in Hematology*; Third. Core Health Services, Inc.: Concord, Ontario, Canada, 2002.
(65) Cohen, I.; De Vries, A. Platelet Contractile Regulation in an Isometric System. *Nature* **1973**, *246*, 36–37.
(66) Suzuki-Inoue, K.; Hughes, C. E.; Inoue, O.; Kaneko, M.; Cuyun-Lira, O.; Takafuta, T.; Watson, S. P.; Ozaki, Y. Involvement of Src Kinases and PLCγ2 in Clot Retraction. *Thromb. Res.* **2007**, *120*, 251–258.
(67) Myers, D. R.; Qiu, Y.; Fay, M. E.; Tennenbaum, M.; Chester, D.; Cuadrado, J.; Sakurai, Y.; Baek, J.; Tran, R.; Ciciliano, J. C.; *et al.* Single-Platelet Nanomechanics Measured by High-Throughput Cytometry. *Nat. Mater.* **2016**, *16*, 230–235.
(68) Lam, W. A.; Chaudhuri, O.; Crow, A.; Webster, K. D.; Li, T.-D.; Kita, A.; Huang, J.; Fletcher, D. A. Mechanics and Contraction Dynamics of Single Platelets and Implications for Clot Stiffening. *Nat. Mater.* **2011**, *10*, 61–66.
(69) Qiu, Y.; Brown, A. C.; Myers, D. R.; Sakurai, Y.; Mannino, R. G.; Tran, R.; Ahn, B.; Hardy, E. T.; Kee, M. F.; Kumar, S.; *et al.* Platelet Mechanosensing of Substrate Stiffness During Clot Formation Mediates Adhesion, Spreading, and Activation. *Proc. Natl. Acad. Sci. U.S.A.* **2014**, *111*, 14430–14435.

(70) Fries, D. The Early Use of Fibrinogen, Prothrombin Complex Concentrate, and Recombinant-Activated Factor VIIa in Massive Bleeding. *Transfusion* **2013**, *53*, 91S–95S.
(71) Girolami, A.; de Marinis, G. B.; Bonamigo, E.; Lombardi, A. M. Recombinant FVIIa Concentrate-Associated Thrombotic Events in Congenital Bleeding Disorders Other Than Hemophilias. *Hematology* **2013**, *17*, 346–349.
(72) Ravikumar, M.; Modery, C. L.; Wong, T. L.; Dzuricky, M.; Gupta, Sen, A., Ph.D. Mimicking Adhesive Functionalities of Blood Platelets Using Ligand-Decorated Liposomes. *Bioconjugate Chem.* **2012**, *23*, 1266–1275.
(73) Haji-Valizadeh, H.; Modery-Pawlowski, C. L.; Gupta, Sen, A. A Factor VIII-Derived Peptide Enables Von Willebrand Factor (VWF)-Binding of Artificial Platelet Nanoconstructs Without Interfering with VWF-Adhesion of Natural Platelets. *Nanoscale* **2014**, *6*, 4765–4773.
(74) Shukla, M.; Sekhon, U. D. S.; Betapudi, V.; Li, W.; Hickman, D. A.; Pawlowski, C. L.; Dyer, M. R.; Neal, M. D.; McCrae, K. R.; Gupta, Sen, A. In Vitro Characterization of SynthoPlate™ (Synthetic Platelet) Technology and Its in Vivo Evaluation in Severely Thrombocytopenic Mice. *J. Thromb. Haemost.* **2016**, *15(2)*, 375–387.
(75) Shoffstall, A. J.; Everhart, L. M.; Varley, M. E.; Soehnlen, E. S.; Shick, A. M.; Ustin, J. S.; Lavik, E. B. Tuning Ligand Density on Intravenous Hemostatic Nanoparticles Dramatically Increases Survival Following Blunt Trauma. *Biomacromolecules* **2013**, *14*, 2790–2797.
(76) Kudela, D.; Smith, S. A.; May-Masnou, A.; Braun, G. B.; Pallaoro, A.; Nguyen, C. K.; Chuong, T. T.; Nownes, S.; Allen, R.; Parker, N. R.; *et al.* Clotting Activity of Polyphosphate-Functionalized Silica Nanoparticles. *Angew. Chem. Int. Ed.* **2015**, *54*, 4018–4022.
(77) Brown, A. C.; Stabenfeldt, S. E.; Ahn, B.; Hannan, R. T.; Dhada, K. S.; Herman, E. S.; Stefanelli, V.; Guzzetta, N.; Alexeev, A.; Lam, W. A.; *et al.* Ultrasoft Microgels Displaying Emergent Platelet-Like Behaviours. *Nat. Mater.* **2014**, *13*, 1108–1114.
(78) Anselmo, A. C.; Modery-Pawlowski, C. L.; Menegatti, S.; Kumar, S.; Vogus, D. R.; Tian, L. L.; Chen, M.; Squires, T. M.; Gupta, Sen, A.; Mitragotri, S. Platelet-Like Nanoparticles: Mimicking Shape, Flexibility, and Surface Biology of Platelets to Target Vascular Injuries. *ACS Nano* **2014**, *8*, 11243–11253.
(79) Bachman, H.; Brown, A. C.; Clarke, K. C.; Dhada, K. S.; Douglas, A.; Hansen, C. E.; Herman, E.; Hyatt, J. S.; Kodlekere, P.; Meng, Z.; *et al.* Ultrasoft, Highly Deformable Microgels. *Soft Matter* **2015**, *11*, 2018–2028.
(80) Voros, E.; Cho, M.; Ramirez, M.; Palange, A. L.; De Rosa, E.; Key, J.; Garami, Z.; Lumsden, A. B.; Decuzzi, P. TPA Immobilization on Iron Oxide Nanocubes and Localized Magnetic Hyperthermia Accelerate Blood Clot Lysis. *Adv. Funct. Mater.* **2015**, *25*, 1709–1718.
(81) Absar, S.; Kwon, Y. M.; Ahsan, F. Bio-Responsive Delivery of Tissue Plasminogen Activator for Localized Thrombolysis. *J. Control. Release* **2014**, *177*, 42–50.
(82) Absar, S.; Nahar, K.; Kwon, Y. M.; Ahsan, F. Thrombus-Targeted Nanocarrier

Attenuates Bleeding Complications Associated with Conventional Thrombolytic Therapy. *Pharm. Res.* **2013**, *30*, 1663–1676.
(83) Korin, N.; Kanapathipillai, M.; Matthews, B. D.; Crescente, M.; Brill, A.; Mammoto, T.; Ghosh, K.; Jurek, S.; Bencherif, S. A.; Bhatta, D.; *et al.* Shear-Activated Nanotherapeutics for Drug Targeting to Obstructed Blood Vessels. *Science* **2012**, *337*, 738–742.
(84) Chen, H.; Mo, W.; Su, H.; Zhang, Y.; Song, H. Characterization of a Novel Bifunctional Mutant of Staphylokinase with Platelet-Targeted Thrombolysis and Antiplatelet Aggregation Activities. *BMC Mol. Biol.* **2007**, *8*, 88.
(85) Chen, C.; Li, S.; Liu, K.; Ma, G.; Yan, X. Co-Assembly of Heparin and Polypeptide Hybrid Nanoparticles for Biomimetic Delivery and Anti-Thrombus Therapy. *Small* **2016**, *12*, 4719–4725.
(86) Absar, S.; Choi, S.; Yang, V. C.; Kwon, Y. M. Heparin-Triggered Release of Camouflaged Tissue Plasminogen Activator for Targeted Thrombolysis. *J. Control. Release* **2012**, *157*, 46–54.
(87) Hashida, M.; Kawakami, S.; Yamashita, F. Lipid Carrier Systems for Targeted Drug and Gene Delivery TI . *Chem. Pharm. Bull.* **2005**, *53*, 871–880.
(88) Hörmann, K.; Zimmer, A. Drug Delivery and Drug Targeting with Parenteral Lipid Nanoemulsions — a Review. *J. Control. Release* **2016**, *223*, 85–98.
(89) Kogan, A.; Garti, N. Microemulsions as Transdermal Drug Delivery Vehicles. *Adv. Colloid Interface Sci.* **2006**, *123–126*, 369–385.
(90) Kalepu, S.; Manthina, M.; Padavala, V. Oral Lipid-Based Drug Delivery Systems – an Overview. *Acta Pharm. Sinica B* **2013**, *3*, 361–372.
(91) Tadros, T. F. Future Developments in Cosmetic Formulations. *International Journal of Cosmetic Science* **1992**, *14*, 93–111.
(92) Lacava, J.; Ouali, A.-A.; Raillard, B.; Kraus, T. On the Behaviour of Nanoparticles in Oil-in-Water Emulsions with Different Surfactants. *Soft Matter* **2014**, *10*, 1696–1704.
(93) Ngai, T.; Behrens, S. H.; Auweter, H. Novel Emulsions Stabilized by pH and Temperature Sensitive Microgels. *Chem. Commun.* **2005**, 331–333.
(94) Wang, H.; Hobbie, E. K. Amphiphobic Carbon Nanotubes as Macroemulsion Surfactants. *Langmuir* **2003**, *19*, 3091–3093.
(95) Cheetangdee, N.; Fukada, K. Protein Stabilized Oil-in-Water Emulsions Modified by Uniformity of Size by Premix Membrane Extrusion and Their Colloidal Stability. *Colloids Surf., A* **2012**, *403*, 54–61.
(96) Solans, C.; Izquierdo, P.; Nolla, J.; Azemar, N.; Garcia-Celma, M. J. Nano-Emulsions. *Current Opinion in Colloid & Interface Science* **2005**, *10*, 102–110.
(97) Tadros, T.; Izquierdo, P.; Esquena, J.; Solans, C. Formation and Stability of Nano-Emulsions. *Adv. Colloid Interface Sci.* **2004**, *108 IS* -, 303–318.
(98) Li, X.; Chen, Y.; Li, P. C. H. A Simple and Fast Microfluidic Approach of Same-Single-Cell Analysis (SASCA) for the Study of Multidrug Resistance Modulation in Cancer Cells. *Lab Chip* **2011**, *11*, 1378–1384.
(99) Ganta, S.; Paxton, J. W.; Baguley, B. C.; Garg, S. Pharmacokinetics and Pharmacodynamics of Chlorambucil Delivered in Parenteral Emulsion. *Int. J. Pharm.* **2008**, *360*, 115–121.
(100) Ramreddy, S.; Kandadi, P.; Veerabrahma, K. Formulation and

Pharmacokinetics of Diclofenac Lipid Nanoemulsions for Parenteral Application. *PDA J. Pharm. Sci. Technol.* **2012**, *66*, 28–37.
(101) Zheng, J.; Tang, Y.; Sun, M.; Zhao, Y.; Li, Q.; Zhou, J.; Wang, Y. Characterization, Pharmacokinetics, Tissue Distribution and Antitumor Activity of Honokiol Submicron Lipid Emulsions in Tumor-Burdened Mice. *Die Pharmazie - An International Journal of Pharmaceutical Sciences* **2013**, *68*, 41–46.
(102) Zhang, X.; Sun, X.; Li, J.; Zhang, X.; Gong, T.; Zhang, Z. Lipid Nanoemulsions Loaded with Doxorubicin-Oleic Acid Ionic Complex: Characterization, in Vitro and in Vivo Studies. *Die Pharmazie - An International Journal of Pharmaceutical Sciences* **2011**, *66*, 496–505.
(103) Ganta, S.; Sharma, P.; Paxton, J. W.; Baguley, B. C.; Garg, S. Pharmacokinetics and Pharmacodynamics of Chlorambucil Delivered in Long-Circulating Nanoemulsion. *J. Drug Target.* **2009**, *18*, 125–133.
(104) Liu, F.; Liu, D. Long-Circulating Emulsions (Oil-in-Water) as Carriers for Lipophilic Drugs. *Pharm. Res.* **1995**, *12*, 1060–1064.
(105) Alayoubi, A.; Alqahtani, S.; Kaddoumi, A.; Nazzal, S. Effect of PEG Surface Conformation on Anticancer Activity and Blood Circulation of Nanoemulsions Loaded with Tocotrienol-Rich Fraction of Palm Oil. *AAPS J.* **2013**, *15*, 1168–1179.
(106) Zhang, X.-X.; Eden, H. S.; Chen, X. Peptides in Cancer Nanomedicine: Drug Carriers, Targeting Ligands and Protease Substrates. *J. Control. Release* **2012**, *159*, 2–13.
(107) The Self-Assembly, Aggregation and Phase Transitions of Food Protein Systems in One, Two and Three Dimensions. *Rep. Prog. Phys.* **2013**, *76*, 046601.
(108) Lu, J. R.; Su, T. J.; Thomas, R. K. Structural Conformation of Bovine Serum Albumin Layers at the Air–Water Interface Studied by Neutron Reflection. *J. Colloid Interface Sci.* **1999**, *213*, 426–437.
(109) Mcclements, D. J. Critical Review of Techniques and Methodologies for Characterization of Emulsion Stability. *Crit. Rev. Food Sci. Nutr.* **2007**, *47*, 611–649.
(110) Jones, D. B.; Middelberg, A. P. J. Interfacial Protein Networks and Their Impact on Droplet Breakup. *AIChE J.* **2003**, *49*, 1533–1541.
(111) Ray, M.; Rousseau, D. Stabilization of Oil-in-Water Emulsions Using Mixtures of Denatured Soy Whey Proteins and Soluble Soybean Polysaccharides. *Food Res. Inter.* **2013**, *52*, 298–307.
(112) Shah, R. K.; Shum, H. C.; Rowat, A. C.; Lee, D.; Agresti, J. J.; Utada, A. S.; Chu, L.-Y.; Kim, J.-W.; Fernandez-Nieves, A.; Martinez, C. J.; *et al.* Designer Emulsions Using Microfluidics. *Mater. Today* **2008**, *11*, 18–27.
(113) Zhao, C.-X. Multiphase Flow Microfluidics for the Production of Single or Multiple Emulsions for Drug Delivery. *Adv. Drug Deliv. Rev.* **2013**, *65*, 1420–1446.
(114) Lovelyn, C.; Attama, A. A. Current State of Nanoemulsions in Drug Delivery. *J. Biomater. Nanobiotechnol.* **2011**, *02*, 626–639.
(115) Vladisavljević, G. T.; Williams, R. A. Recent Developments in Manufacturing

Emulsions and Particulate Products Using Membranes. *Adv. Colloid Interface Sci.* **2005**, *113*, 1–20.
(116) Sugumar, S.; Singh, S.; Mukherjee, A.; Chandrasekaran, N. Nanoemulsion of Orange Oil with Non Ionic Surfactant Produced Emulsion Using Ultrasonication Technique: Evaluating Against Food Spoilage Yeast. *Appl. Nanosci.* **2016**, *6*, 113–120.
(117) Gehrmann, S.; Bunjes, H. Preparation of Lipid Nanoemulsions by Premix Membrane Emulsification with Disposable Materials. *Int. J. Pharm.* **2016**, *511*, 741–744.
(118) Calligaris, S.; Plazzotta, S.; Bot, F.; Grasselli, S.; Malchiodi, A.; Anese, M. Nanoemulsion Preparation by Combining High Pressure Homogenization and High Power Ultrasound at Low Energy Densities. *Food Res. Inter.* **2016**, *83*, 25–30.
(119) Xia, Y.; Whitesides, G. M. Soft Lithography. *Angew. Chem. Int. Ed.* **1998**, *37*, 550–575.
(120) Iler, R. K. Multilayers of Colloidal Particles. *J. Colloid Interface Sci.* **1966**, *21*, 569–594.
(121) Decher, G.; Hong, J.-D. Buildup of Ultrathin Multilayer Films by a Self-Assembly Process, 1 Consecutive Adsorption of Anionic and Cationic Bipolar Amphiphiles on Charged Surfaces. *Makromol. Chem., Macromol. Symp.* **1991**, *46*, 321–327.
(122) Bertrand, P.; Jonas, A.; Laschewsky, A.; Legras, R. Ultrathin Polymer Coatings by Complexation of Polyelectrolytes at Interfaces: Suitable Materials, Structure and Properties. *Macromol. Rapid Commun.* **2000**, *21*, 319–348.
(123) Stuart, M. A. C.; Huck, W. T. S.; Genzer, J.; Muller, M.; Ober, C.; Stamm, M.; Sukhorukov, G. B.; Szleifer, I.; Tsukruk, V. V.; Urban, M.; *et al.* Emerging Applications of Stimuli-Responsive Polymer Materials. *Nat. Mater.* **2010**, *9*, 101–113.
(124) Ariga, K.; Yamauchi, Y.; Rydzek, G.; Ji, Q.; Yonamine, Y.; Wu, K. C. W.; Hill, J. P. Layer-by-Layer Nanoarchitectonics: Invention, Innovation, and Evolution. *Chem. Lett.* **2014**, *43*, 36–68.
(125) Sukhorukov, G. B.; Donath, E.; Davis, S.; Lichtenfeld, H.; Caruso, F.; Popov, V. I.; Möhwald, H. Stepwise Polyelectrolyte Assembly on Particle Surfaces: a Novel Approach to Colloid Design. *Polym. Adv. Technol.* **1998**, *9*, 759–767.
(126) Déjugnat, C.; Sukhorukov, G. B. pH-Responsive Properties of Hollow Polyelectrolyte Microcapsules Templated on Various Cores. *Langmuir* **2004**, *20*, 7265–7269.
(127) Yu, A.; Wang, Y.; Barlow, E.; Caruso, F. Mesoporous Silica Particles as Templates for Preparing Enzyme-Loaded Biocompatible Microcapsules. *Adv. Mater.* **2005**, *17*, 1737–1741.
(128) Shiratori, S. S.; Rubner, M. F. pH-Dependent Thickness Behavior of Sequentially Adsorbed Layers of Weak Polyelectrolytes. *Macromolecules* **2000**, *33*, 4213–4219.
(129) Feng, W.; Zhou, X.; He, C.; Qiu, K.; Nie, W.; Chen, L.; Wang, H.; Mo, X.; Zhang, Y. Polyelectrolyte Multilayer Functionalized Mesoporous Silica Nanoparticles for pH-Responsive Drug Delivery: Layer Thickness-Dependent

Release Profiles and Biocompatibility. *J. Mater. Chem. B* **2013**, *1*, 5886–5898.
(130) Delcea, M.; Schmidt, S.; Palankar, R.; Fernandes, P. A. L.; Fery, A.; Möhwald, H.; Skirtach, A. G. Mechanobiology: Correlation Between Mechanical Stability of Microcapsules Studied by AFM and Impact of Cell-Induced Stresses. *Small* **2010**, *6*, 2858–2862.
(131) Zhou, D.; Xiao, H.; Meng, F.; Zhou, S.; Guo, J.; Li, X.; Jing, X.; Huang, Y. Layer-by-Layer Assembled Polypeptide Capsules for Platinum-Based Pro-Drug Delivery. *Bioconjugate Chem.* **2012**, *23*, 2335–2343.
(132) Peng, C.; Zhang, Y.; Tong, W.; Gao, C. Influence of Folate Conjugation on the Cellular Uptake Degree of Poly(Allylamine Hydrochloride) Microcapsules. *J. Appl. Polym. Sci.* **2011**, *121*, 3710–3716.
(133) Hu, N.; Frueh, J.; Zheng, C.; Zhang, B.; He, Q. Photo-Crosslinked Natural Polyelectrolyte Multilayer Capsules for Drug Delivery. *Colloids Surf., A* **2015**, *482*, 315–323.
(134) Gao, H.; Sapelkin, A. V.; Titirici, M. M.; Sukhorukov, G. B. In SituSynthesis of Fluorescent Carbon Dots/Polyelectrolyte Nanocomposite Microcapsules with Reduced Permeability and Ultrasound Sensitivity. *ACS Nano* **2016**, *10*, 9608–9615.
(135) Pavlov, A. M.; Gabriel, S. A.; Sukhorukov, G. B.; Gould, D. J. Improved and Targeted Delivery of Bioactive Molecules to Cells with Magnetic Layer-by-Layer Assembled Microcapsules. *Nanoscale* **2015**, *7*, 9686–9693.
(136) Chen, H.; Di, Y.; Chen, D.; Madrid, K.; Zhang, M.; Tian, C.; Tang, L.; Gu, Y. Combined Chemo- and Photo-Thermal Therapy Delivered by Multifunctional Theranostic Gold Nanorod-Loaded Microcapsules. *Nanoscale* **2015**, *7*, 8884–8897.
(137) Yashchenok, A. M.; Jose, J.; Trochet, P.; Sukhorukov, G. B.; Gorin, D. A. Multifunctional Polyelectrolyte Microcapsules as a Contrast Agent for Photoacoustic Imaging in Blood. *J. Biophoton.* **2016**, *9*, 792–799.
(138) Li, T.; Yang, M. Electrochemical Sensor Utilizing Ferrocene Loaded Porous Polyelectrolyte Nanoparticles as Label for the Detection of Protein Biomarker IL-6. *Sens. Actuators B Chem.* **2011**, *158*, 361–365.
(139) Yang, Z.; Yang, L.; Zhang, Z.; Wu, N.; Xie, J.; Cao, W. Hollow Spheres of Silver Synthesized Using Polyelectrolyte Capsules as Microreactors. *Colloids Surf., A* **2008**, *312*, 113–117.
(140) Goldberg, M.; Langer, R.; Jia, X. Nanostructured Materials for Applications in Drug Delivery and Tissue Engineering. *J. Biomater. Sci. Polym. Ed.* **2007**, *18*, 241–268.
(141) De Koker, S.; Hoogenboom, R.; De Geest, B. G. Polymeric Multilayer Capsules for Drug Delivery. *Chem. Soc. Rev.* **2012**, *41*, 2867–2884.
(142) De Geest, B. G.; Sukhorukov, G. B.; Möhwald, H. The Pros and Cons of Polyelectrolyte Capsules in Drug Delivery. *Expert Opin. Drug Deliv.* **2009**, *6*, 613–624.
(143) Yurinskaya, M. M.; Kochetkova, O. Y.; Shabarchina, L. I.; Antonova, O. Y.; Suslikov, A. V.; Evgen'ev, M. B.; Vinokurov, M. G. Encapsulated Hsp70 Decreases Endotoxin-Induced Production of ROS and TNFα in Human Phagocytes. *Cell Stress Chaperones* **2017**, *22*, 163–171.

(144) Shukla, P.; Gupta, G.; Singodia, D.; Shukla, R.; Verma, A. K.; Dwivedi, P.; Kansal, S.; Mishra, P. R. Emerging Trend in Nano-Engineered Polyelectrolyte-Based Surrogate Carriers for Delivery of Bioactives. *Expert Opin. Drug Deliv.* **2010**, *7*, 993–1011.
(145) Selina, O. E.; Belov, S. Y.; Vlasova, N. N.; Balysheva, V. I.; Churin, A. I.; Bartkoviak, A.; Sukhorukov, G. B.; Markvicheva, E. A. Biodegradable Microcapsules with Entrapped DNA for Development of New DNA Vaccines. *Russ. J. Bioorg. Chem.* **2009**, *35*, 103.
(146) Gao, H.; Goriacheva, O. A.; Tarakina, N. V.; Sukhorukov, G. B. Intracellularly Biodegradable Polyelectrolyte/Silica Composite Microcapsules as Carriers for Small Molecules. *ACS Appl. Mater. Interfaces* **2016**, *8*, 9651–9661.
(147) De Temmerman, M.-L.; Demeester, J.; De Vos, F.; De Smedt, S. C. Encapsulation Performance of Layer-by-Layer Microcapsules for Proteins. *Biomacromolecules* **2011**, *12*, 1283–1289.
(148) Deng, Y.; Zhang, Y.; Sun, S.; Wang, Z.; Wang, M.; Yu, B.; Czajkowsky, D. M.; Liu, B.; Li, Y.; Wei, W.; *et al.* An Integrated Microfluidic Chip System for Single-Cell Secretion Profiling of Rare Circulating Tumor Cells. *Sci. Rep.* **2014**, *4*, 7499.
(149) Li, Y.; Lu, L.; Zhang, H.; Wang, J. The pH Regulated Phycobiliproteins Loading and Releasing of Polyelectrolytes Multilayer Microcapsules. *Colloids Surf., B* **2012**, *93*, 121–126.
(150) Deo, D. I.; Gautrot, J. E.; Sukhorukov, G. B.; Wang, W. Biofunctionalization of PEGylated Microcapsules for Exclusive Binding to Protein Substrates. *Biomacromolecules* **2014**, *15*, 2555–2562.
(151) Costa, R. R.; Girotti, A.; Santos, M.; Arias, F. J.; Mano, J. F.; Rodríguez-Cabello, J. C. Cellular Uptake of Multilayered Capsules Produced with Natural and Genetically Engineered Biomimetic Macromolecules. *Acta Biomater.* **2014**, *10*, 2653–2662.
(152) Timin, A. S.; Lepik, K. V.; Muslimov, A. R.; Gorin, D. A.; Afanasyev, B. V.; Sukhorukov, G. B. Intracellular Redox Induced Drug Release in Cancerous and Mesenchymal Stem Cells. *Colloids Surf., B* **2016**, *147*, 450–458.
(153) Nematbakhsh, Y.; Lim, C. T. Cell Biomechanics and Its Applications in Human Disease Diagnosis. *Acta Mech. Sinica* **2015**, *31*, 268–273.
(154) Suresh, S. Biomechanics and Biophysics of Cancer Cells. *Acta Mater.* **2007**, *55*, 3989–4014.
(155) Vinogradova, O. I. Mechanical Properties of Polyelectrolyte Multilayer Microcapsules. *J. Phys. Condens. Matter* **2004**, *16*, R1105.
(156) Lulevich, V. V.; Vinogradova, O. I. Effect of pH and Salt on the Stiffness of Polyelectrolyte Multilayer Microcapsules. *Langmuir* **2004**, *20*, 2874–2878.
(157) Mueller, R.; Köhler, K.; Weinkamer, R.; Sukhorukov, G.; Fery, A. Melting of PDADMAC/PSS Capsules Investigated with AFM Force Spectroscopy. *Macromolecules* **2005**, *38*, 9766–9771.
(158) Fernandes, P. A. L.; Delcea, M.; Skirtach, A. G.; Möhwald, H.; Fery, A. Quantification of Release From Microcapsules Upon Mechanical Deformation with AFM. *Soft Matter* **2010**, *6*, 1879–1883.
(159) Volodkin, D. V.; Schmidt, S.; Fernandes, P.; Larionova, N. I.; Sukhorukov, G.

B.; Duschl, C.; Möhwald, H.; Klitzing, von, R. One-Step Formulation of Protein Microparticles with Tailored Properties: Hard Templating at Soft Conditions. *Adv. Funct. Mater.* **2012**, *22*, 1914–1922.

(160) Shattil, S. J.; Hoxie, J. A.; Cunningham, M.; Brass, L. F. Changes in the Platelet Membrane Glycoprotein IIb.IIIa Complex During Platelet Activation. *J. Biol. Chem.* **1985**, *260*, 11107–11114.

(161) Tuddenham, E. G. D.; Schwaab, R.; Seehafer, J.; Millar, D. S.; Gitschier, J.; Higuchi, M.; Bidichandani, S.; Connor, J. M.; Hoyer, L. W.; Yoshioka, A.; *et al.* Haemophilia a: Database of Nucleotide Substitutions, Deletions, Insertions and Rearrangements of the Factor VIII Gene, Second Edition. *Nucleic Acids Res.* **1994**, *22*, 3511–3533.

(162) Payne, A. B.; Miller, C. H.; Kelly, F. M.; Michael Soucie, J.; Craig Hooper, W. The CDC Hemophilia a Mutation Project (CHAMP) Mutation List: a New Online Resource. *Human Mutation* **2013**, *34*, E2382–E2392.

(163) Bogdanova, N.; Markoff, A.; Eisert, R.; Wermes, C.; Pollmann, H.; Todorova, A.; Chlystun, M.; Nowak-Göttl, U.; Horst, J. Spectrum of Molecular Defects and Mutation Detection Rate in Patients with Mild and Moderate Hemophilia A. *Human Mutation* **2007**, *28*, 54–60.

(164) Franchini, M.; Lippi, G. The Use of Desmopressin in Acquired Haemophilia a: a Systematic Review. *Blood Transfusion* **2011**, *9*, 377–382.

(165) Wynn, T. T.; Gumuscu, B. Potential Role of a New PEGylated Recombinant Factor VIII for Hemophilia A. *Journal of Blood Medicine* **2016**, *7*, 121–128.

(166) Gruppo, R. A.; Brown, D.; Wilkes, M. M.; Navickis, R. J. Increased Breakthrough Bleeding During Prophylaxis with B-Domain Deleted Factor VIII – a Robust Meta-Analytic Finding. *Haemophilia* **2004**, *10*, 449–451.

(167) Collins, P. W.; Hirsch, S.; Baglin, T. P.; Dolan, G.; Hanley, J.; Makris, M.; Keeling, D. M.; Liesner, R.; Brown, S. A.; Hay, C. R. M.; *et al.* Acquired Hemophilia a in the United Kingdom: a 2-Year National Surveillance Study by the United Kingdom Haemophilia Centre Doctors' Organisation. *Blood* **2007**, *109*, 1870–1877.

(168) Lulla, R. R.; Allen, G. A.; ZakarijaA, A.; Green, D. Transplacental Transfer of Postpartum Inhibitors to Factor VIII. *Haemophilia* **2010**, *16*, 14–17.

(169) Gawryl, M. S.; Hoyer, L. W. Inactivation of Factor VIII Coagulant Activity by Two Different Types of Human Antibodies. *Blood* **1982**, *60*, 1103.

(170) Prescott, R.; Nakai, H.; Saenko, E. L.; Scharrer, I.; Nilsson, I. M.; Humphries, J. E.; Hurst, D.; Bray, G.; Scandella, D. The Inhibitor Antibody Response Is More Complex in Hemophilia a Patients Than in Most Nonhemophiliacs with Factor VIII Autoantibodies. *Blood* **1997**, *89*, 3663.

(171) Lusher, J. M.; Arkin, S.; Abildgaard, C. F.; Schwartz, R. S. Recombinant Factor VIII for the Treatment of Previously Untreated Patients with Hemophilia a -- Safety, Efficacy, and Development of Inhibitors. *N. Engl. J. Med.* **1993**, *328*, 453–459.

(172) Gouw, S. C.; van den Berg, H. M.; Oldenburg, J.; Astermark, J.; de Groot, P. G.; Margaglione, M.; Thompson, A. R.; van Heerde, W.; Boekhorst, J.; Miller, C. H.; *et al.* F8 Gene Mutation Type and Inhibitor Development in Patients with Severe Hemophilia a: Systematic Review and Meta-Analysis. *Blood* **2012**,

119, 2922–2934.
(173) Astermark, J.; Berntorp, E.; White, G. C.; Kroner, B. L.; GROUP, T. M. S. The Malmö International Brother Study (MIBS): Further Support for Genetic Predisposition to Inhibitor Development. *Haemophilia* **2001**, *7*, 267–272.
(174) Kempton, C. L.; Meeks, S. L. Toward Optimal Therapy for Inhibitors in Hemophilia. *Blood* **2014**, *124*, 3365–3372.
(175) Meeks, S. L.; Chapman, R. L.; Kempton, C.; Dunn, A. L. Late Immune Tolerance Induction in Haemophilia a Patients. *Haemophilia* **2013**, *19*, 445–448.
(176) Nakar, C.; Manco-Johnson, M. J.; Lail, A.; Donfield, S.; Maahs, J.; Chong, Y.; Blades, T.; Shapiro, A. Prompt Immune Tolerance Induction at Inhibitor Diagnosis Regardless of Titre May Increase Overall Success in Haemophilia a Complicated by Inhibitors: Experience of Two US Centres. *Haemophilia* **2015**, *21*, 365–373.
(177) DiMichele, D. M.; Hoots, W. K.; Pipe, S. W.; Rivard, G. E.; Santagostino, E. International Workshop on Immune Tolerance Induction: Consensus Recommendations1. *Haemophilia* **2007**, *13*, 1–22.
(178) Kruse-Jarres, R.; St-Louis, J.; Greist, A.; Shapiro, A.; Smith, H.; Chowdary, P.; Drebes, A.; Gomperts, E.; Bourgeois, C.; Mo, M.; *et al.* Efficacy and Safety of OBI-1, an Antihaemophilic Factor VIII (Recombinant), Porcine Sequence, in Subjects with Acquired Haemophilia A. *Haemophilia* **2015**, *21*, 162–170.
(179) Uchida, N.; Sambe, T.; Yoneyama, K.; Fukazawa, N.; Kawanishi, T.; Kobayashi, S.; Shima, M. A First-in-Human Phase 1 Study of ACE910, a Novel Factor VIII-Mimetic Bispecific Antibody, in Healthy Subjects. *Blood* **2016**, *127*, 1633–1641.
(180) Adverse Events in Trial Dent Hopes for Roche Hemophilia Drug. *Reuters* **2016**.
(181) Carroll, J. Roche confirms patient death in ACE910 PhIII hemophilia trial, spurring new questions about top blockbuster hopeful (accessed May 31, 2017).
(182) Lindenboom, C. R. Alnylam Reports Positive Interim Phase 1 Results for Fitusiran in Hemophilia a and B Patients with Inhibitors. *Alnylam Pharmaceuticals*, 2016.
(183) Konkle, B. A.; Stasyshyn, O.; Chowdary, P.; Bevan, D. H.; Mant, T.; Shima, M.; Engl, W.; Dyck-Jones, J.; Fuerlinger, M.; Patrone, L.; *et al.* Pegylated, Full-Length, Recombinant Factor VIII for Prophylactic and on-Demand Treatment of Severe Hemophilia A. *Blood* **2015**, *126*, 1078–1085.
(184) Mei, B.; Pan, C.; Jiang, H.; Tjandra, H.; Strauss, J.; Chen, Y.; Liu, T.; Zhang, X.; Severs, J.; Newgren, J.; *et al.* Rational Design of a Fully Active, Long-Acting PEGylated Factor VIII for Hemophilia a Treatment. *Blood* **2010**, *116*, 270–279.
(185) Shetty, K. A.; Kosloski, M. P.; Mager, D. E.; Balu-Iyer, S. V. Soy Phosphatidylinositol Containing Nanoparticle Prolongs Hemostatic Activity of B-Domain Deleted Factor VIII in Hemophilia a Mice. *J. Pharm. Sci.* **2015**, *104*, 388–395.
(186) Shetty, K. A.; Kosloski, M. P.; Mager, D. E.; Balu-Iyer, S. V. Factor VIII Associated with Lipidic Nanoparticles Retains Efficacy in the Presence of Anti-

Factor VIII Antibodies in Hemophilia a Mice. *Biopharm. Drug Dispos.* **2016**, *37*, 409–420.
(187) Peng, A.; Kosloski, M. P.; Nakamura, G.; Ding, H.; Balu-Iyer, S. V. PEGylation of a Factor VIII–Phosphatidylinositol Complex: Pharmacokinetics and Immunogenicity in Hemophilia a Mice. *AAPS J.* **2011**, *14*, 35–42.
(188) Ishida, T.; Ichihara, M.; Wang, X.; Yamamoto, K.; Kimura, J.; Majima, E.; Kiwada, H. Injection of PEGylated Liposomes in Rats Elicits PEG-Specific IgM, Which Is Responsible for Rapid Elimination of a Second Dose of PEGylated Liposomes. *J. Control. Release 112*, 15–25.
(189) Angelatos, A. S.; Johnston, A. P. R.; Wang, Y.; Caruso, F. Probing the Permeability of Polyelectrolyte Multilayer Capsules via a Molecular Beacon Approach. *Langmuir* **2007**, *23*, 4554–4562.
(190) She, Z.; Antipina, M. N.; Li, J.; Sukhorukov, G. B. Mechanism of Protein Release From Polyelectrolyte Multilayer Microcapsules. *Biomacromolecules* **2010**, *11*, 1241–1247.
(191) Eubanks, J.; Baldwin, W. H.; Markovitz, R.; Parker, E. T.; Cox, C.; Kempton, C. L.; Meeks, S. L. A Subset of High-Titer Anti–Factor VIII A2 Domain Antibodies Is Responsive to Treatment with Factor VIII. *Blood* **2016**, *127*, 2028–2034.
(192) Colace, T.; Fogarty, P. F.; Panckeri, K. A.; Li, R.; Diamond, S. L. Microfluidic Assay of Hemophilic Blood Clotting: Distinct Deficits in Platelet and Fibrin Deposition at Low Factor Levels. *J. Thromb. Haemost.* **2014**, *12*, 147–158.
(193) Hui, K.; Haber, E.; Matsueda, G. Monoclonal Antibodies to a Synthetic Fibrin-Like Peptide Bind to Human Fibrin but Not Fibrinogen. *Science* **1983**, *222*, 1129–1132.
(194) Gaharwar, A. K.; Avery, R. K.; Assmann, A.; Paul, A.; McKinley, G. H.; Khademhosseini, A.; Olsen, B. D. Shear-Thinning Nanocomposite Hydrogels for the Treatment of Hemorrhage. *ACS Nano* **2014**, *8*, 9833–9842.
(195) Jing, T.; Lai, Z.; Wu, L.; Han, J.; Lim, C. T.; Chen, C.-H. Single Cell Analysis of Leukocyte Protease Activity Using Integrated Continuous-Flow Microfluidics. *Anal. Chem.* **2016**, *88*, 11750–11757.
(196) Hou, H. W.; Petchakup, C.; Tay, H. M.; Tam, Z. Y.; Dalan, R.; Chew, D. E. K.; Li, K. H. H.; Boehm, B. O. Rapid and Label-Free Microfluidic Neutrophil Purification and Phenotyping in Diabetes Mellitus. *Sci. Rep.* **2016**, *6*, 29410.
(197) Ozkumur, E.; Shah, A. M.; Ciciliano, J. C.; Emmink, B. L.; Miyamoto, D. T.; Brachtel, E.; Yu, M.; Chen, P. I.; Morgan, B.; Trautwein, J.; *et al.* Inertial Focusing for Tumor Antigen-Dependent and -Independent Sorting of Rare Circulating Tumor Cells. *Sci. Transl. Med.* **2013**, *5*, 179ra47–179ra47.
(198) Parker, E. T.; Lollar, P. A Quantitative Measure of the Efficacy of Factor VIII in Hemophilia a Mice. *Thromb. Haemost.* **2003**, *89*, 480–485.
(199) Broze, G. J.; Yin, Z.-F.; Lasky, N. A Tail Vein Bleeding Time Model and Delayed Bleeding in Hemophiliac Mice. *Thromb. Haemost.* **2001**, *85*, 747–748.
(200) Healey, J. F.; Parker, E. T.; Barrow, R. T.; Langley, T. J.; Church, W. R.; Lollar, P. The Humoral Response to Human Factor VIII in Hemophilia a Mice. *J. Thromb. Haemost.* **2007**, *5*, 512–519.
(201) Meeks, S. L.; Healey, J. F.; Parker, E. T.; Barrow, R. T.; Lollar, P. Antihuman

Factor VIII C2 Domain Antibodies in Hemophilia a Mice Recognize a Functionally Complex Continuous Spectrum of Epitopes Dominated by Inhibitors of Factor VIII Activation. *Blood* **2007**, *110*, 4234–4242.

(202) Koudelka, S.; Mikulik, R.; Mašek, J.; Raška, M.; Turánek Knotigová, P.; Miller, A. D.; Turánek, J. Liposomal Nanocarriers for Plasminogen Activators. *J. Control. Release* **2016**, *227*, 45–57.